Expression of visual opsins in the retina of Atlantic salmon (*Salmo salar L.*) during smoltification

By Eirik Næss Viken

Master program in Aquaculture biology

Department of Biological Sciences

University of Bergen, Norway

Spring 2020

Content

Acknowledgements:

I would like to sincerely thank my main supervisor Post-doc Mariann Eilertsen for her constant assistance during my stay at the Marine Developmental Biology lab, having her door always open and setting aside time during an otherwise busy schedule, whenever I needed guidance related to laboratory work or while writing my thesis.

I would also like to show my gratitude towards my co-supervisor Professor Jon Vidar Helvik for introducing me to the subject and his encouragement for me to participate in an ongoing project. His experience within the field of Salmon vision came in handy when opinions from an expert was required.

A special thanks is sent to my other co-supervisor Professor Tom Ole Nilsen for his contributions to the thesis with his profound knowledge on the transformations occurring during the smoltification process.

Rita Karlsen deserves some well-earned attention, for immediately aiding me whenever problems occurred. Whether the problems were big or small, she was always available to provide assistance.

Additionally, I would like to thank all the people that have contributed to the friendly and including environment I've experienced in my time at the lab. This made coming into the lab effortlessly.

Abstract:

The visual system of Atlantic salmon is highly adapted to their migratory and dynamic life-history, where the profound transformational process of smoltification is crucial. The retina contain both rod- and cone photoreceptors that express specific classes of opsins. *Rhodopsin* expressed in rod photoreceptors is responsible for the detection of light in dimmed conditions (scotopic vision). Cone photoreceptors, responsible for the detection of light in bright, coloured conditions (photopic vision), consist of the single cones: The first short wavelength-sensitive *sws1* (UV opsin) and the second short wavelength-sensitive *sws2* (blue opsin), and the double cones: the middle wavelength-sensitive *rh2* (green opsin) and the long-to-middle wavelength-sensitive *lws* (red opsin). The main purpose of this study was to establish the topographic distribution of the various photoreceptor classes (opsins) using the *In situ* hybridization (ISH) method on cryosections, during a period where the Atlantic salmon developed from a parr, through the smoltification process, and towards having spent a month in sea water. It was shown that patterns were different between the cone opsins, especially by comparing expression in genes related to single- and double cones. Additionally, comparisons were made between the distribution of the rod- and cone photoreceptor classes, where the constant prominent presence of *rhodopsin* was likely influenced by the continuous incorporation of rod photoreceptors through neurogenesis in rod precursor cells in the outer nuclear layer (ONL). This continuous supply of *rhodopsin* throughout the expanding retina is a consequence of the post-embryonic development common to teleosts. In addition, retinal alterations was observed through the smoltification process, especially in the downregulation of *sws1*. The commonly presented causation of this transformation is a process called opsin changeover, where *sws1* is proposed to be transformed into *sws2* during the alevin stage. However, findings in the literature on Atlantic salmon in addition to the fluctuating pattern of *sws2* observed in this study questioned the influence of this theory in salmon. *Sws2* displayed a central prominence adjacent to the optic nerve on the central eye section during the smolt stage, a finding previously unknown in Atlantic salmon, potentially illustrating the continued importance of the embryonic fissure in single cone generation. The importance of the ciliary marginal zone (CMZ) in the generation of cone photoreceptors was demonstrated in the continuous prominence of *sws2, rh2* and *lws* adjacent to this area through smoltification. However, the reduced presence of *sws1* in this area opposed the theory stating that the appearance of cone opsins in the CMZ would be reflected through the retinal transformation. The topographic distribution and its dynamic patterns in the retina were put into an ecological perspective, demonstrating how the migration from fresh water to salt water has functioned as a natural influencer on the observations made. Additionally, the findings of this study could support the aquaculture industry in their utilization of lighting conditions exposed to the reared salmon.

1. Introduction:

1.1. Atlantic salmon, an anadromous species undergoing transformation:

Atlantic salmon (*Salmo salar L.)* goes through several developmental stages throughout its life cycle. Salmon starts its life in fresh water, where the embryos develop and hatching of alevins occurs while the embryo is safely hidden in gravel. When the yolk sac is fully utilized, the salmon emerge from the gravel as fry. Having to supply itself through external intake of food, it starts feeding exogenously. The juvenile salmon grows and becomes a parr, reaching a certain critical length from which the smoltification process is initiated. This profound transformation of bodily functions culminates in the salmon becoming a smolt, meaning that the downward migration into the oceans can begin. Here the salmon spend several years exploiting the abundance of nutritional food, growing until they're ready to sexually mature. Following this process, the salmon move back to the very same river they once came from to spawn, a pattern facilitated by the olfactory imprinting of familiar odours occurring prior to the seaward migration (McCormick et al., 1998; Verspoor et al., 2007).
This migratory pattern makes the salmon anadromous. By splitting anadromous into two halves, it displays the meaning of the word: *Ana-*, meaning up; and *-dromous*, meaning movement - explaining the upward migration from the oceans into the rivers where salmon breed (McDowall, 2006).

1.2. Smoltification:

As already mentioned, salmon goes through a process called smoltification, which is critical for the salmon as it migrates downwards the river and into the marine environment. In nature, salmon experience several environmental conditions which are of importance in the regulation of smoltification, with photoperiod, temperature and flow being the most prominent factors in this regard (McCormick et al., 1998). Temperature and flow serves to modify and regulate the speed of the transformation, while photoperiod is the most important signal in initiating the process (McCormick et al., 1998). As the year progresses, salmon are exposed to a range of different seasonal variations in photoperiod, causing a set of endocrinal motions (Hoar, 1988; McCormick et al., 1998).
Melatonin, a hormone synthesized in the pineal gland, is an important factor involved in the

initiation of smoltification. During the night, melatonin is synthesized and released in the blood plasma (Porter et al., 2001). In late autumn and start of the winter, the daylength is gradually decreasing, culminating in the increased production of melatonin (Ekström P. & Meissl H., 1997; Iigo et al., 2005). What is termed the "winter signal" in the aquaculture industry, represents a period of sustained, high levels of melatonin caused by the decreasing daylength and the concurrent prolonged night-time (Porter et al., 2001). If the juvenile salmon reaches the sufficient size-threshold for a comprehensive and demanding smolt-process, this signal initiates a range of bodily transformations that will take place as the photoperiod increases in the spring (Folkedal et al., 2010; McCormick et al., 2007).

As the downward migration from fresh water into salt water represents a profound change of habitat in a salmon's life, this requires a set of adaptations in the fish in order to accommodate the drastically changing environmental conditions.

Smoltification involves the morphological, physiological and behavioral changes that prepare the juvenile salmon for a marine life (Boeuf, 1993; Hoar, 1988; McCormick et al., 1998).

1.2.1. Morphology:

*C*haracterizations of a smolt is readily apparent in the outer morphological traits. The colorization patterns change as the salmon goes from being a parr to a smolt. Both the dorsal and ventral side undergo changes, from a brown-green to a silvery dark and from a yellow-light to a silvery light, respectively. The characteristic parr-marks, brown-ish colour-structures on the side of the parr resembling fingermarks, are lost (McCormick et al., 1998; Woo et al., 1978). These transformations in colour patterns are facilitated by the deposition of purines – guanin and hypoxanthin – in the skin (McCormick et al., 1998). This adaptation is natural as the salmon goes from being a benthic parr utilizing the structures of the river for camouflage, to being a pelagic fish exposed to threats in the open waters of the ocean (Johnston & Eales, 2011). Another modification to colorization patterns are observed especially in the dorsal, caudal and pectoral fins. The fins themselves become lighter, almost transparent, while the fin margins become darker (Stefansson et al., 2008). It is hypothesized that this is an adaptation contributing to visual signalling as the salmon starts schooling (Stefansson et al., 2008).

The body itself becomes thinner and lengthier, making the salmon more streamlined (Kipanyula & Maina, 2016). The metabolic activity is reorganized and increased, mobilizing stored lipids to create energy (Sheridan, 1989). The condition factor, which is a parameter for measuring the general condition in the fish by calculating the ratio of body weight to body

length, is decreased (McCormick et al., 1998). These transformations in morphological structures facilitates a pelagic lifestyle (Hoar, 1988).

1.2.2. Behaviour:

The adaptations to behavioural patterns is another way of observing a smoltified salmon through external cues. As a parr, living in a river where competition for covering spots functioning as shelter for the fish is vital for survival, salmon have a distinct territorial behaviour (McCormick et al., 1998). Moving into the oceans as a smolt, salmon typically starts schooling. To accommodate this change in existence, the aggressive behaviour related to territoriality is lost (Björnsson et al., 2011; McCormick et al., 1998).

In order to prevent excessive expenditure of energy while maintaining the position in the constant flow of the river, juvenile salmon have evolved a swimming behaviour called positive rheotaxis (Martin et al., 2012). Positive rheotaxis (upstream orientation) is gradually transformed into negative rheotaxis (downstream orientation) as the salmon develops into an ocean-going smolt preparing to inhabit an environment where this one-way movement of water is absent (Martin et al., 2012; McCormick et al., 1998).

1.2.3. Physiology:

Changing habitats completely by moving from fresh water into salt water requires a profound change in physiological mechanisms of varying significance in the body. One of the most important for the migrating salmon, is the ability to adapt its osmoregulatory capabilities (McCormick & Saunders, 1987; Nilsen et al., 2007). Keeping physiological levels balanced is crucial for survival, and several different regulatory mechanisms are constantly working to maintain homeostasis. This is especially important regarding plasma-ion levels, which is regulated by osmoregulation (McCormick & Saunders, 1987). In order to accomplish this, salmon have specialized chloride cells in the gills accompanied with sodium pumps, the Na+/K+-ATPase, responsible for maintaining the ionic homeostasis through actively pumping ions (McCormick & Saunders, 1987; Nilsen et al., 2007). In fresh water, where the water contain limited amounts of ions, salmon must accommodate this by having chloride cells with sodium pumps specialized for pumping in ions through the gills, spending large amounts of energy in the process (McCormick & Saunders, 1987; Nilsen et al., 2007). Inside the body, ion levels are further preserved through a filtering system in the kidneys, diluting the urine before it's excreted (McCormick & Saunders, 1987). The fish is also reluctant to drinking water at this stage (Tipsmark et al., 2010)

Following smoltification, salmon is adapted to an existence in a completely different environment. Moving from water with limited amounts of ions in rivers to water concentrated with ions in the ocean, the regulatory process is reversed, as the focus is shifted towards getting rid of ions through excretion instead of retaining the ions (McCormick & Saunders, 1987). As this is an energy-intensive process, the gills adapt through modifications, increasing the number and size of chloride cells (McCormick & Saunders, 1987). Hence, as the salmon still resides in fresh water, an adaptation towards the upcoming migration occurs, increasing the amount of chloride cells adapted to sea water in the gills, while their accompanying sodium pumps, the basolateral enzyme Na+/K+-ATPase (NKA), have their activity increased (McCormick & Saunders, 1987; Nilsen et al., 2007). This is also readily apparent in the concentration of mitochondria in the chloride cells, which increases drastically throughout the smoltification process (McCormick & Saunders, 1987). A study by Blake et al. in 1984 on Atlantic salmon displayed how the concentration of mitochondria in chloride cells increased by 50 % in smolts compared to parr (Blake et al., 1984). At the migratory stage, the salmon starts drinking ample amounts of water concentrated with ions to satisfy its requirements for fluid (Tipsmark et al., 2010). An opposite focus is also seen in the kidneys, which in sea water excretes concentrated urine (Tipsmark et al., 2010).

1.2.4. Endocrinology:

Physiological processes regulating levels in the body to keep homeostasis is in itself regulated by another system, the endocrine system (Blanton & Specker, 2007). Hormones are released by glands and transported in the circulatory system, functioning as signalling molecules received at target locations around the body, either inhibiting or setting in motion physiological processes (Blanton & Specker, 2007). As already mentioned, the melatonin hormone released by the pineal gland is an important factor in the regulation of smoltification. Increased levels of melatonin released in the blood plasma binds to specific binding sites in the brain (i.e. the anterior hypothalamus and in the preoptic area), which further signals the pituitary gland, starting a reaction pathway resulting in several hormones being released (Iigo et al., 2005). Hormones with important roles during the smoltification process are the thyroid stimulating hormone (TSH), the thyroid hormones T3 and T4, growth hormone (GH), insulin-like growth factor (IGF-1), cortisol and insulin, all displaying peak levels at different times during smoltification (Dickhoff et al., 1997; Young et al., 1989). Each of these hormones either work and affect the smoltification on its own or in combination with other hormones. GH and cortisol interact in the development of sea water tolerance through the increased

activity of the Na+/K+-ATPase, while T3/T4 are important for morphological adaptations like silvering of the skin (McCormick et al., 2002).

1.3. Photoreceptors (rods and cones) and accompanying visual pigment proteins (opsins):

1.3.1. Photoreception through photoreceptors:

Photoreception is the act of perceiving light by the organism in a medium, leading to vision through a series of neuronal processes performed by the eyes and further processed in the brain (Archer, 1999). Photoreceptors, which are responsible for the processing of information received through electromagnetic waves (photons), were evolved more than 600 Mya, functioning as a fundamental mechanism for the survival of the organism. Having developed a basis for visual perception of the environment increased the possibilities of detecting sources of nutrients through food, avoid predation, etc. (Lamb et al., 2007). To be able to process the electromagnetic waves received through light, which are measured in nanometers (nm), these needs to be within a certain spectrum, called the visible spectrum (Ali, 2008). Animals are exposed to a wide range of different lighting conditions, meaning that the visible spectrum of species differs in accordance with the ability to process the received photons in their respective habitats (Carleton et al., 2020; Levine & Macnichol Jr, 1982). Hence, species living in dimmed lighting conditions, like deep-sea teleosts, have a visible spectrum within a more limited range of wavelengths compared to teleosts inhabiting brighter habitats, like Atlantic salmon (Ali, 2008).

1.3.2. Complex eyes with retinal photoreceptors (rods and cones):

Retina:

The complex eyes are thought to have evolved following the Cambrian explosion, some 540 Mya (Lamb et al., 2007). Eyes, composed of specialized compartments with distinct functions, made it possible to process complex images to a bigger extent than before, perceiving the surroundings in higher detail (Lamb et al., 2007; Reece et al., 2015). One of these specialized compartments mentioned is the retina, a layer of tissue positioned at the innermost section of the eye (Lamb et al., 2007). In Fig. 1, the morphology and layers of the retina of an adult zebrafish (*Danio rerio)* are displayed (Fig, 1A) with the accompanying cells located in each layer (Fig, 1B). Starting from the inner section of the retina closest to the

vitreous humour and moving outward towards the section closest to the choroid, the layers are listed in positional order: The retinal ganglion layer (RGL), the inner plexiform layer (IPL), the inner nuclear layer (INL), the outer plexiform layer (OPL), the outer nuclear layer (ONL), the photoreceptor layer (PL) and the pigment epithelium (PE). The rod- and cone photoreceptors which are of importance to the research performed in this thesis, are located in the outer segments of the retina, protruding from the ONL, growing through the PL, and ending up in the PE. The rods and cones are connected to bipolar cells, to which the information received in the pigment epithelium are transported after being processed in the photoreceptors. From here, the information is transmitted further to the ganglion cells, before moving towards the optic disc, the optic nerve, and further towards the brain where the signals of light are perceived and processed in the optic tectum. Horizontal- and amacrine cells are important in the assistance of processing and making sense of the array of information received from the outer medium (Gramage et al., 2014).

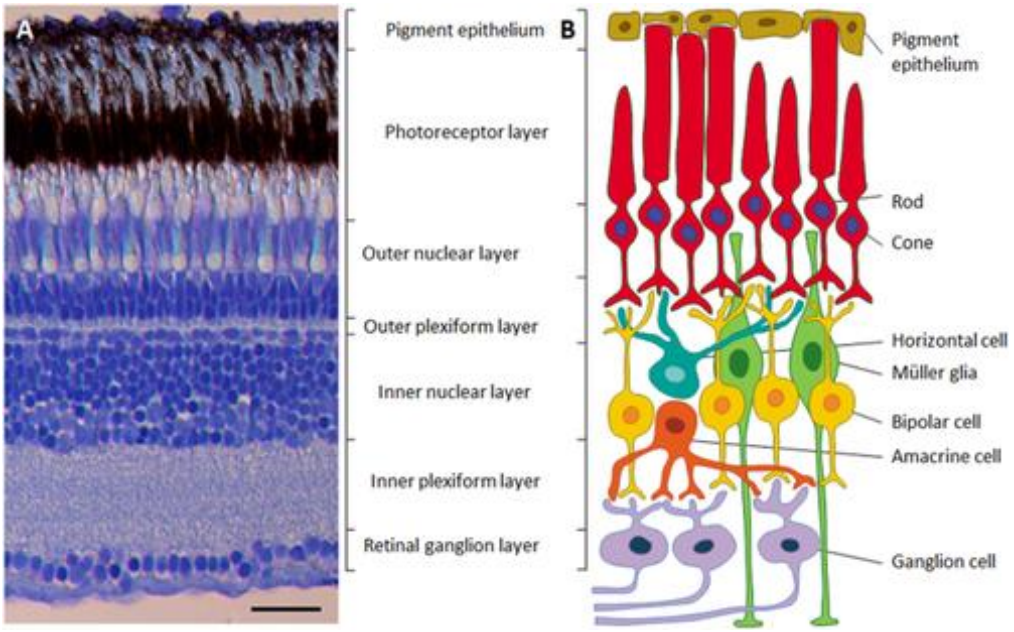

Figure 1: Retinal morphology and structure in an adult Zebrafish. **A:** Histological section of the retina presenting the retinal layers. **B:** Retinal cells and their location in the retinal layers. (modified from Gramage, Li and Hitchcock, 2014)

Photoreceptors:

In vertebrates, the retina consists of two kinds of photoreceptors, the rods and cones, responsible for detecting light and forwarding the visual information to the brain (Lamb et al., 2007). The rods are responsible for detecting light at low levels; so-called scotopic vision –

and the cones are responsible for detecting light at higher levels, with an important function being the detection of colour; so-called photopic vision (Bowmaker, 2008; Valen et al., 2016). Photoreceptors consists of two segments: the inner- and the outer segment. The outer segment is the receiver of photons, a primary cilium with a large area developed for maximal absorption of light, and is the segment where photopigments are located. The inner segment is the metabolic part of the cell, maintaining cellular functions while forwarding the signal absorbed by the outer segment through a change in membrane potential (Baker & Kerov, 2013). These photoreceptors are further separated into different classes. However, in the case of rods, these commonly only consist of one class in vertebrates. The scotopic vision is therefore monochromatic (Sabouhanian, 2015). Colour vision being more complicated to process, requires at least two classes of cones that are spectrally distinct and connected to a nervous system that can compare the visual detection received in each cone (Bowmaker, 2008).

Opsins:

Rods and cones are classified through the differentiation of their visual pigments composed of opsins located in the photoreceptors outer segment, a group of G-protein-coupled receptors linked to the chromophore retinal, either represented by an 11-*cis* retinal (A1) or an 11-*cis* 3,4-dehydroretinal (A2). Photons are captured and absorbed by the vitamin-A chromophore, leading to photoisomerization of the 11-cis isomer to the all-*trans* form, causing a change in opsin protein structure (Peirson et al., 2009; Terakita, 2005). Opsins are typically composed of about 350 amino acids arranged in a structure of seven alpha-helical transmembrane regions enclosing a ligand-binding pocket, where the Schiff base linkage is bound to a lysine residue in the seventh helix (Bowmaker & Hunt, 2006). The structural composition explained above is displayed in Fig. 2. Interactions between retinal and specific amino acids determines the spectral sensitivity of the pigment (Bowmaker & Hunt, 2006; Carleton et al., 2020).

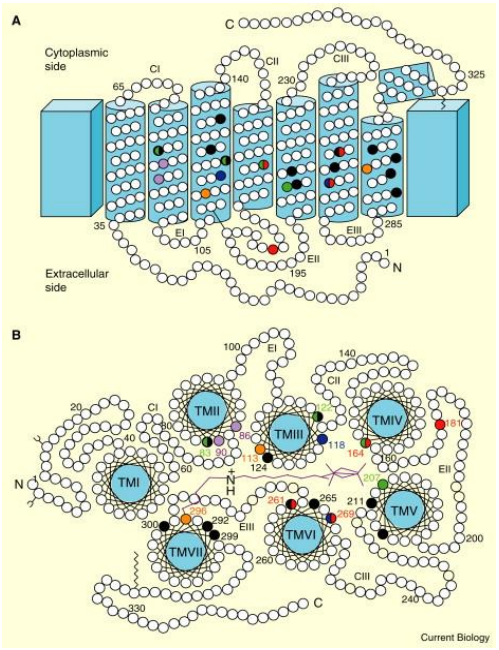

Figure 2: Visual pigment molecule structure. **A.** The seven alpha-helical transmembrane regions. **B.** Arrangement of the amino acid (AA) helices around the vitamin-A chromophore. The respective tuning sites of each individual opsin are displayed in colours: black (*rhodopsin*), violet (*sws1*), blue (*sws1*), green (*rh2*) and red (*lws*), positions of spectral tuning caused by modifications to the amino acid sequence surrounding the chromophore. (modified from Bowmaker and Hunt, 2006)

Classes of photoreceptors:

Vertebrates have as mentioned only one class of rods, the *rhodopsin* (*rh1*). Cones, however, are arranged into four spectrally distinct classes, responsible for the perception of light with different wavelengths (Helvik et al., 2001; Yokoyama, 2000).

These classes are thought to have developed from a single opsin about 450 Mya (Bowmaker & Hunt, 2006). Through a series of processes involving gene duplications, this ancestral opsin functioned as a base gradually developing into the four distinct classes seen in vertebrates today (Bowmaker & Hunt, 2006; Lin et al., 2017; Nathans et al., 1986).

Towards the upper end of the photopic spectrum is the long-to-middle wavelength class (*lws*), sensitive to light in the red-green spectral region (490-570 nm). Next is the middle wavelength class (*rh2*), which is sensitive to light in the green spectral region (480-535 nm). Following is the short wavelength class (*sws2*), which is sensitive to light in the blue-violet spectral region (410-490 nm). Last of the cone opsins, the second short wavelength class (*sws1*), is sensitive to light in the violet-ultraviolet (UV) spectral region (355-440 nm) (Bowmaker & Hunt, 2006). *Rhodopsin* expressed in rod photoreceptors, is sensitive to light in the mid- upper part of the spectral region (447-525 nm) (Carleton et al., 2020). The absorption

ability of opsins is commonly calculated by determining the λmax, which is the wavelength at which the pigment shows maximal absorption of light (Lin et al., 2017). In Atlantic salmon, the λmax of the various opsins is as follows: *Rhodopsin* (515 +/- 5), *sws1* (361 +/- 5), *sws2* (435 +/- 5), *rh2* (518 +/- 4) and *lws* (578 +/- 6) (Cheng et al., 2006).

A study by Lin et al. in 2017 observed 10 functional visual opsins in Atlantic salmon (*rhodopsin, sws1* and *sws2*: 1 paralogue; *rh2*: 4 paralogues; *lws*: 3 paralogues) (Lin et al., 2017), while a more recent study performed by Eilertsen and Helvik revealed that the salmon retina in fact contain 11 visual opsins (*lws:* 4 paralogues instead of 3). These findings are contrary to the former theory based on cloning stating the presence of only five opsins, a belief that was current prior to the publication of the salmon genome. Fig. 3 shows the phylogenetic tree where Eilertsen and Helviks findings are displayed.

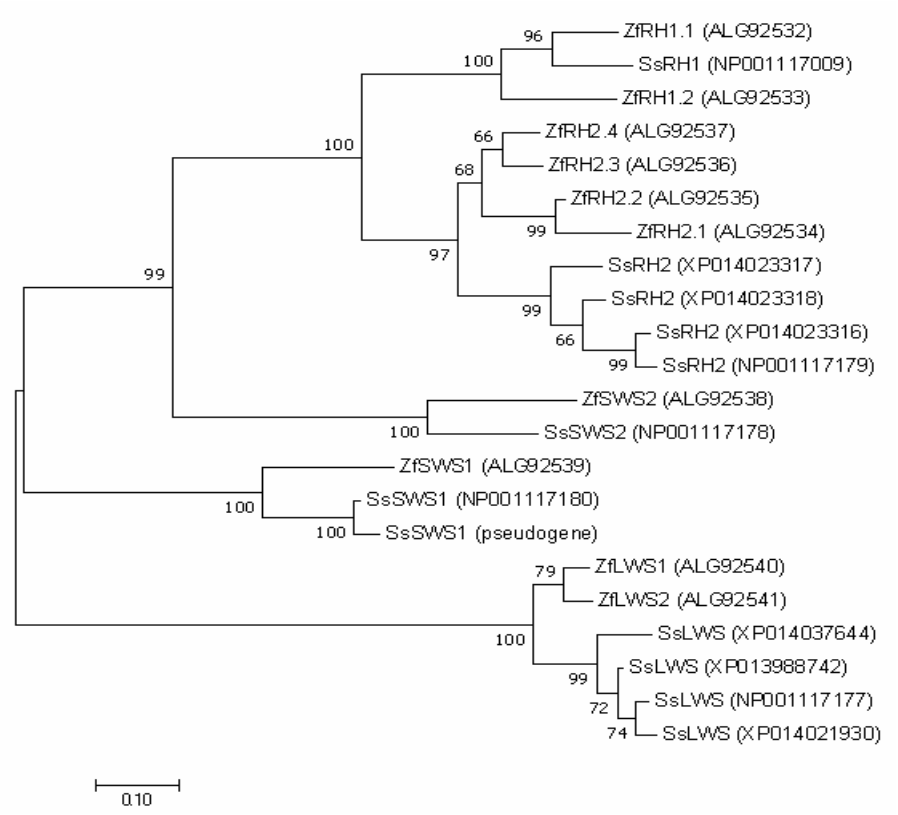

Figure 3: Maximum likelihood tree of the visual opsins in *Atlantic Salmon* (Ss) and *Zebrafish* (Zf) with a bootstrap value of 1000. The accession number (protein) of the opsins are indicated and the NP numbers in salmon are the opsins previously described in the literature by cloning. The salmon genome also contains an additional *sws1*, however this is a pseudogene (Phylogenetic tree provided by Eilertsen et al. (unpublished data)).

1.4. Photoreception in teleosts:

Teleosts, so-called bony fishes, also tend to have the same four classes of cone photoreceptors as other vertebrates, being tetrachromatic species (Bowmaker, 1998). Above water, light is distributed relatively evenly throughout all habitats – if it's on a beach or in the mountains (Cronin & Marshall, 2011). In water, however, the viscosity and concentration of the medium makes for refraction, a bending of light waves as it passes from one medium to the other (Lythgoe, 1988). Additionally, light is either scattered or absorbed by the particles dissolved in the water, interacting with the absorption capability in the medium (Lythgoe, 1988; Wozniak & Dera, 2007). Compared to air, where light passes relatively freely with few obstructions (i.e. clouds) (Ilyas, 1967), and the light intensity is mainly dependent of the time of the day, the intensity drops exponentially in water as the depth increases (Jerlov, 1976; Kirk, 1994; Lythgoe, 1988). Living in a marine habitat, teleosts has had to accommodate this by developing an eye-function adaptable to environmental conditions in constant change, with light being no exception (Carleton et al., 2020). In contrast to other vertebrates, like mammals, teleosts therefore undergo a continuous retinal growth, being able to modify its optical senses and visual acuity as the fish develops (Evans & Fernald, 1990). Compared to mammals, which are released from the mother's womb as well-developed, miniature models of their parents through direct development (Schachtel, 2013), many teleosts undergo an indirect development, being under-developed larvae at hatching (Flegler-Balon, 1989). Hence, a profound transformational metamorphosis is required to develop these species from a larvae and into their adult counterparts (Balon, 1985; Björnsson et al., 2012). Compared to other teleosts strictly following the strategy of indirect development, commonly observed in marine fish like Atlantic cod (*Gadus Morhua)* or Atlantic halibut (*Hippoglossus hippoglossus)*, salmonids differ slightly from these species in their developmental progression, possessing a shorter larval period and having proceeded further in the development at the time of start-feeding (Balon, 1990). Hence, determining whether salmonids follow the direct- or indirect developmental strategy can be difficult.

Research on zebrafish has displayed how the growing and developing retina stretches out, increasing the surface area, while at the same time thinning out the retinal layers. In order to accommodate this retinal growth and maintain optimal sight throughout the whole life-cycle, a regular generation of rod photoreceptors through neurogenesis has been a crucial adaptation (Fadool, 2003).

In deeper waters where light is scarce, species have generally developed a retina mainly consisting of rods, specialized for visual processing in a dark environment. The necessity for cones is reduced as their function of detecting colours no longer is prioritized (Carleton et al., 2020). Research performed on Escolar (*Lepidocybium flavobrunneum*), a large deep-sea living predatory teleost, has shown a retina solely composed of rods (Landgren et al., 2014). However, research performed by Busseroles et al. in 2017 on the *Maurolicus sp.*, commonly called pearlsides; a small, deep-sea fish mostly active during dusk and dawn, close to the surface where the light is intermediate in the twilight or mesopic spectrum, have established the development of another type of opsin – the transmuted cone photoreceptor. This is a specialized cell combining the morphological properties of a rod photoreceptor with a cone opsin and a cone phototransduction cascade, which has proved to be the most evolutionary optimal solution in the environment the pearlsides inhabit (De Busserolles et al., 2017). Although vertical migrations towards deeper waters are performed by recently ocean-migrated smolts in order to avoid predation (Davidsen et al., 2008), Atlantic salmon frequently inhabits the shallow parts of the water column. This is reflected in their eyes, customized to the processing of colours in a habitat where the light intensity is high. As most other vertebrates, all the cone opsins (*lws, rh2, sws1* and *sws2*) are intact. The cone opsins are either single or double - the single being either maximally sensitive to UV or blue light (*sws1* and *sws2*), and the double having two members fused together that is maximally sensitive to green and red light (*rh2* and *lws*) (Deborah L. Stenkamp et al., 1996). Through research the distribution of cone opsins in the salmonid retina has been established, being organized into either row- or square mosaics. The target of this study being juvenile Atlantic salmon, during a period of which the square mosaic is most prominent in the retina (Cheng et al., 2007; Cheng & Novales Flamarique, 2007b; Novales Flamarique, 2018), later discussions regarding this structural topic will be focused towards the square mosaic. The sides of this mosaic consist of four paired cones, either expressing the same opsin (twin cones) (Cheng et al., 2006), or both, where the accessory member of the double cone express *rh2*, and the long member of the double cone express *lws*, while short single cones located centrally express *sws2*, and the accessory corner cone express *sws1* (Cheng & Novales Flamarique, 2007a, 2007b; Veldhoen et al., 2006).

1.5. Topographic distribution of photoreceptors in the retina:

How these photoreceptors and their respective opsins are topographically distributed in the retina is important to establish in order to understand the visual perception of the animal. Opsins are distributed in the retina according to function and requirements in the specific environment the organism experiences (Temple, 2011), which is reflected in a retinal topography facilitating the animal's detection of colours in different directions of their field of vision (Beaudet et al., 1997; Temple, 2011). In relation to the surroundings perceived by the animal, a ventral-dominated photoreceptor distribution facilitates the detection of external cues in the upper parts of the animal's visual field, while a central- and dorsal-dominated photoreceptor distribution promotes visual acuity in front and below the animal, respectively (Ahlbert, 1976; Carleton et al., 2020). The areas of the retina of importance to the visual perception of colours commonly consist of a dense concentration of cone photoreceptors, clearly expressing the visual photopic opsins mentioned (Ahlbert, 1976). How these photoreceptor cells are generated and spatially organized early in the developmental process have been thoroughly studied in a wide range of teleosts. As already mentioned, the retina of species developing post-embryonically expand correspondingly as the animal grows. To accommodate the increasing retinal size, rod photoreceptor cells are continuously added, while the presence of all other retinal cells (cone photoreceptors included) are reduced (P. R. Johns, 1982; Pamela Raymond Johns & Fernald, 1981; Julian et al., 1998; Otteson & Hitchcock, 2003; Deborah L. Stenkamp, 2007). In order to maintain their visual requirements in the growing retina synchronously with the decreasing cell population, cones therefore perform a gradual growth in size, which was measured and observed in an increased diameter (Novales Flamarique & Hawryshyn, 1996). At what period during development these photoreceptor cells (rods and cones) are synthesized and start expressing the different opsins is heavily debated. Studies performed on cyprinid fishes has shown that opsin appearance likely proceeds in one of the following orders: *rhodopsin, lws, rh2, sws1* and then *sws2* (zebrafish) (Raymond et al., 1995) or: *rhodopsin, lws, rh2, sws2* and *sws1* (goldfish (*Carassius auratus*)) (D. L. Stenkamp & Raymond, 1994). In rodents and other mammals, however, the order of opsin appearance is as follows: violet-blue, *rhodopsin,* then followed by green and/or red opsin (Cheng et al., 2007). In salmonids, it was presented by Cheng et al. in 2007 that the appearance of *sws1* and *lws* occurred almost simultaneously (*sws1* slightly preceding *lws),* while *rhodopsin* first was expressed after the first cone opsin. Both *sws2*

(transformed from *sws1)* and *rh2* appeared later in the development (Cheng et al., 2007). What is generally presented as a truth, however, is that neurogenesis of new photoreceptor cells occurs concurrent with the creation of new retina. During the earliest embryonic stages, the embryonic fissure is the main source of neurogenesis (Novales Flamarique & Hawryshyn, 1996), and research has shown that the embryonic fissure continues to provide the retina with photoreceptors in older fish (Kunz, 1987). Later in development, however, the largest proportion of cones are generated and differentiated where the retina meets the iris epithelium, at an area called the ciliary margin (also termed ciliary marginal zone, CMZ) where a circumferential germinal zone (CGZ) is formed. These zones will be mutually termed as CMZ throughout this thesis. Rods, on the other hand, are mainly created by rod precursors located in the ONL throughout the retina (Otteson & Hitchcock, 2003; Deborah L. Stenkamp, 2007). Neurogenesis is the cellular process where new neurons (nerve cells) are generated through asymmetric cell divisions of stem cells. This process results in two daughter cells, one cell replacing the former stem cell, and the second cell (commonly referred to as a progenitor cell) potentially differentiating into photoreceptors (Otteson & Hitchcock, 2003). The topographic patterning of photoreceptors in the retina being an important aspect of this thesis, this topic will be discussed thoroughly in the discussion.

1.6. Alterations to expression patterns in retinal opsins, a natural adaptation in salmonid species:

1.6.1. Migration between habitats:

Most species living in water inhabit the same medium throughout their whole life, it being in fresh water or salt water. In fresh water, the varying degree of available light is commonly regulated by the amount of phytoplankton and dissolved organic materials in the water (Levine & Macnichol Jr, 1982). In salt water, the most prominent cause of diminishing light intensity is increasing depths (Bowmaker & Hunt, 2006; Carleton et al., 2020).

For salmon, living in both fresh water and salt water (either anadromous or catadromous), an adaptation to the habitation of both environments has been necessary. In salmon, this adaptation is most readily apparent through the smoltification process (Hoar, 1988; McCormick et al., 1998).

However, the changing of light regimes from the shallow rivers to the deep oceans, which is demonstrated in Fig. 7 (Levine & Macnichol Jr, 1982), has put focus towards the optical system. Alterations to the eyes on a histological level has proved to be an important

adaptation in salmon, as requirements regarding observation and sensing through vision changes as the salmon migrates from one photic environment completely different from the other (Carleton et al., 2020; Dann et al., 2004).

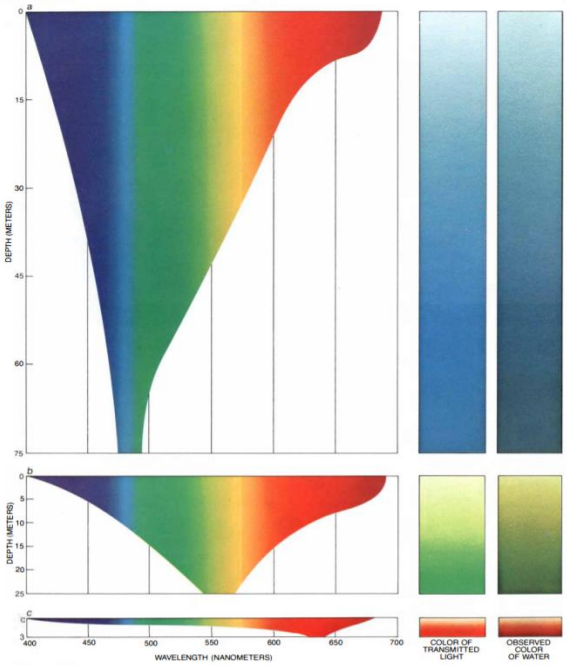

Figure 4: Penetration of light with different wavelengths of the electromagnetic spectrum in the water column. A: Clear lakes and the ocean. B: Fresh water with green organic matter. C: River, swamps and marshes concentrated with plant and animal decay. Columns on the right demonstrate the colour of transmitted light and how it is perceived (modified from Levine and Macnichol Jr, 1982).

1.7. Retinal alterations through different mechanisms:

1.7.1. Loss of corner cones as a consequence of apoptosis:

Studies on salmonids have displayed that they can adapt their vision through modifications in the eyes. One of these adaptations commonly seen in wild salmonid species is the gradual change of expression patterns in opsins, especially to the single cones expressing either UV- or blue opsins. As the salmonid grows and intensifies its adaptation to salt water through smoltification, the ability to absorb light in the ultraviolet spectre is lost, while the ability to absorb light in the blue spectre is increased (Cheng et al., 2006; Cheng & Novales Flamarique, 2007a, 2007b). Previously, it was thought that this transformation was solely caused by apoptosis, a process involving programmed cell death of photoreceptors. The theory was built on the knowledge of opsin composition in square mosaics, hypothesizing that the reduction of sensitivity to UV light prior to the migration into sea water was caused by the

loss of corner cones expressing UV opsins through apoptosis during the smoltification process, initiated by the release of the thyroid hormone precursor, T4 (Kunz et al., 1994). Newer research, however, have raised questions regarding this theory.

1.7.2. Apoptosis and opsin changeover as coherent mechanisms:

Tests performed on several Pacific salmon and Rainbow trout (*Oncorchynchus mykiss*) have proved that single cones (both corner and central) only express UV opsins at hatching – i.e., there are no expression of blue opsins. Hence, it was theorized that the decreased absorption of UV light and increased absorption of blue light as the salmonid grows does not only involve apoptosis, but an additional process called opsin changeover (Cheng et al., 2006). During the alevin period, just before the salmonid has fully absorbed its provided yolk sac, these single corner cones expressing UV opsins are starting to be gradually transformed into cones expressing blue opsins, in good time before the smoltification process is initiated (Cheng et al., 2006). This opsin switch is observed in photoreceptors possessing UV sensitivity at the tip and blue sensitivity at the base of the outer segment. The timing of this transformation seems to depend on the duration of the fresh water residency, with species migrating early (pink- (*Oncorchynchus gorbuscha*) and chum salmon (*Oncorchynchus keta*)) losing their single corner cones at an earlier stage than species migrating later (Chinook- (*Oncorchynchus tshawytscha*) and Coho salmon (*Oncorchynchus kisutch*)) (Cheng et al., 2006). A contrasting and interesting theory about Atlantic salmon presented by the same study, demonstrates the fact that if opsin changeover actually occurs in this species, it would have to commence during embryonic stages, ultimately questioning the process' relation to smoltification (Cheng et al., 2006). With this potentially having a great impact on the expression patterns presented, it will be discussed thoroughly later.

The absorption of the yolk sac results in a surge of thyroid hormones in the blood, a natural process influencing the initiation of the transformational process in single cones. Research has also proved that salmonids reared in water treated with T4 has its opsin changeover process prematurely induced (Cheng et al., 2009). In order for this exogenous treatment with T4 to have any effect, however, exposure has to occur prior to the naturally induced opsin switch (Cheng et al., 2009; Novales Flamarique, 2013). Hence, Kunz et al. (1994) were right in their observance of T4 having an important role in the loss of UV sensitivity, but were wrong in determining which process it influenced. Additionally, the study by Novales Flamarique in 2013 demonstrated a previously unknown consequence of growth hormone (GH), potentially accelerating the opsin changeover process in transgenic rainbow trout where this hormone

was overexpressed (Novales Flamarique, 2013). The transformation of the corner cone opsins proceeds until photoreceptors expressing UV opsins are restricted to a few cells in the dorsotemporal region as a young smolt, and only slightly observable in certain areas in the retina of adult salmonids (Cheng et al., 2006; Cheng & Novales Flamarique, 2007a; Novales Flamarique, 2013). The reasoning behind this transformation is debatable.

1.7.3. External cues facilitating transformation in opsins:

The importance of UV opsins in a wide range of vertebrate species have long been debated, potentially having an influence in foraging, mate selection, communication and/or orientation (Novales Flamarique, 2013). In salmonids, UV sensitivity have long been thought to be related to foraging and detection of prey in a habitat with shallow and shiny water, by improving the contrast enhancement of zooplankton (Novales Flamarique & Hawryshyn, 1994). However, a study performed in 2006 on several salmonid species proposed that the ability to absorb light in the ultraviolet part of the spectrum was lost during a period of which zooplankton is the only source of nutrients. Losing the ability and advantage of detecting prey which is critical for the survival of the salmonid would be counterproductive, so questions were raised against the theory that opsin changeover primarily is an adaptation mediated by dynamic foraging patterns (Cheng et al., 2006). Further, by investigating zooplankton on different spectral backgrounds, it was established by the same study that contrast in the blue wavelength was similar or even better than in the UV wavelength (Cheng et al., 2006). A newer study performed by Novales Flamarique on Rainbow trout in 2013, however, presented findings that backed up Novales Flamarique and Hawryshyns theories published in 1994, revealing how fish treated with thyroid hormone initiating the *sws1-sws2* opsin switch, had their foraging performance on their natural prey, the zooplankton *Daphnia magna*, considerably reduced by up to 20 % (Novales Flamarique, 2013). Hence, the reduced ability to perceive the contrast of zooplankton following thyroid treatment indicates that the following loss of UV sensitivity affects the salmonid negatively in their search for prey (Novales Flamarique, 2013). Additionally, UV sensitivity have been theorized to be an important factor in the orientation of the salmonid, with its function being related to the detection of celestial polarization signals (Hawryshyn et al., 1990). However, since *sws1* is either lost (Kunz et al., 1994) or solely restricted to the dorsal retina in juvenile salmon (Cheng et al., 2006; Cheng & Novales Flamarique, 2007a), this orientational-related role is also questioned. These findings have put forth a new theory about the role of UV opsins, linking it to being an important factor regarding the distribution of the retina, necessary for

the chromatic organization (Cheng et al., 2006). Three facts that increase the credibility of this theory are:

1. UV opsins are early expressed during retinal development.
2. UV opsins are restricted to single cones forming a regular mosaic pattern.
3. The reduction of UV sensitivity facilitated by the loss of UV opsins materialize as the salmonid gradually becomes more active.

Hence, the role of UV opsins as the salmonid develops into a more dynamic, full-grown specimen, is questionable (Cheng et al., 2006). As demonstrated, there are many studies performed on the UV opsin, *sws1,* and the reasoning behind the observed downregulatory mechanism. In addition, there are proposed theories emphasizing the importance of the upregulation of the blue opsin, *sws2.* As was the case in the regulation of *sws1,* the increased presence of *sws2* seems to be related to prey search (Novales Flamarique, 2013). In addition to the greater depths experienced in the oceans, where the exposure to photons in the UV part of the spectrum is greatly reduced or absent (i.e. requirement for UV sensitivity reduced) (Lin et al., 2017), the detection of larger, opaque prey is dependent on increased ability to absorb light in the blue part of the spectrum (Novales Flamarique, 2013). From these presented theories explaining the switch in opsin expression through opsin changeover, a process occurring naturally in salmonids when preparing for a life in another habitat, the natural relevance of this retinal alteration is evident.

1.7.4. Amino acid (AA) substitution and positive selection:

Through history, a process commonly known as amino acid (AA) substitution has been established as an important factor in the development of the visual opsins seen in salmon and other fishes (Carleton et al., 2020). Following gene duplications, which is the creation of two identical copies of the same gene, mutations to nucleotide sequences leading to AA substitutions has been able to spectrally tune one of the copied genes, gradually transforming it into a new one. From a basis of a single, prehistoric opsin, these mutations have through evolution resulted in the 5 renowned opsins (Carleton et al., 2020; Yokoyama, 2000). Following this knowledge, another study performed by Dann et al. in 2004 displayed a modification of these AA substitutions in a process called positive selection. This is an occurrence of non-synonymous nucleotide substitutions happening more often than synonymous nucleotide substitutions ($dN > dS$), a process that has provided fish with the ability to modify their opsins by making small shifts in λmax as a consequence of amino acid (AA) substitutions on positions surrounding the chromophore (Dann et al., 2004). This is

especially widespread in species living in deeper waters, but has also been proved to be prominent in several species of Pacific salmon in addition to Atlantic salmon (Dann et al., 2004).

What was also discussed in the same study, and analysed further in a study by Temple et al. from 2006, is the utilization of a combination of the two chromophore types A1 and A2 throughout the retina, with an opsin conjugated to a A1 chromophore having a λmax which is lower than that of an opsin conjugated to a A2 chromophore (Temple et al., 2006). This has presented another opportunity of spectrally tuning the ability to observe through vision. Depending on the habitat of which the fish inhabits and the photic conditions in the current environment, this process represents the possibility of shifting the A1/A2 chromophore ratio towards what is preferred (Carleton et al., 2020; Temple et al., 2006). The reasoning behind the development of this method of improving the opsins potential for absorption is debated, and three theories are demonstrated in the article:

1. Migration/metamorphosis: Spectral tuning due to the migration from one photic environment into another, commonly coinciding with the smoltification process.
2. Seasonal: A spectral tuning based on the changing photic conditions throughout the year.
3. A combination of the two.

With the focus of the research being on Coho salmon, a shift towards an A1-dominated retina in +1 parr (> 12 months old) was displayed, coincident with the thought that these shifts is a result of the migration into the oceans. However, the same shift was observed in landlocked 0+ parr (< 12 months old), challenging the migrational/metamorphosis-based theory and raising questions regarding this hypothesis. Hence, what was presented as the main hypothesis by Temple et al., and a more likely explanation to the observed spectral shift, is that the salmon's reaction to changing light conditions is following a cyclical, seasonal pattern, with an increased ability to absorb light with higher wavelengths during the winter (A2 chromophore dominant) and lower wavelengths during the summer (A1 chromophore dominant) (Dann et al., 2004; Novales Flamarique, 2005; Temple et al., 2006). This seasonal theory was further substantiated by another study performed by Temple et al. in 2008, where it was shown that the rod photoreceptors displayed minimal shifts in mean λmax in alevins, parr and ocean smolt of Coho salmon that was measured at the same time of the year (Temple et al., 2008). Additionally, the fact that this seasonal shift in A1/A2 ratio is found in a diverse range of species (Carleton et al., 2020) builds additional support to this hypothesis, while at the same time increasingly disproving the migrational/metamorphosis hypothesis, a theory that was more established in the past (Crescitelli, 1958).

1.8. Expression patters in Salmon reared under controlled conditions:

During the past few centuries, the productivity of aquaculture has increased tremendously. In Norway, the intensively driven aquaculture on Atlantic salmon has been one of the most prominent industries, producing large quantities of high-quality fish either consumed locally or exported abroad, generating income crucial for the Norwegian economy (Xiaowei & Junning, 2018). In previous years prior to the exponential growth of aquaculture, fish sold on the market primarily came from fisheries, where fish developed and were caught in their natural habitat (Nash, 2010). As aquaculture expanded and became increasingly intensified, the environmental conditions which previously were exposed to the fish in natural fashion, could now be manipulated by the producers. Environmental factors like light, temperature, feeding regimes etc., are controlled during every stage of the salmon's life cycle, streamlining the production even further (Oppedal et al., 2011). Well known examples from the aquaculture industry where environmental conditions are utilized for the benefit of the producer are many:

The timing of smoltification can be manipulated, producing either +0 or +1 smolt (Duncan et al., 1998; Duncan & Bromage, 1998; Thrush et al., 1994); the somatic growth can be accelerated, reducing the time it takes before the fish is harvested (Hansen et al., 1992; Maiolo et al., 2015; Oppedal et al., 2011; Strand et al., 2018); and sexual maturation can be prevented (Hansen et al., 1992; Oppedal et al., 2003; Stefansson et al., 1991; Taranger et al., 1999).

These are all procedures that are well known in aquaculture for its importance in the matter of production, where light functions as the primary factor in regulating salmon development.

In this thesis, we wish to build further on the knowledge studies on photoreception in salmon has provided by investigating the retinal development during the smoltification process, and how the expression patterns of photoreceptors are altered throughout this period. As previously mentioned, similarly to other organisms living in water, salmon undergo continuous changes to the retinal function and formation during its life-cycle in their natural habitat, especially in order to accommodate the downward migration into the oceans (Carleton et al., 2020; Cheng et al., 2006, 2007; Cheng & Novales Flamarique, 2007a, 2007b). Hence, the purpose of this project is:

Objectives:

To characterize the expression pattern of visual opsins classes and topographic distribution of visual photoreceptors in the retina of Atlantic salmon (*Salmo salar L.*) through smoltification.

Hypothesis:

1. Exposing Atlantic salmon parr to a winter signal by light treatment will induce smoltification.

2. In general, the topographic profile of visual opsins in Atlantic salmon is different in the various cone opsin classes.

3. The topographic pattern of *rhodopsin* is different from cone opsins.

4. During retinal transformation the topographic patterns of visual opsins classes change.

5. The appearance of visual opsins in ciliary marginal zone is reflected in the retinal transformation.

2. Methods:

2.1. Setup of experiment:

This master thesis is conducted as a part of the project "The effect of narrow banded LED light on development and growth performance" (Project No. 254894) financed by the Research Council of Norway. I joined the project in January 2018 when the fish described in this thesis had reached the parr stage.
Eggs and sperm used in the experiment (from one female and one male) were provided by Marine Harvest Tveitervågen, Askøy. Eggs were fertilized at October 19th 2017 and reared in egg-incubators with a temperature of approximately 6 °C until start-feeding were initiated at February 19th 2018, from which the fish were kept in 3 separate tanks of approximately 60 cm (diameter) with a temperature that was increased and kept stable at approximately 11 °C. From this point, the feed provided by Bjørsvik, Lerøy were given to the fish with a gradually increasing size; starting at 0.5 mm at February 19th 2018, further increasing to 1.0 mm at April 15th, 1.5 mm at June 10th and 2.0 mm at November 14th. The fish were kept in these tanks until the transfer into sea water. At this point, a salt water tolerance test was performed on the fish to establish that they were fully smoltified and able to handle the changed conditions accordingly, before they were moved into corresponding tanks with salt water for further rearing. At March 25th, 2019, all the fish had been moved into the 3 sea water tanks, where they were kept under a temperature of 11 °C for approximately 5 weeks until the last sampling at April 29th.

2.2. Light exposure:

The project was performed with multiple light stimulations, but the fish used for analyses in this thesis were from fertilization until start-feeding exposed to Philips warm white 2700 K LDw (14:10) with a light-intensity of 0,1 W/m^2. At the end of July 2018, these lights broke, and were replaced by the light tubes already present in the room, GE Starcoat T5 Long Last 1449mm Fluorescent Tube 49W, 3000K Warm white (General Electric), exposed to the fish all the way through the smoltification process. At start-feeding, the larvae were placed in 3 different tanks and they were all exposed to an LD of (20:4) with an intensity of 1 W/m^2 from start feeding to 11.12.18 when the "winter signal" was turned on, by changing the light period

to 12:12 for 6 weeks. After the winter signal stimulation for 6 weeks, a gradual change to continuous light was initiated (light was dimmed up and down (30 min) to 18:6 (17.15 hours full light, 5.45 hours full dark)), a procedure followed to acclimatize the fish. At 27.01.19, the light was changed to continuous light (24:0) to induce smoltification.

2.3. Sampling:

Four samplings were done in this experiment (Fig. 5):
1st Sampling: After 6 weeks of winter signal ((22.01.19) (SS01/19) (4280 day-degrees (dd))) just prior to turning the light back to 24:0.
2nd Sampling: Approx. 3 weeks after turning on the continuous light ((12.02.19) (SS02/19) (4515 dd)).
3rd Sampling: Approx. 7 weeks after turning on the continuous light ((12.03.19) (SS03/19) (4835 dd)).
4th Sampling: Approx. 5 weeks after the transfer into sea water, 14 weeks after turning on the continuous light ((29.04.19) (SS04/19) (5370 dd)).

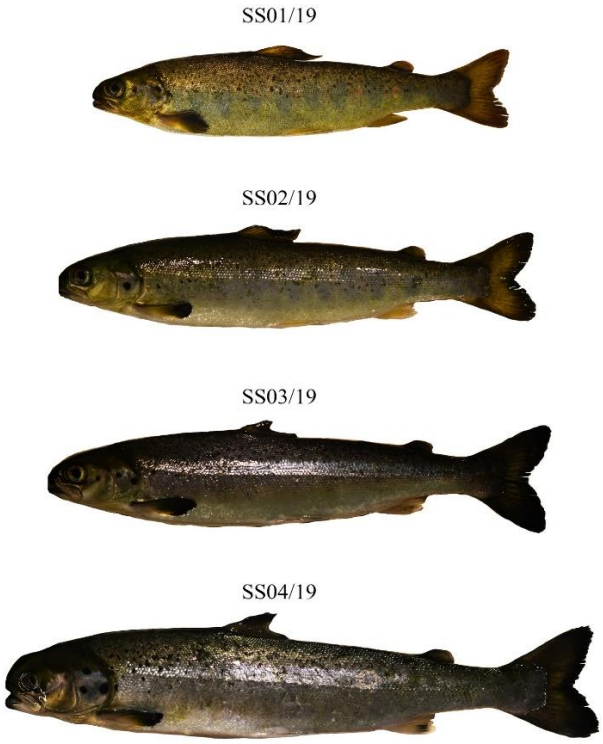

Figure 5: Morphological changes occurring as the Atlantic salmon develops through the smoltification process, represented by 4 stages (SS01/19 (parr), SS02/19 (mid-smolt), SS03/19 (smolt) and SS04/19 (1 month in sea water)).

Procedures:

In order to avoid generating biased results through manual selection of fish for further analysis, the 6 fish selected for tissue analysis were randomly chosen by randomizer.org from 1 of the 3 tanks.
The salmon were placed in a bucket with a lethal dose of MS222 (Cat. No 140729).
Following are the procedures performed on the salmon, in order:

1. Each fish was measured – weight and length were calculated.
2. Blood samples were collected from the fish.
3. Muscle samples were collected from the fish.
4. Gill samples were collected from the fish.
5. Eye samples were collected from the fish.
6. Brain samples were collected from the fish.
7. Sex and maturation status was established (there were no signs of early maturation in the individuals sampled).

For this thesis, the eye-dissection is of highest importance, and procedures followed are explained below:

Day 1:

First, the eyes were dissected from the fish using a small scissor. The left eye was placed in a cryo-tube directly moved to liquid nitrogen (stored at -80°C), and the right eye (punctured by a needle) was placed in falcon-tubes, fixated in 4% PF at 4°C for 48 hours.

Day 2:

The 4% PF used as a fixative on the right eyes in falcon-tubes were firstly washed in 1x PBS. Next, the eyes were placed in petri-dishes inside a fume hood, where a small scissor was used to clip a small hole in the lens. Then, the eyes were incubated in sucrose/Tissue-tek OCT compound (Cat. No 4583, Sakura) overnight at 4°C.

Day 3:

10 mL of sucrose/Tissue-tek was pipetted out of the falcon-tubes for the eyes to be stored in a more concentrated solution for 1 hour. Eyes were then placed in petri-dishes before they were moved to 2 mL Eppendorf tubes. The Eppendorf tubes with eyes were filled with sucrose/Tissue-tek using a pipette, before they were moved to be stored at -80 °C.

2.4. Moulding of the eye:

First, the eyes used in the procedure were gathered from -80°C to be thawed before moulding. Inside the fume hood, the thawed eyes embedded in sucrose/Tissue-tek were moved onto petri dishes. To remove excessive fat-tissue from the eyes, two tweezers (one coarse and one fine) were used. After this, the fine tweezer and a small scissor were carefully utilized to make a small cross into the cornea, creating a hole. Through this hole the lens was extracted by using the coarse tweezer to pinch on the eye from above, while the fine tweezer was pushed down on the cornea. This procedure is followed carefully, as any injuries to the eye needs to be prevented.
To make the eye look more complete and presentable, a syringe was used to fill the open hole with Tissue-tek. Further, the embryonic fissure was located by looking for a dark line in the least pigmented area of the eye. The eye was then oriented with the embryonic fissure facing towards the person performing the procedure, with the posterior side facing left and the anterior side facing right.
The fine tweezer was then used to pinch the eye on the left (posterior side), lifting it up, before placing it in a tube (upper section of a 15 ml falcon tube) on a sample glass, filled with Tissue-tek (halfway up the tube). The eye was held in place by the tweezer, orienting it with the embryonic fissure facing towards the black line, the anterior side facing down into the tube, and the posterior side facing up. To mould the eye in place, the sample glass was placed on a flat “rock” pre-frozen in liquid nitrogen. As the Tissue-tek started to freeze, slowly building a foundation for the eye, Tissue-tek was filled to the top of the tube. To know the orientation of the eye, a black line was drawn onto the Tissue-tek. The knob was then wrapped in biofilm and aluminium, before it was frozen and stored at -20 °C.

2.5. Sectioning of the eye:

The eye to be sectioned was moved from storage at -20°C and into the LEICA CM3050 S cryostat. To build a foundation for the knob, Tissue-tek was added in a circle to the disc, before the knob was attached to the disc as straight as possible. The knob was then placed onto the machine and the orientation-settings adjusted, with the black line representing the embryonic fissure facing downwards, readying the knob for sectioning.
The settings of the machine was then adjusted for the current sectioning, mainly adjusting the section-thickness to 10 μm. To initiate the procedure, sections were tossed until the first eye-tissue in the Tissue-tek was reached. At this point, tissue samples were gathered and attached to each of the five object glasses (Superfrost Plus; Menzel, Braunschweig, Germany), which were pre-frozen in the cryostat. After this, 15 sections were tossed – i.e., 5 tissues gathered -> 15 tissues tossed -> 5 tissues gathered -> 15 tissues tossed, etc. This procedure was followed in order to gather tissue from all the sections of the eye without it exceeding a certain number of tissue-samples. When the five object glasses were filled with samples, they were placed to dry in room temperature for approximately 30 minutes. The gathering of tissue proceeded until the eye was fully depleted, with object glasses containing tissue-samples from every section of the eye in an anterior-to-posterior axis. After the eyes had dried completely, they were moved into the oven to be baked at 65°C for a minimum of 30 minutes. This step is important, as it will secure the attachment of tissue to the object glass in the *In Situ* hybridization (ISH)-process to follow. Following the baking, the object glasses were placed in labelled boxes and put in -20°C for storage.

2.6. PCR:

The PCR was performed according to the Advantage 2 PCR kit (Takara) in order to generate template for the RNA to attach to during the RNA probe synthesis of the visual opsins (*rhodopsin, lws, sws1, sws2* and *rh2*) present in this study, required for *In Situ* Hybridization. The templates utilized in the PCR procedure are plasmids with inserts generated through molecular cloning, created in the lab. The synthesis of the *rh2* opsin used all 4 paralogues presented in table 2 as template, due to an identity of above 86% when two and two paralogues were aligned, generating a probe mix of all the paralogues. In the synthesis of the *lws* opsin, all 4 paralogues showed an identity of above 87%, but only the two paralogues

presented in table 2 were used as template. However, the probe created hybridized to the remaining two paralogues of *lws* not used in the PCR (XM_014182169 and XM_014133267), as the similarity of these paralogues with the individual PCR-probes were above 90%.

Advantage 2 buffer (10x) (Cat. No S1799, Clonetech)	5,0 µl
dNTP (10 µM)	1,0 µl
T3_Ss_gene_of_interestF1 (10 µM)	1,5 µl
T7_Ss_gene_of_interestR1 (10 µM)	1,5 µl
Template (1:10) (20 ng)	2,0 µl
Advantage 2 Polymerase (50x)	1,0 µl
Nuclease free water to 50 µl	38 µl

PCR conditions:

1. 95 °C for 3 minutes
2. 95 °C for 30 seconds
3. 55 °C for 30 seconds
4. 68 °C for 1 minute and 30 sec
5. Go to step 2 34 times
6. 68 °C for 10 minutes
7. 4 °C forever

Table 1: Sequence information, primers utilized and length of probes used for the various opsins (Ssrhodopsin, SsSWS1, SsSWS2, SsRH2 and SsLWS).

Gene	Primer	Sequence	Probe length (bp)
Ssrhodopsin (NM_001123537)	T3SsrhodF1	CATTAACCCTCACTAAAGGGAAGCCGGAACACCATCTGAAGAAG	1159
	T7SsrhodR1	TAATACGACTCACTATAGGGTTCTTTGTGGACGCTGGATCG	
SsSWS1 (NM_001123708)	T3SsSWS1F1	CATTAACCCTCACTAAAGGGAAGGAAGATCCGCAGAAGAAGC	1182
	T7SsSWS1R1	TAATACGACTCACTATAGGGGCTCCTGATGGACTGAGACC	
SsSWS2 (NM_001123706)	T3SsSWS2F1	CATTAACCCTCACTAAAGGGAACATGCGATCAACCTTCGAGC	1231
	T7SsSWS2R2	TAATACGACTCACTATAGGGGAGATGCCCTCTTTAACCAGC	
SsRH2 (NM_001123707, XM_014167841, XM_014167842, XM_014167843)	T3SsRH2allF1	CATTAACCCTCACTAAAGGGAACAACTTCTACATTCCCATGTCC	999
	T7SsRH2allR1	TAATACGACTCACTATAGGGGACACTTCTGTCTTGCTTGTTG	
	T3SsLWSF3	CATTAACCCTCACTAAAGGGAACAGAAATGGCAGAGGTTTGG	1079

SsLWS (NM_001123705, XM_014166455)	T7SsLWS_allR1	TAATACGACTCACTATAGGGTTATGCGGGTGTCACAGAGG	

2.7. Rinsing of PCR product:

- The AmiconR Ultra-0.5 (Cat. No UF505096, Sigma-Aldrich) device was inserted into microcentrifuge tubes.
- Ultra-Pure water was added to 450 µl PCR product to a total volume of 500 µl, and the RNA was added to the Amicon® Ultra filter device. It was then centrifuged at 14,000×g for 20 minutes. The filter had to be dry after centrifugation.
- The Microcon column was turned upside down into a new microcentrifuge tube, before it was spun for 2 minutes at 1000×g at room temperature.
- The rinsed PCR product was stored at -20 °C.
- 1 µl of the PCR product was then analyzed on a 1% agarose gel (1xTAE).
- The concentration of the rinsed PCR product was measured on the NanoDrop OneC (Thermo fisher Scientific).

2.8. Agarose gel electrophoresis:

(The PCR was extracted using the QIAEX II Gel Extraction Kit (Qiagen, Germany))

The 1% agarose gel was made by mixing 0.5g of Seakem LE agarose (Cat. No 50004) and 50 mL 1x TAE, before it was heated for 2 minutes using a microwave oven. The solution was then cooled until it reached approximately 40 °C. 5 µl of "Gel-red" was added to the solution, and the 1% agarose gel was poured into the container in the machine and was left to polymerize for 30 minutes.
When the gel had polymerized, 1x TAE was added to the container until it reached a point just above the agarose gel. Of the 6 wells in the gel, 1 was filled with ladder mix, and the next 5 was filled with freshly made PCR-product (4 µl Ultra-Pure water, 1 µl PCR-product and 1 µl loading dye). Prior to starting the electrophoresis, the machine's settings was adjusted (mainly the voltage to 80V), before the process was run for 40 minutes. After this, a picture was taken of the gel in the G-Box GeneSnap (Syngene).

2.9. RNA probe synthesis:

The RNA probe synthesis was performed in order to create the specific probes for each of the 5 opsins investigated in the study.

Template (50 ng/µl)	3,0 µl
10xTranscriptionsbuffer	0,5 µl
DTT (0,1M)	0,5 µl
DIG-RNA labeling mix (10x)	0,5 µl
RNAsein (40 U/µl)	0,25 µl
T3 or T7 polymerase (20 U/µl)	0,25 µl

- RNA synthesis was done by running the PCR machine for 3-4 hours at 37 °C.
- The tubes were kept on ice following this procedure.
- The reaction was stopped by adding 0,5 ul sterile 0.5 M EDTA and 4,5 ul sterile water to each tube.
- 1/20 of the probe reaction (1 µl probe reaction and 19 µl Ultra-Pure water) was analyzed on 1% agarose gel (1x TAE). The RNA was denatured prior to the Agarose gel electrophoresis by placing it at 95 °C for 3 minutes in the PCR machine before directly putting it on ice.

2.10. tRNA precipitation:

- 0,9 µl 4 M LiCl (ice cool), 2,2 µl 4,2 µg/µl tRNA and 27 µl 100 EtOH (ice cool) was added to each probe reaction.
- The solutions were vortexed and put on -20 °C for at least 30 minutes.
- It was then centrifuged at 13.2 x1000 rpm at 4 °C for 20 minutes.
- The pellet was washed in 200 µl 70% EtOH.
- The pellet was then air dried for a certain period.
- 20 µl nuclease free water was used to dissolve the pellet.
- The probe was stored at -80 °C.

2.11. *In situ* hybridization (ISH):

(ISH on cryosections of the retina will be performed according to protocols described in Sandbakken et al., 2012 and Eilertsen et al., 2014.)
Pre-sectioned eye tissue on object glasses stored at -20°C was used in this procedure. Each ISH-procedure was performed on two eyes, analysing 3 eyes from each of the 4 sampling periods (SS01/19, SS02/19, SS03/19 and SS04/19).

Day 1:

(In order to prevent the degradation of mRNA, it is very important to avoid the interaction of RNase with the tissue during day 1. Hence, gloves were required throughout the whole process, and all the buffers and solutions used during day 1 was made with DEPC-water – water treated with Diethylpyrocarbonate (DEPC) – to make it RNase free.)

Tissue pre-treatment:
(All washing steps explained below were performed in room temperature.)
The object glasses were placed in glass cuvettes, before they were rehydrated with the introduction to ethanol in DEPC, being washed for 1 minute in each of 95%-, 70%- and 50%-ethanol, respectively. This gradual implementation of decreasing ethanol-concentrations was performed to prevent the tissue from bursting during the rehydration. The tissue was then washed in 2x SSC for 1 minute, in order to increase the stringency and prevent unspecific binding.
Next, a treatment with the protein-degradative Proteinase K (10µg/ml) of the tissue for 4 minutes would stop the enzyme activity and increase the permeability of the tissue.
Then, to maintain the permeabilitized state provided by the proteinase K, the tissue was post-fixated in 4% PF (paraformaldehyde) for 5 minutes. The tissue was further washed in 1xPBS for 2x2 minutes.
The tissue was then embedded in 0.1 M Triethanolamine (TEA) pH 8.0 for 3 minutes, before being introduced to acetic anhydride (0.25% acetic anhydride in 0.1 M TEA, pH 8.0) for 10 minutes. These two washing steps were performed to reduce the background staining caused by the phosphatase activity in the tissue. Both these solutions were freshly made just prior to the ISH-experiment.

Next, the tissue was washed in 2x SSC for 1 minute, before being gradually introduced to increasing concentrations of ethanol, 50%, 70%, 95% and 100% x2, respectively, for 1 minute each. All washing steps explained above were performed in room temperature.
The tissue was then left on an aluminium plate for 1 hour to dry. During this stage, a hydrophobic frame was made around the tissue on the object glasses with a PAP pen.

Hybridization with RNA probe:

The hybridization solution with the probe (hyb+) to be added to the tissue firstly had to be prepared by preheating the hybridization solution without the probe (hyb-) in eppendorf tubes at 65°C. The RNA probe (antisense) added to DEPC water was boiled for 5 minutes to stretch out the supercoiled state, and directly moved into ice to prevent the tissue from re-coiling. The RNA probe solution was then added to the correct hyb- Eppendorf tubes (labelled according to the genes present in the study (*rhodopsin, lws, sws1, sws2* and *rh2*)) – creating the hyb+. 120 µl of hyb+ (now in 5 different Eppendorf tubes representing the 5 genes mentioned) was now pipetted onto the respective object glasses (hyb+ (*rhod*) -> object glass (*rhod*), hyb+ (*lws*) -> object glass (*lws*), etc.), before Hybri-Slips were added to prevent evaporation.
The object glasses were placed in boxes and incubated with paper embedded in 2xSSC overnight at 65°C.

Day 2:

Post hybridization treatment:

(All solutions used in the steps performed under higher temperatures (37°C or 65°C) were preheated in advance.)

Excessive RNA probe and the Hybri-Slips were flushed away by using a pipette, before the tissue was embedded in 2xSSC for 2x 30 minutes. After this, the tissue was treated with 50 % deionized formamide in 2xSSC for 30 minutes in 65°C to increase the stringency and further remove the RNA probe. Then, the tissue was washed in 2xSSC for 2x 10 minutes, before it was treated with 0.02 mg/ml RNase A for 20 minutes on 37°C. This is done to reduce the unspecific staining by removing unbound probe. To remove and inactive RNase, the tissue was washed in RNase buffer for 20 minutes at 65°C.

Immunohistochemical detection:

The tissue was left in 2xSSC, 0.05% Triton X-100, 2% Blocking reagent for 2-3 hours, before it was washed in 1x maleate buffer for 2x 5 minutes. 120 µl of freshly made antibody solution with Anti dioxigenin-alcaline phosphatase FAB-fragment (1:2000) was then added to the object glasses, and incubated over-night at room temperature in boxes with paper embedded in dH_2O.

Day 3:

Visualization:

Excessive antibody solution was quickly dried off, before the object glasses were washed in 1x maleate buffer for 2x 10 minutes. The sections were then washed in visualization buffer for 10 minutes, before 200 µl of freshly made chromagen substrate (NBT/BCIP) was added to cover wells which the object glasses are placed upon – a process that initiates the visualization reaction. As the chromagen substrate is sensitive to light, the falcon tube containing the solution was wrapped in aluminium foil, and the object glasses were quickly placed into sealed boxes for incubation.

After this follows a period of observation, where the object glasses were regularly checked under a microscope for staining. An important note during this period, is that the 5 genes investigated in this study ranges significantly regarding the time it takes before the staining becomes visible. When the staining became apparent, and the background staining was still low, the cover wells were removed, and the visualization reaction was stopped by embedding the tissue into a stop buffer. Because of the high pH of the stop buffer, the alkaline phosphatase was inhibited, and the staining was stopped.

In the end, the object glasses were mounted with 70% glycerol and covered with cover glasses, before they were sealed with a nail polish and stored in boxes at -20°C.

2.12. Figure preparations of ISH-sections:

(The steps explained below are important in order to make the sections prepared in the ISH-process presentable for the thesis. The “best” eye out of the 3 eyes from each sampling that went through an ISH-process (Anti-Sense probe), in addition to 1 eye from the 1st sampling that was treated with the Sense probe, was selected for further processing – 5 eyes in total.)

First, the object glasses were cleaned thoroughly with 70% EtOH, removing any excessive 70% glycerol or nail polish covering the sections. Then, the sections were scanned in the Axio Scan.Z1 (Zeiss), a process enhancing the quality of the sections, revealing the necessary details.
The selected sections most optimally visualizing the investigated gene's expression patterns were further edited into figures using photoshop, with each figure representing the results for every gene as the salmon developed. The figures were presented in a "4x4" manner, vertically displaying one eye from each of the 4 sampling points, and horizontally displaying different parts of the retina (central, dorsal and ventral), with each picture being separated by a margin of 10 mm. Table 3 in the appendix shows the settings utilized to create the 5 figures mentioned, where the size of the eyes for each gene were adjusted according to the eye from the first sampling. Hence, an example of the sizes displayed for each of the last 3 eyes for each gene is as follows: "16 (eye-number), 101% (size of the current eye compared to the first as they were imported)". Additionally, the results displayed in Fig. 16 demonstrating the negative control using a sense probe, was also edited in photoshop.
The schematic visualization of expression in photoreceptors displayed in Fig. 15, and the anterior-to-posterior axis of expression displayed in Fig. 17, was drawn in Incscape, before the figures were finalized in photoshop.

2.13. Na+/K+-ATPase activity test:

The NKA activity in the gills was measured in a Spark multimode microplate reader (Tecan, Mannedorf, Switzerland) under strict temperature control (25 °C) according to the microassay method of McCormick, 1993 (McCormick, 1993).

An assay mixture (AM: 5.0 U/ml Pyruvate Kinase (PK) and 4.0 U/ml Lactic Dehydrogenase (LDH), 2.8 mM phosphenylpyruvate (PEP), 0.22 mM β-Nicotinamide Adenine Dinucleotide (NADH), 0.7 mM Adenosine Triphosphate (ATP) and 50 mM immidazole) without (AM) and with (AM-O) 0.5 mM Oubain (ATPase enzyme inhibitor) was prepared. The assay medium was completed by adding salt solution in order to achieve the final concentrations of 50 mM immidazole, 189 mM NaCl, 10.5 mM $MgCl_2$ and 42 mM KCl in both the AM and AM-O mixtures. Prior to analyzing the samples, the AM solution was quality assessed by running a 10 µl triplicate standard curve from 0 to 20 nmol ADP per well using the slope of the

endpoint. The standard curve in the kinetic reading should be within 17-19 mOD nmole ADP per well.

Protein:

Protein concentrations in the samples were determined using the Pierce BCA Protein Assay kit (Thermo fisher Scientific, Massachusetts, USA). 200 µl of reagents (50 parts A:1 part B) from the Pierce BCA Protein Assay kit (Thermo fisher Scientific, Massachusetts, USA) were added to each triplicate sample and covered with parafilm, shaken for 30 seconds and incubated for 30 min at 37 °C in an INCU-Line digital incubator (IKA, Staufen, Germany). After having cooled for 2-3 min, the absorbance was measured in the Spark multimode microplate reader at 562 nm. The final enzyme activity was then calculated as follows:

$$\frac{\text{nmoles ADP/10µl/min}}{\text{µg/10µl protein}} = \text{ µmoles ADP/mg protein/min}$$

$$(\text{µmoles ADP/mg/min})(60\text{ min}) = \text{µmoles ADP/mg protein/hour}$$

The NKA enzyme activity is reported as µmoles ADP per mg protein per hour.

2.14. Statistical analysis:

All statistical analyses were performed using Prism GraphPad software v. 8 (San Diego, California, USA). Normality of distributions was tested using the Shapiro-Wilk W-test. A one-way Analysis of Variance (ANOVA) was performed to determine changes over time (weight, length, condition factor (CF) and gill NKA activity). When the ANOVA null-hypothesis of equal means was rejected, Tukey's HSD post-hoc test was used to identify differences. Data are presented as means +/- standard error of mean (SEM), and results were considered significant when $p<0,05$.

3. Results:

3.1. Growth calculated through weight, length and condition factor:

Fig. 6 and 7 displays how the reared fish increased both in weight and length as the salmon developed. Fig. 8 shows how the condition factor increased from the 1st stage measured (a couple months before the 1st sampling in this study) towards the parr stage, before gradually decreasing during the 2nd and 3rd sampling. This indicates that from the 1st to the 2nd stage, the fish increased its weight faster than its length, meaning that the weight/length ratio favoured the former, ultimately resulting in an increase of the condition factor. From the 2nd stage onwards, the condition factor was gradually reduced, before a significant decrease was observed between the 3rd and 4th stage, meaning that the fish favoured growing its length rather than its weight during this period.

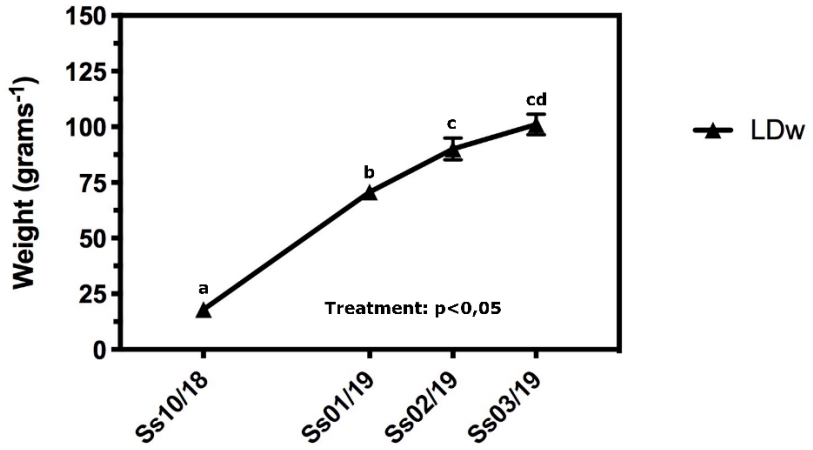

Figure 6: Wet weight (grams^{-1}) in Atlantic salmon during the smoltification process. The timepoints are represented by samplings at 09.10.18 (SS10/18), 22.01.19 (SS01/19), 12.02.19 (SS02/19) and 12.03.19 (SS03/19). Different letters presented indicate significant difference between the sampling points. The tanks were exposed to LDw (14:10) from fertilization until start-feeding. Different letters presented indicate significant difference between the sampling points. Data are presented as mean values +/- the standard deviation of mean. N = 18 for each group. Results were considered significant since p<0,05.

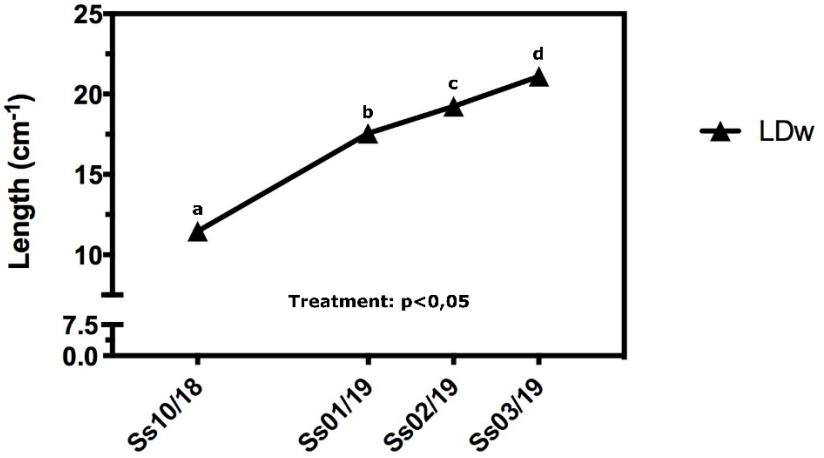

Figure 7: Length (cm^{-1}) in Atlantic salmon during the smoltification process. The timepoints are represented by samplings at 09.10.18 (SS10/18), 22.01.19 (SS01/19), 12.02.19 (SS02/19) and 12.03.19 (SS03/19). The tanks were exposed to LDw (14:10) from fertilization until start-feeding. Different letters presented indicate significant difference between the sampling points. Different letters presented indicate significant difference between the sampling points. Data are presented as mean values +/- the standard deviation of mean. N = 18 for each group. Results were considered significant since p<0,05.

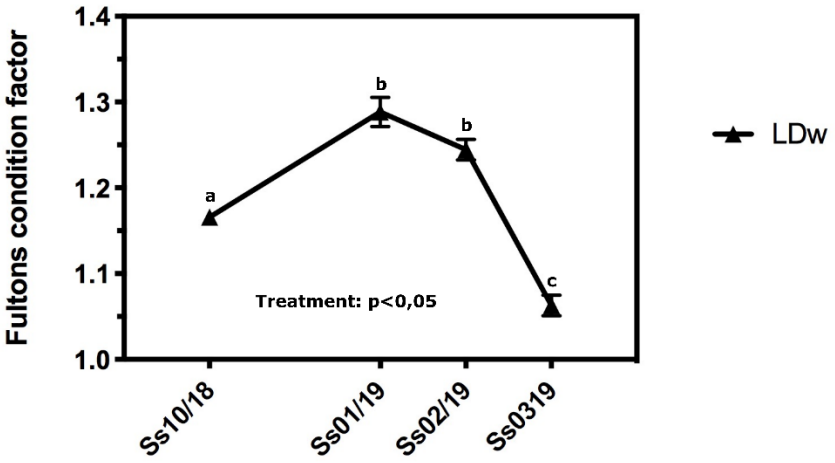

Figure 8: Condition factor (CF) in Atlantic salmon during the smoltification process. The timepoints are represented by samplings at 09.10.18 (SS10/18), 22.01.19 (SS01/19), 12.02.19 (SS02/19) and 12.03.19 (SS03/19). The tanks were exposed to LDw (14:10) from fertilization until start-feeding. Different letters presented indicate significant difference between the sampling points. Data are presented as mean values +/- the standard deviation of mean. N = 18 for each group. Results were considered significant since p<0,05.

3.2. Gill NKA activity:

Fig. 9 shows a slight decrease in gill NKA activity from the 1st measuring (SS10/18) towards the 2nd measuring (SS01/19), before slowly increasing between the 2nd measuring as a parr

and the 3rd measuring (SS02/19) as a mid-smolt, and finally a rapid increase in activity from the 3rd measuring towards the 4th measuring (SS03/19, at a stage which the salmon were nearing full smolt status, having adapted to the upcoming seaward migration.

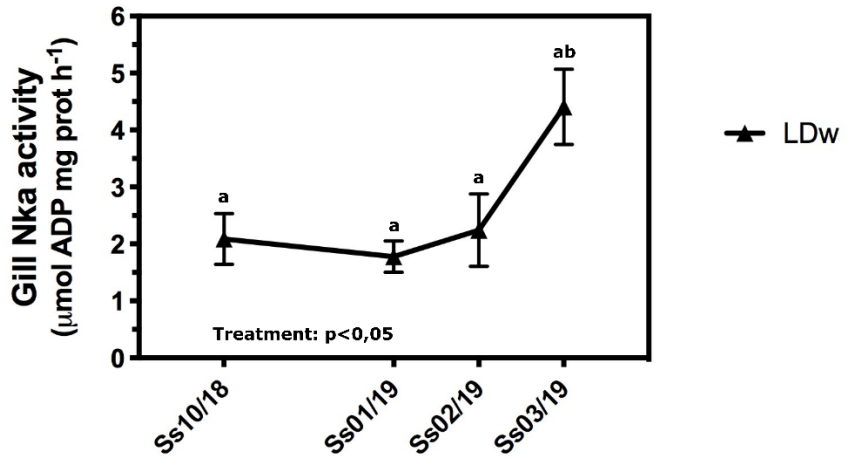

Figure 9: Gill NKA activity (µmol ADP mg prot h^{-1}) in Atlantic salmon during the smoltification process. The timepoints are represented by samplings at 09.10.18 (SS10/18), 22.01.19 (SS01/19), 12.02.19 (SS02/19) and 12.03.19 (SS03/19). The tanks were exposed to LDw (14:10) from fertilization until start-feeding. Different letters presented indicate significant difference between the sampling points. Different letters presented indicate significant difference between the sampling points. Data are presented as mean values +/- the standard deviation of mean. N = 16-18 for each group, and N_{total} = 69. Results were considered significant since p<0,05.

3.3. Topographic distribution and alterations to expression patterns of visual opsins in the retina of Atlantic salmon through smoltification:

In their natural habitat, wild Atlantic salmon have proved to undergo alterations to their retinal photoreceptors through the smoltification process, as they prepare to enter an environment visually different from the natal river streams where they were born. In this study, the expression pattern of visual opsins in salmon were investigated. Fig. 10-14 display the expression pattern of the *rhodopsin* in rod photoreceptors crucial for scotopic vision, the photopic single cone opsins *sws1* (UV-sensitive) and *sws2* (blue-sensitive), and the double cone opsins *rh2* (green-sensitive) and *lws* (red-sensitive), respectively, as the salmon grows from a parr recently exposed to the winter signal, to a mid-smolt, to a smolt, and finally after having spent 1 month in sea water. Fig. 10-14, A1-D1 show the whole eye section investigated for the 5 mentioned opsins during the 4 sampling points, which also is demonstrated as schematic drawings of expression in Fig. 15. Fig. 10-14, A2-A4, B2-B4, C2-

C4 and D2-D4 display the focused areas of the central, dorsal and ventral retina, of which a closer look at the morphology was required to fully understand the retinal alterations. In Fig. 10-15, the topographic morphology of the respective photoreceptor classes is difficult to differentiate, meaning that the expression observed is only assumed to be originated from the respective rods, single cones and double cones. For the purpose of differentiating between photoreceptor classes, tangential sections would be required. However, from this point onwards, the terms rod (Fig. 10 - *rhodopsin*), single cones (Fig. 11-12 - *sws1* and *sws2*) and double cones (Fig. 13-14 - *rh2* and *lws*) will be used to describe the observed photoreceptor classes. In the schematic drawing of Fig. 16, an overview of the retinal expression is displayed in an anterior-to-posterior axis. Fig. 16 shows the differences in retinal appearance in eyes treated with the anti-sense probe and the sense probe.

3.3.1. Rhodopsin:

The *rhodopsin* in rod photoreceptors is responsible for the detection of scotopic vision. Rod photoreceptors greatly outnumbers cone photoreceptors in the retina, which is an apparent fact in the *rhodopsin* expression, being clearly expressed throughout the whole retina during all the stages investigated. Looking at Fig. 10, A2-A4, B2-B4, C2-C4 and D2-D4, a tightly packed layer of photoreceptor cells display a strong expression adjacent to the ciliary marginal zone (CMZ), with the cell layer seemingly thickening slightly towards the central retina. Comparing the eyes gathered from each stage investigated, there are no considerable alterations observed as the salmon develops, with the rod photoreceptor showing similar distribution patterns throughout the whole period.

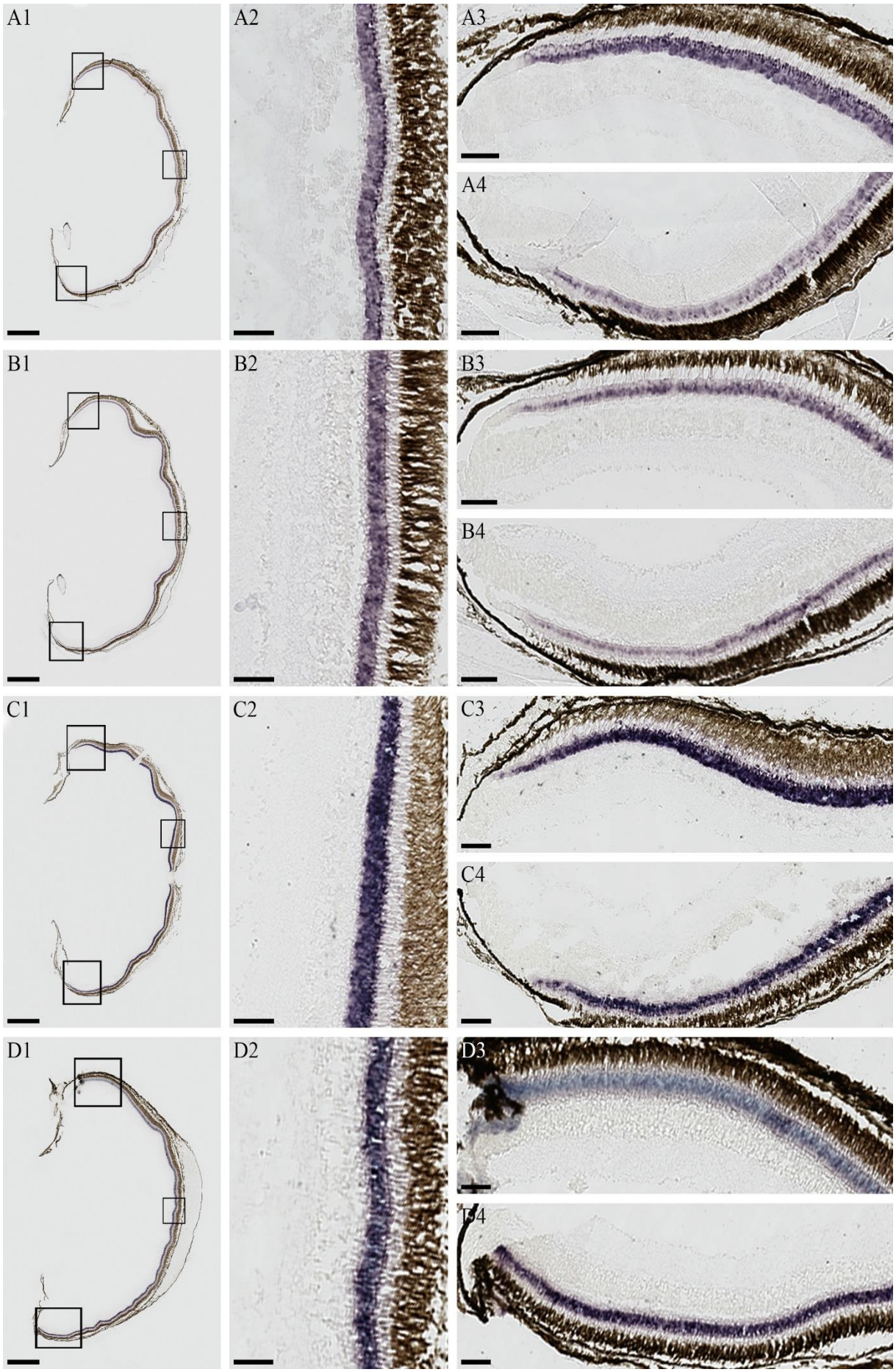
A1
A2
A3
A4
B1
B2
B3
B4
C1
C2
C3
C4
D1
D2
D3
D4

Figure 10: Expression patterns of the *rhodopsin* through the smoltification process in Atlantic salmon. **A1-D1.** The whole eye-sections chosen to display the expression patterns of *rhodopsin* in rod photoreceptors through the retina during 4 different sampling points. Added boxes represents the selected areas of the retina which were studied more closely. **A2-A4, B2-B4, C2-C4, D2-D4.** Distribution and expression patterns through the retina as a parr just after the winter signal, a mid-smolt, a smolt, and 1 month after transfer into sea water, respectively, of which the pictures displays the results from the focused areas centrally (2), dorsally (3) and ventrally (4). Through this whole period, the *rhodopsin* is strongly expressed in the rod photoreceptor cells throughout the whole retina. **Scalebar. (A1-D1):** 1000 µm, **(A2-D4):** 100 µm.

3.3.2. Sws1:

The *sws1* single cone opsin responsible for the detection of UV light, has in nature proved to undergo a downregulation as the salmon develops, being most strongly expressed during the earliest stages. Fig. 11, A3 (dorsal) shows that *sws1* is expressed in a small cluster of cells adjacent to the CMZ. Towards the central retina, individual cells expressing *sws1* are apparent. In Fig. 11, A4 (ventral), this same row of *sws1* positive cells can be seen near the CMZ, but there are no cells expressing *sws1* apart from this area. Centrally, there are no expression observable. Fig. 11, B3 and B4 shows that the expression level of the *sws1* cluster near the CMZ has diminished in strength both dorsally and ventrally during the mid-smolt stage, though there are more *sws1* positive cells expressed towards the central retina compared to the previous stage. Like the parr stage, there are no expression centrally during the mid-smolt stage. During the smolt stage, Fig. 11, C3 and C4 shows that the *sws1* positive cell layer near the CMZ has nearly vanished. Only being slightly visible, it is now difficult to point out the specific cells expressing *sws1* which were previously distinguishable. Centrally there are no expression visible. During the last stage, as the salmon has spent 1 month in sea water, Fig. 11, D3 and D4 shows that the expression levels adjacent to the CMZ has decreased further and faded almost completely, while there are no observable expression of *sws1* apart from this area, neither dorsally, ventrally or centrally. The acknowledged natural downregulation of the *sws1* single cone opsin and the ability to absorb light in the ultraviolet part of the photopic spectrum is clearly illustrated to be current also in Salmon reared under artificial lighting conditions. The general trend of Fig, 11 is that the *sws1* opsin in cone photoreceptors is more strongly expressed adjacent to the CMZ during the early stages investigated (parr and mid-smolt), with clearly observable individual *sws1* positive cells expressed outwards from this area, especially in the dorsal retina – before gradually being downregulated, especially apparent during the smolt-stage and following the migration.

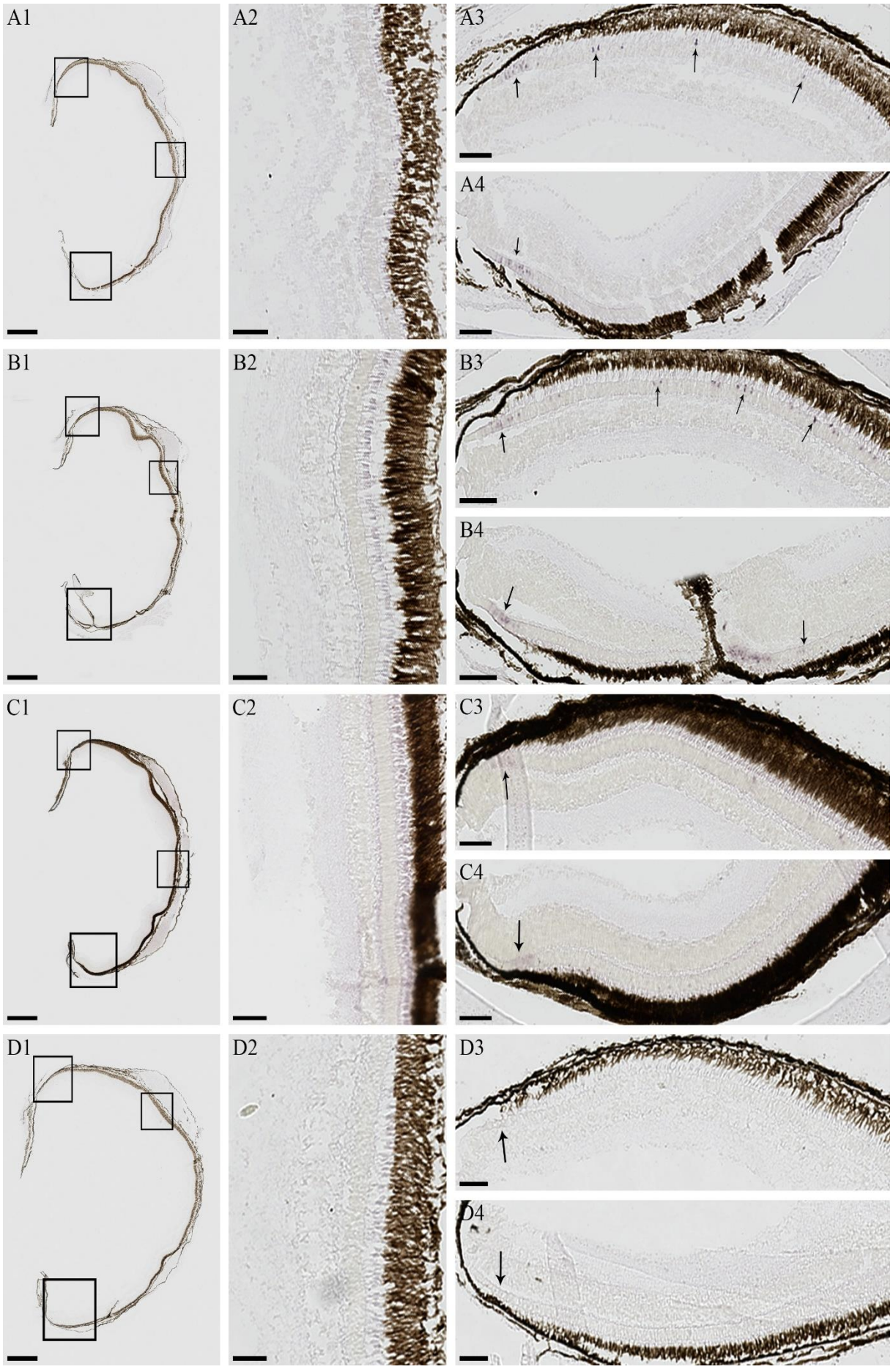
A1
A2
A3
A4
B1
B2
B3
B4
C1
C2
C3
C4
D1
D2
D3
D4

Figure 11: Expression patterns of the *sws1* single cone opsin (UV-sensitive) through the smoltification process in Atlantic salmon. **A1-D1.** The whole eye-sections chosen to display the expression patterns of the *sws1* in cone photoreceptors through the retina during 4 different sampling points. Added boxes represent the selected areas of the retina which was studied more closely (except for pictures D3 and D4, displaying the dorsal and ventral areas of another section from the same eye, as this better represented the general expression in the tissue). **A2-A4.** Distribution and expression patterns through the retina just after the winter signal. Pictures display the results from the focused areas centrally, dorsally and ventrally, respectively. At this point, *sws1* is clearly expressed in a row of photoreceptor cells adjacent to the CMZ. From this area and towards the central retina, the density of cells expressing *sws1* are gradually decreasing, with arrows pointing towards individual *sws1* positive cells. **B2-B4**. Distribution and expression patterns through the retina during the mid-smolt period. The expression level near the CMZ has been slightly reduced, while still showing a gradual loss of density of cells expressing *sws1* towards the central retina. **C2-C4.** Distribution and expression patterns through the retina during the smolt-period. The cluster of cells near the CMZ is now only slightly visible, while there seems to be little to no expression apart from this area. **D2-D4.** Distribution and expression patterns through the retina 1 month after sea water-transfer. The expression level in the cell cluster near CMZ has decreased further, and there are no visible *sws1* expression apart from this area. **Scalebar. (A1-D1):** 1000 µm, **(A2-D4):** 100 µm.

3.3.3. Sws2:

The *sws2* single cone opsin responsible for the detection of blue light, has through research on a series of salmonid species (including Atlantic salmon) proved to be gradually upregulated parallelly to the downregulation of the *sws1* opsin as the fish develops during the early life stages. Fig. 12, A3 and A4 displays that *sws2* is most strongly expressed adjacent to the CMZ, with expression levels diminishing slightly towards the central retina, most clearly apparent ventrally. Fig. 12, A2 shows that the *sws2* opsin is still strongly expressed in the central retina, however distributed more in a layer of cells expressing *sws2*. As a mid-smolt, Fig. 12, B3 and B4 display how *sws2* is still strongly expressed near the CMZ both in the dorsal and ventral retina, but that the expression levels decrease more rapidly towards the central retina compared to the previous sampling. By looking at Fig. 12, B2, it becomes apparent that there's a total loss of *sws2* positive cells centrally during the mid-smolt period. As a smolt, Fig. 12, C3 and C4 show that the expression levels of *sws2* has decreased slightly both in the dorsal and ventral retina adjacent to the CMZ. By looking at Fig. 12, C2, there is an area surrounding the optic nerve where a cluster of cells expressing *sws2* is observable in the central retina. After having spent a month in sea water, by looking at Fig. 12, D3 and D4, the expression levels has clearly increased both dorsally and ventrally near the CMZ, as well as there being more *sws2* positive cells apart from this area. Fig. 12, D2 shows that the amount of cells expressing *sws2* generally has increased also centrally (in all central areas apart from the optic nerve) compared to the previous smolt-stage.

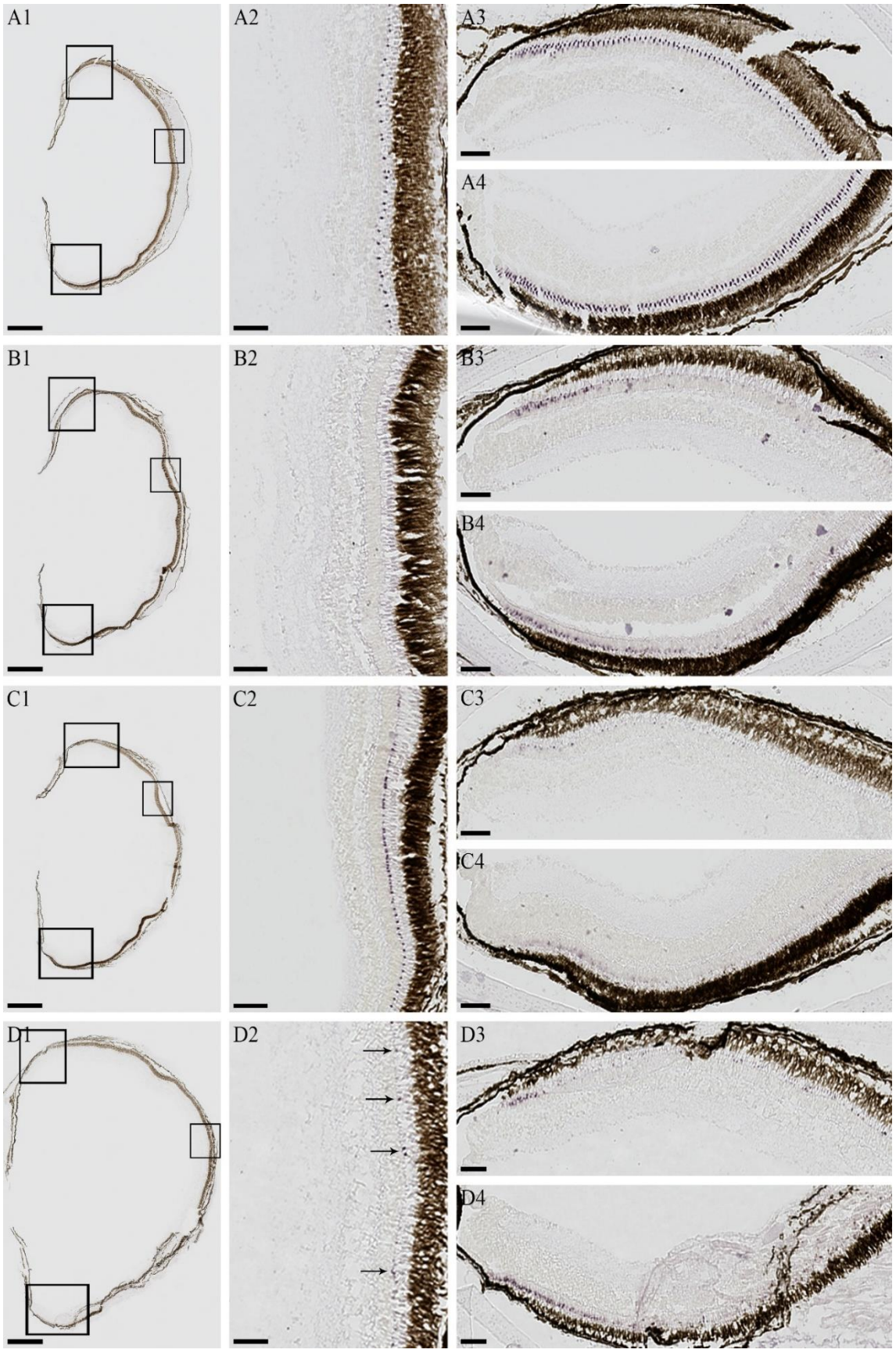
A1
A2
A3
A4
B1
B2
B3
B4
C1
C2
C3
C4
D1
D2
D3
D4

Figure 12: Expression patterns of the *sws2* single cone opsin (blue-sensitive) through the smoltification process in Atlantic salmon. **A1-D1.** The whole eye-sections chosen to display the expression patterns of the *sws2* in cone photoreceptors through the retina during 4 different sampling points. Added boxes represent the selected areas of the retina which was studied more closely (except for pictures C2 and D2, displaying the central area of another section from the same eye, as this better represented the general expression in the tissue). **A2-A4.** Distribution and expression patterns through the retina just after the winter signal. Pictures display the results from the focused areas centrally, dorsally and ventrally, respectively. At this point, *sws2* is strongly expressed in cells adjacent to the CMZ, with the expression levels diminishing closer to the central retina. **B2-B4**. Distribution and expression patterns through the retina as a mid-smolt. *Sws2* is still clearly expressed adjacent to the CMZ, with distribution most widespread ventrally, while the magnitude of *sws2* positive cells shows a considerable reduction from this point towards the central retina, where expression seems to have ceased completely. **C2-C4.** Distribution and expression patterns through the retina as a smolt. Expression have been reduced slightly adjacent to the CMZ, especially dorsally. Towards the center, singular cells expressing *sws2* are observable, with an area adjacent to the optic nerve displaying a cluster of tightly packed *sws2* positive cells. **D2-D4.** Distribution and expression patterns through the retina 1 month after sea water-transfer. The expression is clear near the CMZ (most widespread ventrally as the previous periods), and has increased slightly towards the central retina, where even more cells are expressing *sws2*. **Scalebar. (A1-D1):** 1000 µm, **(A2-D4):** 100 µm.

3.3.4. Rh2:

The *rh2* opsin, representing one member of the double cone structure located on the sides of the mosaic pattern of photoreceptors in the retina, is responsible for the detection of green light. Fig. 13, A3 shows that *rh2* is strongly expressed and evenly distributed in cells in the dorsal part of the retina. Fig. 13, A4, however, display an expression level of a more moderate nature, only slightly visible adjacent to the CMZ and towards the central retina. During this stage, it is difficult to pinpoint any *rh2* positive cells in the central retina, as shown in Fig. 13, A2. Having grown to a mid-smolt, the expression levels of the *rh2* opsin has increased considerably, being clearly visible and seems to be evenly distributed near the CMZ, and showing a layer of cells strongly expressing *rh2* in the central retina. During the next stage, as a smolt, the expression of *rh2* has decreased slightly, being most strongly expressed near the CMZ, gradually reducing the expression levels towards the central retina, where individual cells expressing *rh2* can be detected in a more scattered distribution. After having spent 1 month in sea water, the expression of *rh2* has again increased, being strongly expressed near the CMZ, with expression levels decreasing more rapidly towards the centre in the ventral part of the retina compared to the dorsal. This pattern is also detectable in Fig. 13, D2, where the *rh2* positive cells are more strongly expressed in the upper (dorsal) part of the picture compared to the lower (ventral) part.

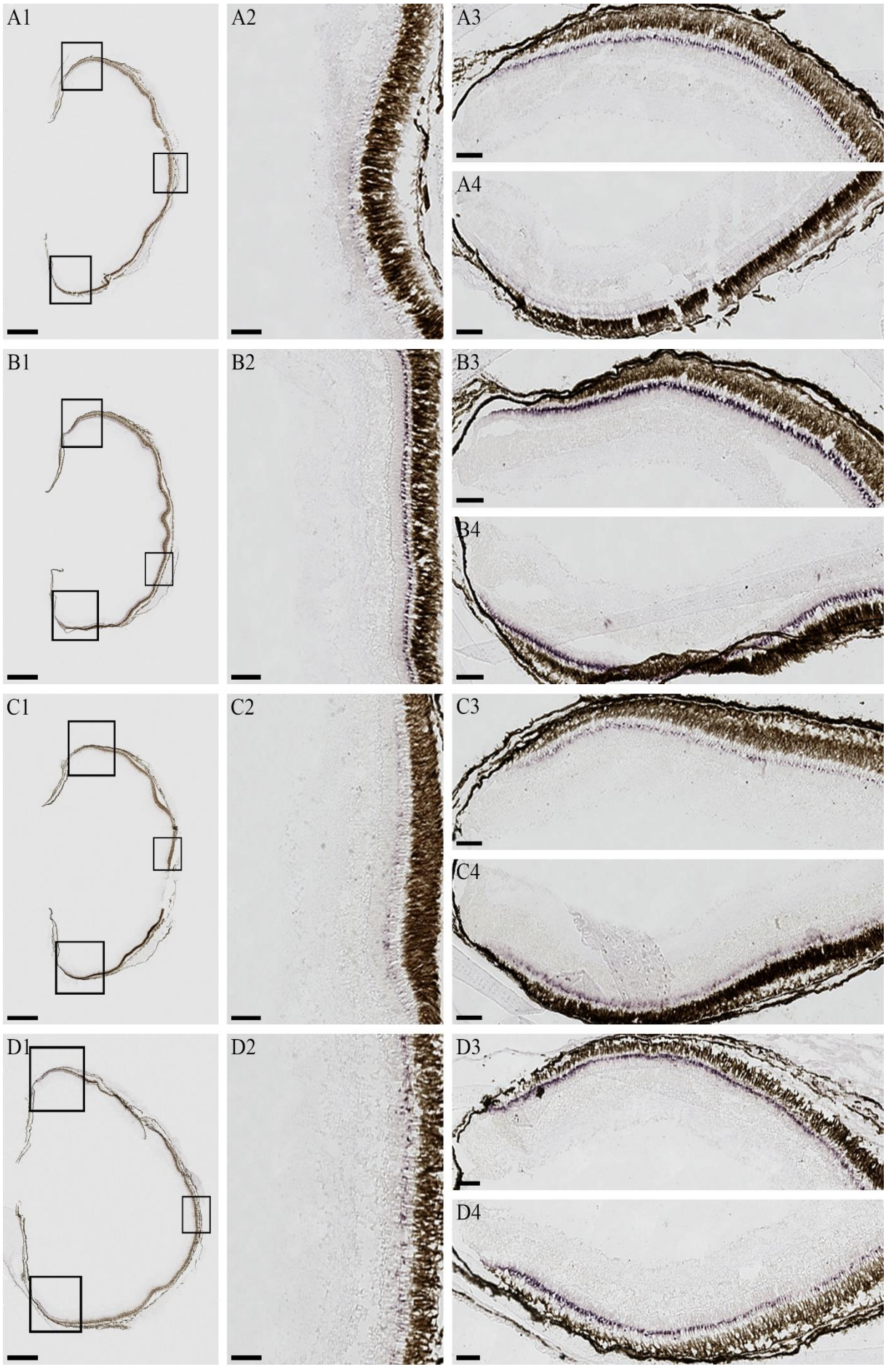
A1
A2
A3
A4
B1
B2
B3
B4
C1
C2
C3
C4
D1
D2
D3
D4

***Figure 13**:* Expression patterns of the *rh2* double cone opsin (green-sensitive) through the smoltification process in Atlantic salmon. **A1-D1.** The whole eye-sections chosen to display the expression patterns of the *rh2* in cone photoreceptors through the retina during 4 different sampling points. Added boxes represent the selected areas of the retina which was studied more closely (except for pictures A2 and A4, displaying the central and ventral areas of another section from the same eye, as this better represented the general expression in the tissue). **A2-A4.** Distribution and expression patterns through the retina just after the winter signal. Pictures display the results from the focused areas centrally, dorsally and ventrally, respectively. The expression of the *rh2* opsin is most clearly apparent adjacent to the CMZ dorsally of the lens, with the strength of expression reduced ventrally. Towards the central retina, distribution is reduced considerably, with *rh2* expression only slightly observable. **B2-B4**. Distribution and expression patterns through the retina as a mid-smolt. Expression is clear and strong near the CMZ both dorsally and ventrally. Towards the central retina, the expression is reduced slightly while still being clearly apparent. **C2-C4.** Distribution and expression patterns through the retina as a smolt. Expression is clear near the CMZ both dorsally and ventrally, but the expression levels has decreased slightly compared to the previous sampling period. Distribution of *rh2* positive cells are reduced gradually towards the central retina, where *rh2* shows a more scattered distribution. **D2-D4.** Distribution and expression patterns through the retina 1 month after sea water transfer. Expression of *rh2* in photoreceptor cells is strong and clear near the CMZ both dorsally and ventrally, while the expression level is decreased slightly towards the central retina. **Scalebar. (A1-D1):** 1000 µm, **(A2-D4):** 100 µm.

3.3.5. Lws:

The *lws* opsin, representing the other member of the double cone structure located on the sides of the mosaic pattern of photoreceptors in the retina, is responsible for the detection of red light. By looking at Fig. 14, the *lws* opsin is generally strongly expressed through the whole retina, displaying a layer of tightly packed *lws* positive cells, where the expression in individual cells is difficult to pinpoint. Looking at the areas adjacent to the CMZ, *lws* displays a clear and similar expression both in the dorsal and ventral retina, with an expression that seems to be slightly more prominent dorsally than ventrally during the mid-smolt stage. Some eye sections (not displayed in the figure), showed an expression more widespread dorsally than ventrally, and others showed an expression more widespread ventrally than dorsally. Hence, the general trend demonstrated an expression pattern similarly distributed in the dorsal and ventral retina. Centrally, there's a strong and clear expression in *lws* positive cells during all the stages investigated in this study.

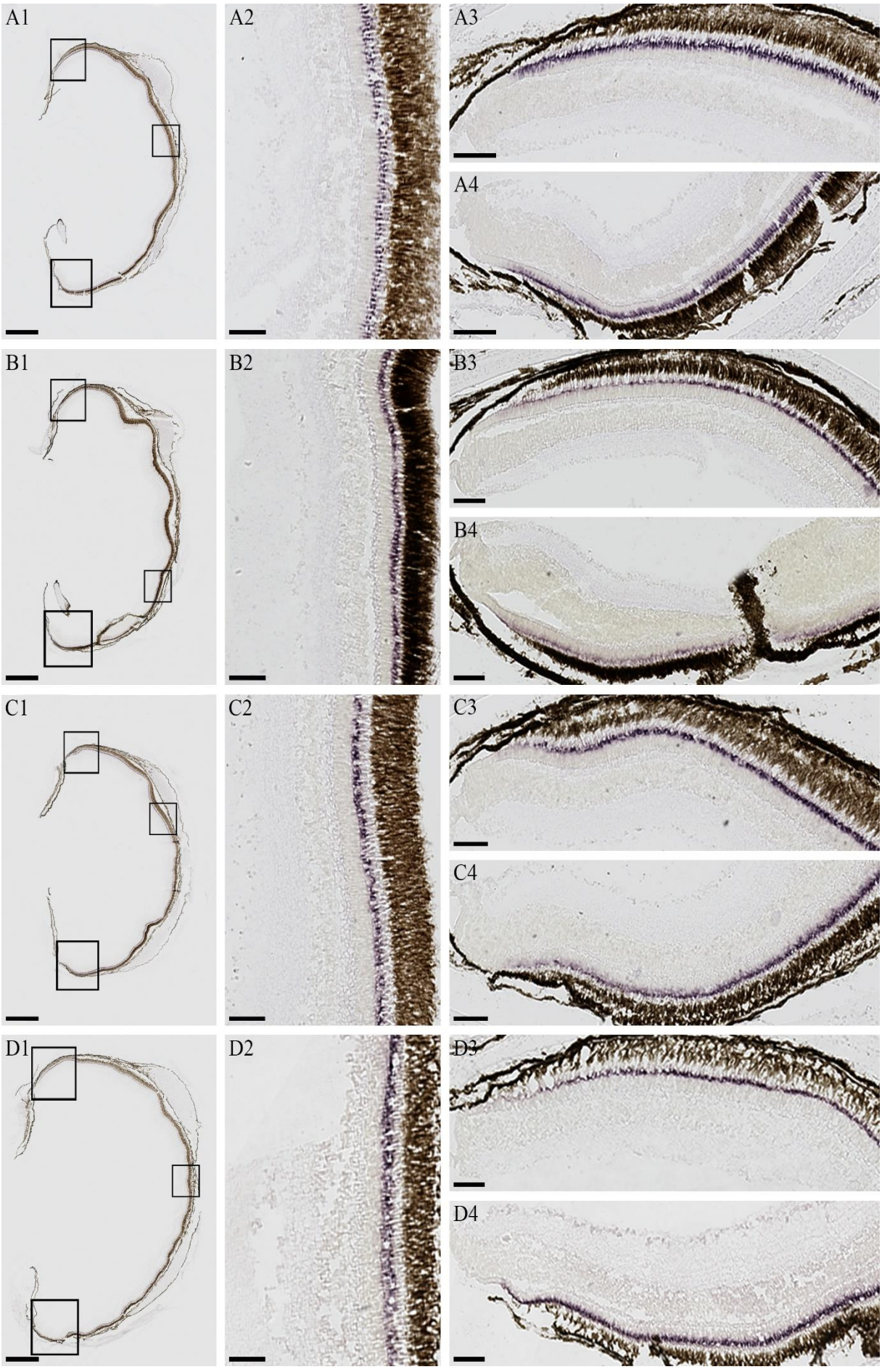
A1
A2
A3
A4
B1
B2
B3
B4
C1
C2
C3
C4
D1
D2
D3
D4

Figure 14: Expression patterns of the *lws* double cone opsin (red-sensitive) through the smoltification process in Atlantic salmon. **A1-D1.** The whole eye-sections chosen to display the expression patterns of the *lws* opsin in cone photoreceptors through the retina during 4 different sampling points. Added boxes represent the selected areas of the retina which was studied more closely (except for pictures D2 and D4, displaying the central and ventral areas of another section from the same eye, as this better represented the general expression in the tissue). **A2-A4, B2-B4, C2-C4, D2-D4.** Distribution and expression patterns through the retina as a parr just after the winter signal, a mid-smolt, a smolt, and 1 month after transfer into sea water, respectively, of which the pictures display the results from the focused areas centrally (2), dorsally (3) and ventrally (4). *Lws* is clearly expressed throughout the whole retina through all the stages investigated. A layer of tightly clustered *lws* positive cells are most strongly expressed adjacent to the CMZ, and expression seems to be similarly distributed both dorsally and ventrally, while slightly decreasing the expression levels towards the central retina. **Scalebar. (A1-D1):** 1000 µm, **(A2-D4):** 100 µm.

3.4. A schematic display of the topographic distribution of photoreceptors in the retina:

Fig. 15 displays a schematic drawing of the topographic distribution of the various photoreceptor classes presented in Fig. 10-14. *Rhodopsin* expression seems evenly distributed through all retinal sections (dorsal, ventral and central) throughout the whole smoltification process. The expression of *sws1* is readily observable adjacent to the CMZ both dorsally and ventrally during the earliest stage, diminishing gradually through the mid-smolt and smolt stage, until most (if not all) expression have ceased after 1 month in sea water. Fig. 15, B1-B2 shows how individual *sws1* positive cells are expressed in the dorsal retina as a parr and mid-smolt. The expression of *sws2* is during the parr stage clear adjacent to the CMZ both dorsally and ventrally, while diminishing slightly towards the central retina, where individual cells are expressed in a structural pattern. Towards the next stage, the expression levels seems to have been reduced considerably. Expression is still clear adjacent to the CMZ, while all expression seems to have ceased towards the central retina. During the latter two stages, expression is gradually increased both adjacent to the CMZ and centrally. As a smolt, an area surrounding the optic nerve displays a prominent presence of *sws2* positive cell. A general trend is that the expression of *sws2* is distributed most widely in the ventral retina, especially observed as a mid-smolt, smolt and after 1 month in sea water. *Rh2* is most clearly expressed in the dorsal retina both adjacent to the CMZ and centrally as a parr. During the next three stages, however differing slightly in the level of expression, *rh2* is clearly expressed adjacent to the CMZ both in the dorsal and ventral retina, with an expression pattern being slightly less packed towards the central retina. *Lws* is throughout the whole period expressed clearly in the whole retina,

with tightly clustered *lws* positive cells located adjacent to the CMZ both dorsally and ventrally, as well as in the central retina.

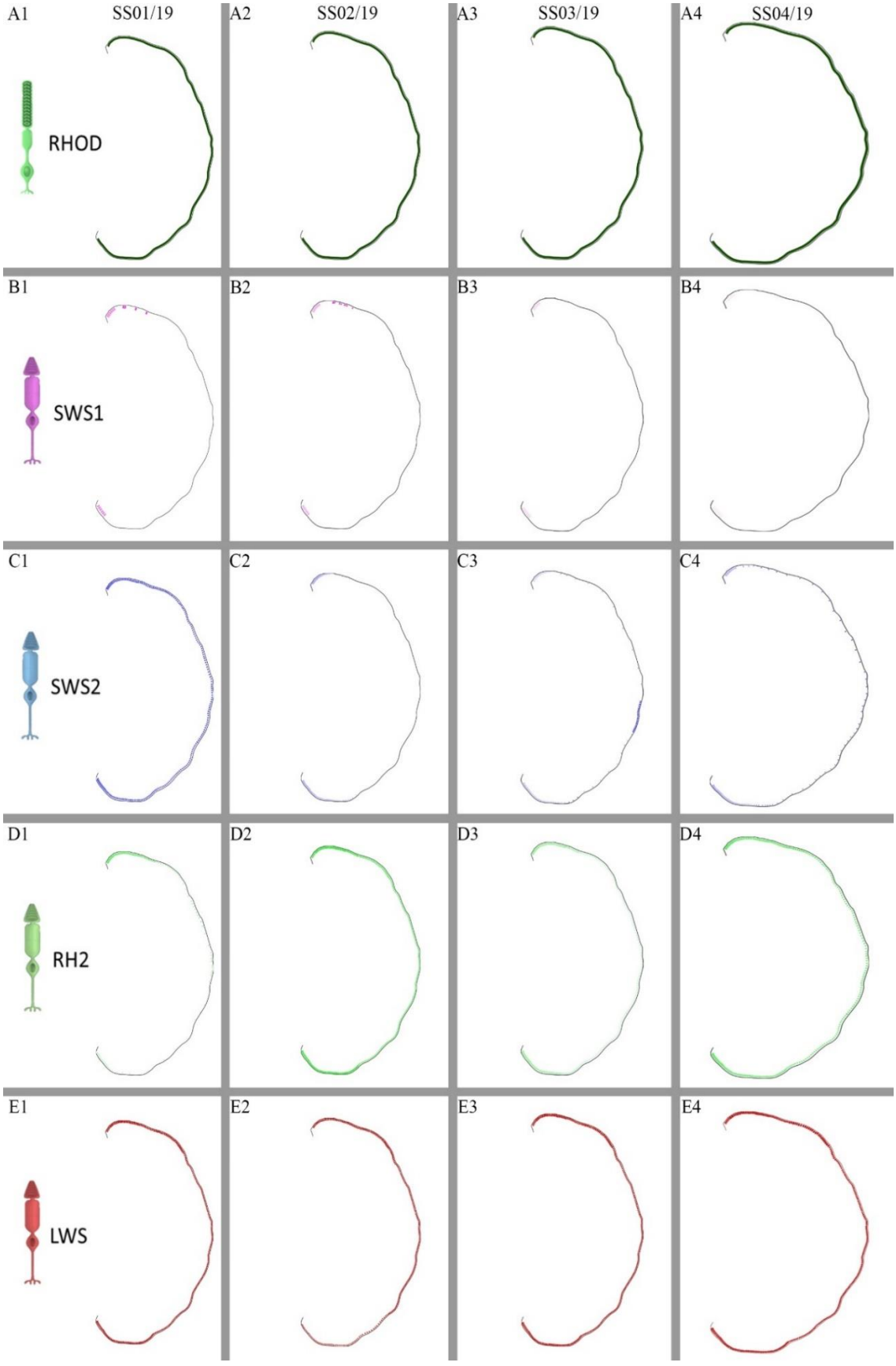

Figure 15: A schematic display of the topographic distribution of photoreceptor cells expressing opsins through the smoltification process. Pictures displaying expression are obtained from sections located in the central parts of the eye. **A1-A4:** Expression patterns of the *rhodopsin* in rod photoreceptors as a parr (A1), mid-smolt (A2), smolt (A3) and after 1 month in sea water (A4). Expression is clear and readily observable in the dorsal, ventral and central retina during the whole period. **B1-B4:** Expression patterns of *sws1* in single cone photoreceptors as a parr (B1), mid-smolt (B2), smolt (B3) and after 1 month in sea water (B4). Expression is generally restricted to an area adjacent to the CMZ, and is gradually downregulated through the period studied. *Sws1* positive cells are also observed apart from the CMZ in the dorsal retina during the parr and mid-smolt stage. **C1-C4:** Expression patterns of *sws2* in single cone photoreceptors as a parr (C1), mid-smolt (C2), smolt (C3) and after 1 month in sea water (C4). During the parr stage, expression is clear adjacent to the CMZ and diminishing slightly tow ards the central retina. As a mid-smolt, expression has diminished considerably. *Sws2* positive cells are readily observable adjacent to the CMZ, but have ceased almost completely in the central retina. During the last two stages, *sws2* expression is gradually upregulated, especially in the central retina. A general observation is that *sws2* expression is most prominent in the ventral retina (C2-C4). **D1-D4:** Expression patterns of *rh2* in double cone photoreceptors as a parr (D1), mid-smolt (D2), smolt (D3) and after 1 month in sea water (D4). Except for the parr stage where *rh2* expression is mostly distributed in the dorsal and central retina, the general observance during the latter three stages is a seemingly similarly distributed topography of *rh2* positive cells, being slightly less dense in the central retina. **E1-E4:** Expression patterns of *lws* in double cone photoreceptors as a parr (E1), mid-smolt (E2), smolt (E3) and after 1 month in sea water (E4). *Lws* is expressed clearly both adjacent to the CMZ and centrally during the whole period.

3.5. Negative control using a sense probe:

Fig. 16 clearly displays how the ISH process performed on eye #7 utilizing an anti-sense probe yielded observable expression (Fig. 16, A1-E1), while the ISH process performed on eye #8 utilizing a sense probe showed an absence of expression (Fig. 16, A2-E2) – both during the parr stage. Performing an ISH using the sense probe functioned as a negative control in differentiating between potential background staining and actual expression in the eye treated with the anti-sense probe.

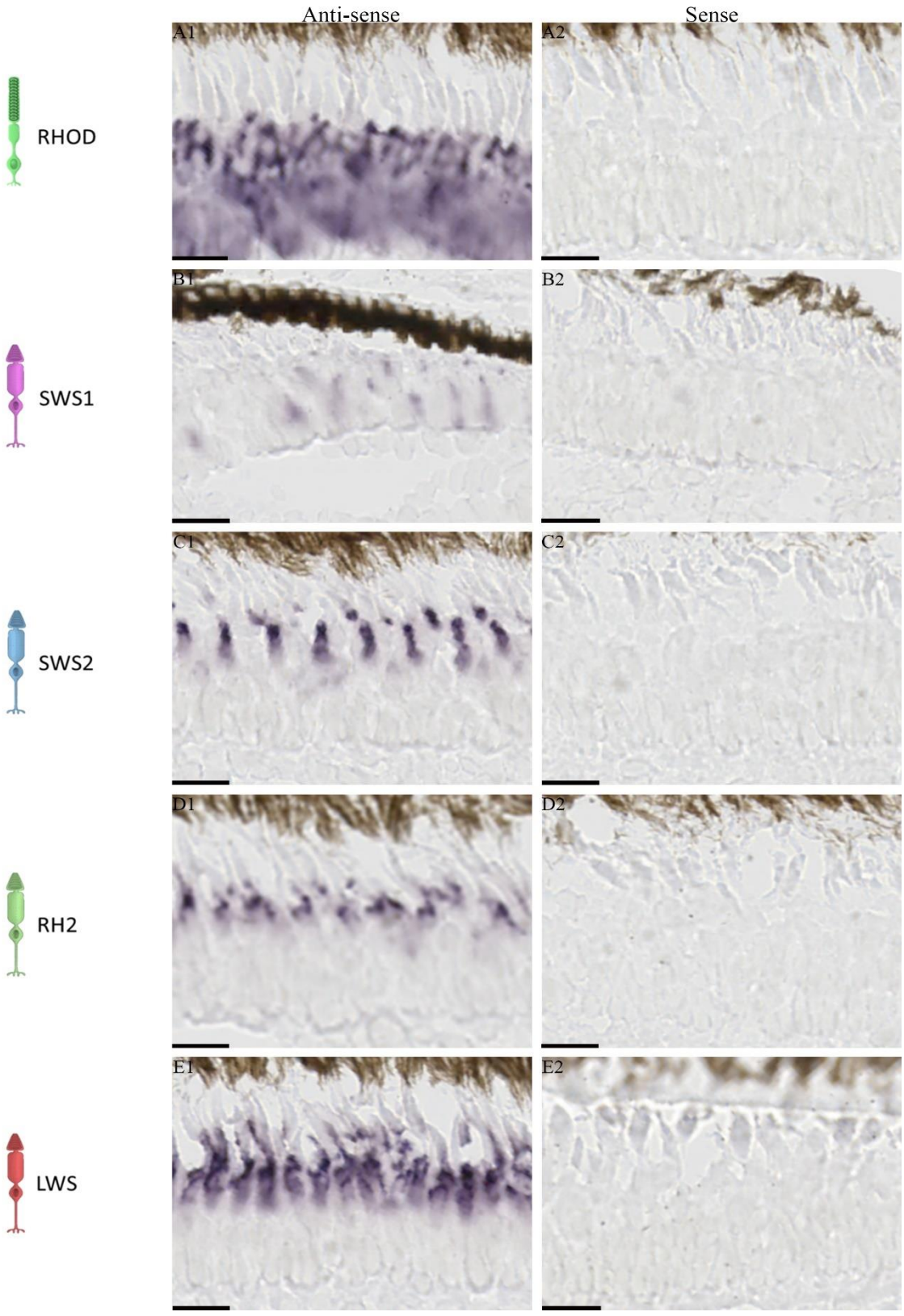

Figure 16: Results from the parr stage of ISH performed on the various opsins, using an antisense probe (A1-E1) or a sense probe (A2-E2) on eye #7 and #8, respectively. All pictures representing the results yielded by the antisense probe display expression in the tissue, while there's no expression in the tissue treated with the sense probe. **Scalebar. (A1-E1):** 50 µm.

4. Discussion:

This study was conducted in order to better understand the visual system and its development through the smoltification process in Atlantic salmon. The choice of Atlantic salmon as a target organism for the purpose of this study is justified through its economic role in Norwegian food production, functioning as the leading commodity for foreign export produced in the Aquaculture industry (Xiaowei & Junning, 2018).

The main goal of this study was to reveal the expression patterns of opsins in photoreceptor cells and to determine if the topographic distribution is altered throughout the retina as the salmon develop through smoltification.

Based on the analysis performed on Atlantic salmon through the smoltification process, targeting the 5 known visual opsins in the retina; the scotopic *rhodopsin*, and the photopic *sws1*, *sws2*, *rh2* and *lws* – a number of hypothesis were presented. The utilization of an artificial winter signal did in fact induce smoltification in the reared salmon, proven through changes in condition factor and gill NKA activity (Fig. 8 and 9). Moving onto the visual system, there were clear differences in topographic distribution between the various cone opsins – especially by comparing the single- and double cones (Fig. 11-15). *Sws2* was shown to be expressed in central areas surrounding the optic nerve during the smolt stage of smoltification, a previously unknown finding that could further highlight the continued importance of the embryonic fissure. In the case of *rhodopsin*, the hypothesized difference between the expression pattern in this opsin compared to cones was readily observed (Fig. 10). Additionally, the post-embryonic development known to salmon and its influence on retinal transformations were observed in the changing expression patterns of single cone opsins, especially seen in the downward regulation of *sws1*. This downregulation of *sws1* challenged the last hypothesis stating that the appearance of opsin expression in the CMZ would be reflected in the retinal transformation, being the only opsin questioning the continuous proliferation proposed to occur in the CMZ through the smoltification process.

4.1. Discussion of material and method:

4.1.1. Setup of experiment:

Induction of smoltification of Atlantic salmon by light stimulation:

The environmental factors of utmost importance for the growth and development of salmon is light, termed as the seasonal "zeitgeber" in physiologically determining when the salmon is ready to proceed with the smoltification process (Ebbesson et al., 2008; McCormick et al., 1998), and temperature (Handeland et al., 2008; McCormick et al., 1998; Solbakken et al., 1994). In aquaculture, the benefit of photoperiod has been utilized to produce out-of-season smolt, maintaining an equal production all throughout the year (Duncan et al., 1998; Duncan & Bromage, 1998; Thrush et al., 1994); to increase somatic growth, especially during the darker seasons (Maiolo et al., 2015; Oppedal et al., 2003) through an increased appetite, food intake and feed conversion ratio (Nordgarden et al., 2003); and prevent sexual maturation (Oppedal et al., 2003; Taranger et al., 1999) due to this process' gonadal development and its unappetizing effects on the fish through changes in color, texture and taste (Hansen et al., 1992). In this study, the salmon was reared under Philips warm white 2700 K (14:10 (LDw)) with a light-intensity of 0,1 W/m^2 from fertilization until start-feeding. From start-feeding, the light exposure was adjusted and increased to 20:4 until the winter signal was given, exposing the salmon to 12:12 light for 6 weeks. From this point, the fish were gradually acclimatized to the increased exposure of light, upregulating the lighting period towards 24:0 (Duncan & Bromage, 1998; Stefansson et al., 1991). The usage of continuous light has proved to be the most efficient way of stimulating growth in salmon, being the preferred lighting conditions utilized for this purpose (McCormick et al., 1998; Stefansson et al., 1991).

High temperature control in the experiment:

The other environmental factor of great importance controlled in the aquaculture industry, is the water temperature (Handeland et al., 2008; Solbakken et al., 1994). Where light is most crucial in the initiation of processes, such as smoltification and increased appetite, temperature mainly functions as an accelerator – speeding up the processes as they proceed (Handeland et al., 2008; Solbakken et al., 1994). However, temperature may also serve as an instigator for smoltification in itself, as studies have proved that the photoperiod's ability to affect smoltification is restricted at low temperatures (McCormick et al., 1998). In this experiment, the fish were reared under a temperature of approximately 6 °C from fertilization

till first-feeding, which was increased and kept stable at approximately 11℃ for the remainder of the period. The temperature in the tanks was thoroughly measured throughout the whole period, a procedure followed to secure that equal conditions were maintained in all the 3 tanks containing fish, and therefore not being a causation of potential growth-differences.

Sampling points through smoltification and sea water tolerance test:
The four sampling points were chosen thoughtfully in order to best represent the changes occurring during the smoltification process. Hence, it was of importance to separate the timing of each sampling sufficiently, and by this securing that the fish had in fact developed and differed from the previous sampling. The 1st sampling represented salmon during a stage of which smoltification had recently been initiated at 4280 dd, the 2nd sampling as a mid-smolt at 4515 dd, the 3rd sampling as a smolt at 4835 dd, and the 4th and final sampling represented a fully smoltified, ocean-going salmon – following the fish from the start and until the end of the smoltification process. In order to establish that the fish were fully adapted for the transfer into salt water through a successful smoltification process, a salt water tolerance test was performed on random fishes from all tanks following the 3rd sampling (Sigholt et al., 1995; Staurnes et al., 2001). At March 25th, all fish had survived the test and were observed to possess the morphological traits resembling a smolt (ref. Fig. 5, SS03/19), and could therefore be placed in 3 new tanks filled with salt water, where they were kept and proceeded their development as post-smolts towards the 4th and final sampling.

4.1.2. In situ *hybridization (ISH) for the purpose of visually detecting expressed genes in the retina of Atlantic salmon:*

Choice of ISH as a method for visualizing opsin expression:
In this study, ISH was done to visualize the expression patterns of visual opsins in the eye of Atlantic salmon. ISH is performed on sections (as in this study), targeting specific cells in the tissue; or on whole-mount, where the whole embryo is used, generating a more profound knowledge of cellular expression on a wider scale (Acloque et al., 2008). ISH has the advantage of not only detecting the expression of genes, but also to determine the topographic distribution of photoreceptor cells in the tissue (Novales Flamarique, 2018; Nuovo, 1994). As this was of importance to yield satisfying results in this thesis, ISH was favoured in comparison to q-PCR (Novales Flamarique, 2018) and RNA-seq – methods quantifying the expression without displaying the actual location (Wu et al., 2014). There are certain

drawbacks to the ISH, however, one of them being the fact that the targeted mRNA in certain cases won't translate into functional proteins. Thus, in the regard of reliably detecting genetic activity in the tissue, performing immunocytochemistry would be the better option, as operating proteins and their locations are the targets of this method (Acloque et al., 2008). However, specific antibodies can be difficult to produce, making it less favourable for this study (Acloque et al., 2008). Performing ISH in this thesis allows visualization of expressional alterations occurring in the salmon during the period investigated on a cellular level.

The ISH protocol, requirement of replicates and a negative control:

ISH requires a sheer amount of time to reach the desired end-product, involving fixation of tissue in advance, the synthesis of RNA-probe to be required for the method - in addition to all the intricate steps performed throughout the process (Acloque et al., 2008; Nuovo, 1994). Performing the entire procedure to perfection is of great importance to secure the results required to optimally present the expression patterns of the visual opsins, making it difficult to point towards a certain flaw made during the process if the product proves to be inadequate. With this knowledge in mind, it was deemed necessary to take certain precautions. For each stage investigated, ISH were performed on eyes from 3 different fish. This was an important step in order to certify the results of the chosen eye from each sampling, by having the potential to support the displayed distribution of visual opsins in the figures by comparing them to the distribution patterns in the other eyes analysed. Additionally, ISH was performed on an eye from the 1st sampling, utilizing the sense probe for each of the 5 genes investigated, revealing no staining. This was done with the purpose of distinguishing between actual opsin expression and potential background staining in the retina of the eyes analysed with the antisense probe (Eilertsen et al., 2014; Sandbakken et al., 2012).

Probes:

It is of importance to state that the probes used in this thesis reveal the expression of all the various paralogues within an opsin class. For example, the green and red opsin probes visualize the expression of all four genes presented within the *rh2* and *lws* opsins, respectively (see chapter 2.6 for further details). In order to determine the expression patterns of all the individual paralogues present within these opsins, ISH with short probes targeting the upstream or downstream sequence of the opsin genes, having less sequence identity, must be performed. However, as this was out of the scope of this thesis, long probes ensuring a strong

signal in the tissue were used to describe the retinal dynamics of opsin classes through smoltification.

The time of colour reaction reflects expression level:
The time it took before the colour reaction revealed expression differed greatly between the opsins investigated. *Rhodopsin* (of which only half the probe was utilized) had its expression revealed after approx. 30 minutes, while *sws1* and *sws2* could spend in the upper parts of 7 hours before expression became visible and ready for analyzation. The timing it takes before the colour reaction reveals expression in the tissue is highly related to the amount of cells expressing the respective opsins, with *rhodopsin* expression distributed clearly and widely throughout the retina (i.e., rapid reaction time), and *sws1* and *sws2* restricted to certain areas (i.e., slower reaction time).

4.1.3. Imaging and analyses:

The expression displayed in Fig. 10-15 is the result of a thorough examination of all eyes which ISH were performed on, before selecting the most presentable eyes from each sampling to be scanned in the Axio Scan.Z1 (Zeiss). Additionally, this accurate tissue-assessment served to further support the findings representing the scanned eyes displayed in the figures, as the presented results was determined to be a good representation of the actual expression in all three eyes analysed from each developmental stage. The advantage of running the scanning process is to display the visualization of expression in the tissue in a high and presentable resolution, while at the same time separating the individual sections into separate pictures for a more accessible assessment of the retinal topography. Following an examination of the scanned eyes, the central part of the eye was established to best present the retinal expression universally observed across all the eyes studied. Hence, the expression patterns of the various opsins discussed later will be based on the expression displayed in this central section of the eye. However, in order have an overall understanding of the expression throughout the entire eye, a thorough examination was conducted to display the anterior-to-posterior axis of expression shown in Fig. 17, which showed that the general expression was similarly distributed in all sections of the axis.

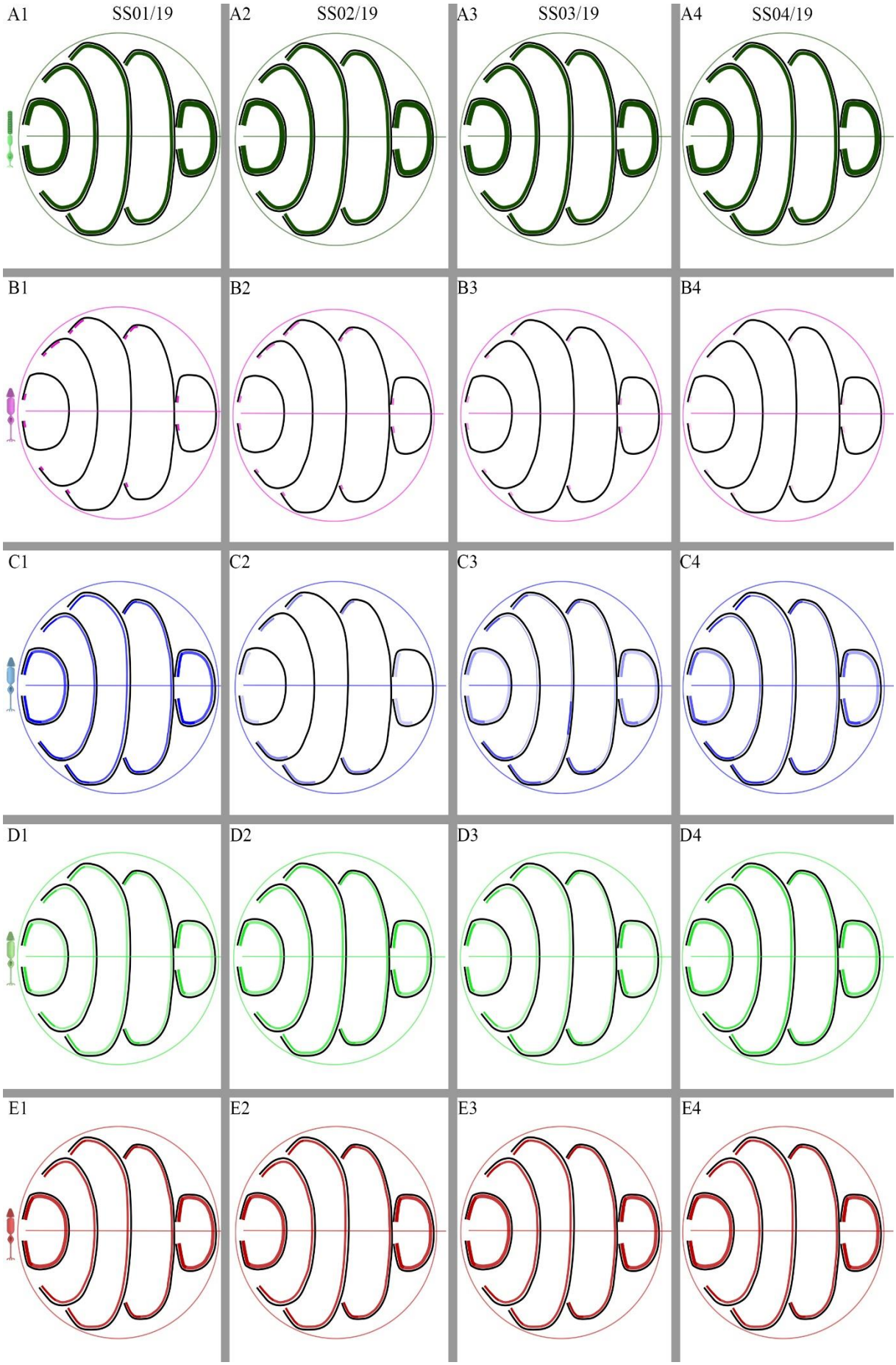
A1
SS01/19
A2
SS02/19
A3
SS03/19
A4
SS04/19
B1
B2
B3
B4
C1
C2
C3
C4
D1
D2
D3
D4
E1
E2
E3
E4

Figure 17: A schematic overview of the topographic distribution of photoreceptor cells expressing opsins through the smoltification process, shown in an anterior (left)-to-posterior (right) axis. **A1-A4:** Expression patterns of the *rhodopsin* in rod photoreceptors as a parr (A1), mid-smolt (A2), smolt (A3) and after 1 month in sea water (A4). Expression is similarly distributed throughout the eye during the whole period. **B1-B4:** Expression patterns of *sws1* in single cone photoreceptors as a parr (B1), mid-smolt (B2), smolt (B3) and after 1 month in sea water (B4). Expression is similarly distributed throughout the eye, however slightly less observable on the anterior and posterior sections. *Sws1* expression is located adjacent to the CMZ both in the dorsal and ventral retina during the whole period, in addition to a section of expression dorsally during parr and mid-smolt stage (B1-B2). The observable expression is downregulated gradually as the salmon develops. **C1-C4:** Expression patterns of *sws2* in single cone photoreceptors as a parr (C1), mid-smolt (C2), smolt (C3) and after 1 month in sea water (C4). As for *sws1*, the expression level of *sws2* is slightly lower in the anterior and posterior sections. Expression is clear throughout the eye during the parr stage, decreased considerably towards the mid-smolt stage where central expression is absent, and increased gradually during the smolt stage and after 1 month in sea water. The central prominence of *sws2* positive cells during the smolt stage is only observable in the centre-most section. **D1-D4:** Expression patterns of *rh2* in double cone photoreceptors as a parr (D1), mid-smolt (D2), smolt (D3) and after 1 month in sea water (D4). Expression is similarly distributed throughout the eye during the whole period, with expression levels more prominent adjacent to the CMZ. **E1-E4:** Expression patterns of *lws* in double cone photoreceptors as a parr (E1), mid-smolt (E2), smolt (E3) and after 1 month in sea water (E4). Expression is similarly distributed throughout the eye during the whole period, with expression levels slightly more prominent adjacent to the CMZ.

4.1.4: Choice of methods for statistical analyses:

The dataset presented in figures 6-9 representing the dynamic pattern of the dependent variables (weight, length, condition factor and gill NKA activity) was obtained from only one group ((14:10) LDw light exposure) consisting of 4 sampling points. Parametric statistical tests are based on a set of underlying assumptions. Hence, before running an ANOVA, three assumptions should be made: 1. The 4 sampling points are independent; 2: Homogeneity of variance; and 3: The dependent variables should be normally distributed. Because of its good power, the Shapiro-Wilk W-test was used to assess normality. Most parameters in the present study conformed to these assumption, with the exception of normal distribution for gill NKA activity (Ref. appendix Table 7). It is not uncommon, however, that biological data may exhibit deviations from some of these assumptions. However, this does not necessarily preclude the use of parametric tests (Zar, 1996). Hence, a one-way ANOVA was chosen as they are found to be robust comparing variances between groups, and only severe deviations from normality will create challenges with respect to validity of F statistics (Zar, 1996)

4.2. Discussion of results:

4.2.1. Smoltification:

Exposing Atlantic salmon parr to a winter signal by light treatment will induce smoltification:
After having been exposed to LD (20:4) from their initial placement into separate tanks at start-feeding, the fish were given the winter signal through exposure to LD (12:12) at December 11th 2018, lasting for a period of six weeks (Duncan & Bromage, 1998; Stefansson et al., 1991). From this information, it was hypothesized that this period of artificial light treatment followed by another period of continuous light (24:0) would induce smoltification in the reared salmon. By looking at Fig. 8 and 9, displaying the condition factor and gill NKA activity, respectively, there are observations that clearly indicates that the light treatment has functioned as an initiator of the smoltification process. Following the graph in Fig. 8, there is a gradual reduction in condition factor between the 1st sampling at the 2nd sampling (February 12th), before it is rapidly reduced from the 2nd sampling and towards the 3rd (March 12th). The condition factor being a measurement for the weight/length ratio (McCormick et al., 1998; Thrush et al., 1994), these findings display how the fish favoured growing its length rather than weight during this period. By looking at Fig. 9, the gill NKA activity develops with a similar dynamic to that of the condition factor, but in the opposite direction – increasing slightly from the 1st to the 2nd sampling, before the graph rises rapidly between the 2nd and 3rd sampling. These findings are in accordance with what is termed as clear indicators in the industry of a proceeding smoltification process.

The condition factor was reduced during smoltification:
Regarding the condition factor, there are two main hypothesis to this lengthening of the body occurring in salmon as they prepare for an entry into sea water (McCormick et al., 1998). The 1st is related to the energetic expenditure required during this profound process, utilizing their stored energy towards the modification and adaptation of all the bodily functions mentioned in the introduction (Kipanyula & Maina, 2016; Sheridan, 1989). Hence, as the salmon becomes lengthier, the leftover energy available isn't sufficient to grow its weight proportionally, and the condition factor is reduced accordingly (McCormick et al., 1998). The 2nd hypothesis proposed is that the lengthier and streamlined appearance obtained by smolts is an adaptation facilitating a pelagic life-style, where the fish transitions from a stationary

habituation in the rivers towards constant movement in the oceans (Kipanyula & Maina, 2016; McCormick et al., 1998). These two factors likely occur simultaneously in the developing salmon, both displaying the magnitude and importance of smoltification.

Gill NKA activity was increased during smoltification:

One of these energy-demanding efforts accumulating in the observed decrease in condition factor is the physiological transformation in gill function. Being the main organ working towards maintaining ionic homeostasis through osmoregulation, a movement from ion-deprived fresh waters into ion-rich salt waters requires a profound transformation in function (McCormick & Saunders, 1987; Nilsen et al., 2007). In order to commence the active outward pumping of ions occurring in smolts, the gill function is gradually reversed (from retaining to excreting ions) while the salmon is still residing in fresh water, modifying the gills by developing salt water adapted mitochondria-rich chloride cells equipped with Na-K-ATPase enzymes (McCormick & Saunders, 1987; Nilsen et al., 2007). The increased activity of this Na-K-ATPase pump (NKA) observed in the graph in Fig. 9 is a consequence of this transformational procedure taking place in the gills, and is a finding being supported by a wide range of studies on salmonids to be an essential adaptation for survival in sea water. Hence, the upward trend of this graph is a renowned indication of smoltification taking place (McCormick & Saunders, 1987; Nilsen et al., 2007).

Morphological changes:

In addition to the presented graphs of condition factor and gill NKA activity evidently suggesting the initiation of smoltification following the winter signal, external bodily cues could also be observed in the sampled fish, further supporting this hypothesis. In the morphological aspect, factors being readily apparent to the naked eye, the colorization patterns changed as the salmon developed. The fish obtained a more silvery appearance while their fin margins became darker (ref. Fig. 5, SS03/19 and SS04/19) (Hoar, 1988; McCormick et al., 1998).

These presented results demonstrate how the Atlantic salmon studied in this thesis in fact underwent the smoltification process following the exposure to the winter signal.

4.2.2. Topographic profile of cone opsins:

In general, the topographic profile of visual opsins in Atlantic salmon is different in the various cone opsin classes:

In higher vertebrates, the visual system is highly adapted to the species' respective photopic environments. This is reflected in a retinal topography consisting of specialized regions where certain opsins expressed in photoreceptors are preferred (Carleton et al., 2020; Temple, 2011). This knowledge was used as a foundation for the hypothesis stating that the topographic profile of visual opsins in Atlantic salmon in general is different in the various cone opsin classes. By looking at Fig. 11-14, and with a special attention to Fig. 15 displaying an overview of the retinal expression of the various opsins, there are clear tendencies to be observed in the patterns followed by the opsins. There are certain distinctions observed between the individual opsins, but the clearest differences are most readily detectable by comparing the expression patterns of single- and double cones. What is generally observed through the whole period, is that the single cone opsins *sws1* and *sws2* are concentrated mainly in the areas adjacent to the CMZ. *Sws1* is almost solely restricted to this area of generation (apart from a few *sws1* positive cells located in the dorsal retina during the parr and mid-smolt stages), while *sws2* are more widely distributed across the dorsal and ventral sections. Moving towards the central retina, there's a considerable reduction in photoreceptors expressing these opsins, with expression of *sws1* having completely disappeared and only a few *sws2* positive cells being detectable. This makes for a natural transition towards discussing the double cone opsins *rh2* and *lws*, which both display expression patterns greatly contrasting those of the single cone opsins. Comparable to *sws1* and *sws2*, the expression of *rh2* and *lws* is most prominent in the areas adjacent to the CMZ, displaying similar expression levels in the dorsal and ventral retina. It is in the central retinal areas, however, that the difference between these opsin classes becomes apparent. Although displaying different levels of expression, both *rh2* and *lws* are generally distributed in a magnitude of tightly packed photoreceptors all across the central retina.

Cones are most widespread in the ventro-temporal part of the retina:

The topographic distribution of cone opsins in the retina reflects their spectral requirement in the visual field. Generally, photoreceptors required for the detection of visual cues in the upper parts of the visual field (above the animal) are most prominent in the ventral retina, photoreceptors exposed to frontal visual signals are located in the central retina, while

photoreceptors developed with the purpose of detecting visual cues from below the animal are located dorsally (Carleton et al., 2020; Temple, 2011). The local densities of cone photoreceptors have been studied in a wide range of salmonids, and the general consensus is that cones are most widespread in the ventro-temporal retina, a fact that is shown to be current for all four cone opsins (Ahlbert, 1976; Beaudet et al., 1997). This ventro-temporal domination of cones seen in salmonids is a likely natural adaptation to their benthic habituation in fresh water where the parr resides near the sentiments, facing the water current frequently searching for zooplankton drifting along a few meters in front and above their heads (Ahlbert, 1976). When these zooplankton are exposed to light, a visual signal is emitted that strikes the salmonid's eye, entering dorsally through the lens and is absorbed by the photoreceptors located ventrally (Ahlbert, 1976). This ventro-temporal domination of cones is shown to persist in the retina as the salmonid grows and enters the oceans, at a stage where it becomes increasingly more difficult to make a connection between the salmonid's feeding habit and it's retinal topography (Ahlbert, 1976). In the oceans, their exogenous feeding becomes more diverse, preying on a range of different species located more unevenly in the water column (Jacobsen & Hanse, 2001). However, the fact that most ocean-residing salmonids spend the largest proportion of their life in the upper few meters of the water column (Reddin et al., 2011), foraging for schooling fish and organisms near the surface (Jacobsen & Hanse, 2001), has likely had an influence on the observed distribution (Ahlbert, 1976).

By comparing our results to those presented in these studies, this ventro-temporal domination of cone photoreceptors can only evidently be observed in the *sws2* opsin. By studying Fig. 12 and 15, especially focusing on the stages of mid-smolt, smolt and after 1 month in sea water, there's a clear tendency of a more widespread distribution of *sws2* positive cells in the ventral retina compared to the dorsal retina. For *sws1*, however, it becomes difficult to clearly differentiate between the dorsal and ventral expression, making it infeasible to speculate whether these results can support the ventro-temporal domination theory or not. This can also be said for both members of the double cone structure, where a general consensus gathered from Fig. 13, 14 and 15 is their representation in all retinal sections, being seemingly evenly distributed in the dorsal and ventral retina. Hence, the distribution of the both *rh2* and *lws* being rather proportional in the dorsal and ventral retina, clearly expressed in the areas adjacent to the CMZ, is in contrast to what was presented by Ahlbert (1976), a distribution following the studied Atlantic salmon and trout (*Salmo trutta)* from a parr and into adulthood (Ahlbert, 1976).

The ratio between double- and single cone opsins:

Another finding that is more related to our results, as it is universally current for all the cone opsins investigated in this thesis, is the accepted knowledge of the ratio of double- to single cones universally favouring the presence of double cones in the salmonid retina, which in the study by Ahlbert (1976) were at its highest ventrally, gradually being evened out towards the dorsal retina (Ahlbert, 1976). What has been shown in our study, is that the number of double cones expressed in the central retina compared to the single cones greatly favours the former, a finding that supports this ratio-theory. The importance of double cones being heavily distributed in the central areas are commonly related to intra- and/or interspecific recognition of species, with immature salmonids reflecting a silvery-green colour requiring green sensitivity, and spawning salmonids displaying red coloration requiring red sensitivity (Dann, 1997). The *lws* being the most prominent cone opsin expressed in the retina indicates that the ability to perceive these electromagnetic waves are of utmost importance to the fish. The more densely packed distribution of double cones compared to single cones in the central retina makes for a transition towards discussing the square mosaic patterns developed in salmonids. The square mosaic have single cones positioned in the centre (blue sensitive) and the corner (UV sensitive) of the mosaic, and four paired cones (either green- or red sensitive (twin cones), or both (double cones)) located on the sides (Cheng et al., 2006). The morphological structure of the mosaic structures distributed throughout the retina, consisting of a larger number of double cones compared to the singular, central blue cone, have likely influenced the findings of this study of a more prominent presence of *rh2* and *lws* in the central retina compared to the scattered distribution of *sws2*.

Fig. 10-15 shows how both members of the double cone structure, the *rh2* and *lws*, displays an expression that is considerably more dense and widespread compared to the single cones throughout the retina, *sws1* and *sws2*. However, the topographic distribution of *rh2* and *lws* displayed in our results only demonstrates the expression provided by the utilized probes targeting all the underlying paralogues of these opsins. This means that the actual expression of the various paralogues could differ from what is presented in this study, potentially being distributed in more specific locations than the widespread expression displayed in Fig. 13 and 14. Hence, to fully understand the complexity of the expression patterns of double cones and their dynamics in Atlantic salmon, future research should aim to generate paralogue specific probes for a more accurate establishment of the actual retinal topography. This has been done successfully in Atlantic cod, visualizing the individual topography of the underlying paralogues of *sws2* and *rh2* during development (Valen et al., 2016, 2018).

The general conclusion obtained from the thorough examination of the expression patterns of the cone opsins in photoreceptors presented in this study, is that there are clear evidences to confirm that cone opsins have different topographic profiles in the retina, which are supported by findings in the literature.

4.2.3. Topographic profile of rhodopsins:

The topographic pattern of rhodopsin is different from cone opsins:
Rhodopsin is expressed in rod photoreceptors and is in contrast to the photopic cone opsins, responsible for scotopic vision (Lin et al., 2017). Knowing this, in addition to the different methods followed in the differentiation of rods and cones towards the expression of their respective opsins, it was hypothesized that the topographic pattern of *rhodopsin* is different to that of cone opsins. By studying Fig. 10 and 15, the expression of *rhodopsin* is consistent in all retinal areas throughout the whole period studied, and seems to be evenly distributed in the dorsal, ventral and central retina. This consistency followed by *rhodopsin* is contrasting to what is observed in cones, displaying alterations to opsin topography to varying degrees as the fish develops. This transformational observation will be discussed thoroughly in the next section. These findings are supported by a wide range of studies performed on several teleosts, which demonstrates how the differences observed in expression patterns can be related to the way these photoreceptors are generated (Fadool, 2003; Otteson & Hitchcock, 2003; Deborah L. Stenkamp, 2007).

Continued generation of rod photoreceptors:
Where neurogenesis of newly differentiated cone photoreceptors and their respective opsins are originated in the CMZ (Otteson & Hitchcock, 2003)(a procedure that will be discussed in a later section), rod photoreceptors are produced by rod precursors located in the outer nuclear layer (ONL) (Fadool, 2003). These proliferating precursor cells are originated from progenitor cells within the inner nuclear layer (INL), generated with the purpose of continuously supplying the growing retina with rod photoreceptors (Fadool, 2003; Otteson & Hitchcock, 2003). Rod precursors readily generate new *rhodopsin* positive cells to be positioned in the available spaces opened up between cone square mosaics, commonly thought to be distributed in a random and sporadic manner (Novales Flamarique & Hawryshyn, 1996; Raymond et al., 1995; Schmitt & Dowling, 1996), but also proposed to be arranged into regularly spaced rows of formations resembling mosaics (Fadool, 2003). This process maintains the scotopic acuity

facilitated by these photoreceptors as the retina expands in a balloon-like fashion during growth (in goldfish, a 4-fold increase in body size is accompanied by a 6-fold increase in retinal size) (Pamela Raymond Johns & Easter, 1977), a mechanism stretching out the retinal area while thinning out the retinal layers (Deborah L. Stenkamp, 2007). This is an important adaptation typically seen in species undergoing post-embryonic development, and is a developmental aspect that has resulted in the ratio between the two photoreceptor classes present in the retina (rods and cones) changing considerably as the fish becomes older. As has been shown in goldfish, the rod-cone ratio was 1:1 in larvae at 1-2 months, 6:1 after a year, and 15:1 in 4-5 year old fish (P. R. Johns, 1982). This is in accordance with the established theory that all other retinal cells (cones included) decrease in density as the fish grows, while the amount of rods are increased (P. R. Johns, 1982; Pamela Raymond Johns & Fernald, 1981; Julian et al., 1998; Li & Maaswinkel, 2006; Deborah L. Stenkamp, 2007). Salmonids follow the same line of development as goldfish, with photoreceptor ratio gradually favouring the presence of rods as the fish grows (Kunz et al., 1994). For vertebrates in general, rod photoreceptors are generally distributed more widely and less restricted to certain areas compared to cones. The ratio of rods to cones favouring the former is the case for most vertebrates, and the most considerable differences are observed in many primates and other mammals, equipped with a retinal topography that is likely affected by the nocturnal lifestyle of these species (Carleton et al., 2020; Hunt et al., 2009). The prominent presence of rods together with the less developed photopic system (many mammals have 2 cone opsins (dichromats) while primates have 3 (trichromats)) have facilitated the ability to perceive the animal's surroundings in dimmed lighting conditions (Hunt et al., 2009). This is reflected in the number of photoreceptors seen in the retina of the Pigtail macaque (*Macaca nemistrina*), having an average of 3.1 million cones and 60.1 million rods (Packer et al., 1989). The continuous proliferation of rod precursors throughout the retinal layers in the Atlantic salmon consequently leading to the ratio of rods and cones greatly favouring the former, is an occurring event having influenced the clear and constant expression of *rhodopsin*, evidently confirming that the topographic pattern of this opsin differs from the various cone photoreceptors.

4.2.4. Retinal transformation and changed topographic patterns:

During retinal transformation the topographic patterns of visual opsins change:

After having discussed how the presented opsins are distributed and expressed throughout the

retina with a general overlook, transitioning towards the potential alterations occurring as the Atlantic salmon develops becomes natural. Hence, it was hypothesized that as the fish develops and a transformation to the retinal structure proceeds, the topographic patterns of visual opsins change. The post-embryonic development seen in a wide range of teleosts, commonly seen in species following an indirect development (Evans & Fernald, 1990; Flegler-Balon, 1989), have provided these species with the retinal plasticity required to transform their visual system and its properties as the fish develops, a golden opportunity present in an environment of constant change (Carleton et al., 2020; Valen et al., 2016, 2018). This is in great contrast to species following a strictly direct development, equipped with a fully functional retina prior to the appearance of visual sense (Hitchcock et al., 2004). With the previous section having focused on how this developmental approach have affected the population of rod photoreceptors, the contents of this section will be directed towards the various cone opsins. By comparing the expression displayed during the smoltification process in Fig. 10-15, the developmental nature of *sws1* stands out in the aspect of transformation.

Expression of sws1 is downregulated through the smoltification process:

The most constant change in expression patterns is detected in *sws1,* which by taking a closer look at Fig. 11 and 15 can be seen to be downregulated through the smoltification process, where the expression level of the cluster of UV sensitive cells located adjacent to CMZ both in the dorsal and ventral retina are gradually diminishing as the fish develops from a parr towards an ocean-residing smolt. These findings correspond to what is already known to be the case for many other salmonids, having their ability to sense light in the UV part of the spectrum considerably reduced during growth (Cheng et al., 2006; Cheng & Novales Flamarique, 2007a, 2007b). This is an adaptation initiated at the yolk-sac stage, gradually depriving the salmon's UV sensitive cones (which at hatching were saturated in the retina) (Kunz et al., 1994), following the salmon all the way into the oceans until most or all expression is erased (Kunz et al., 1994). Looking at the downregulatory matter through an evolutionary perspective, the general and most plausible cause of the loss of a function is the reduced requirement of this very function (Pichaud & Desplan, 2016), with the *sws1* opsin being the prime example in salmonids having this developmental fate. The importance of *sws1* in visual perception was for a long time questioned by pointing towards its restricted distribution in the retina, being almost solely confined to a small section adjacent to the CMZ (Kunz, 1987; Novales Flamarique, 2013). However, the profound conditional transformations occurring during a transfer from one aquatic habitat to the other, a natural manner that will be

discussed further later, has likely influenced the gradual loss of UV sensitivity, as the need for perceiving light in the UV section of the spectrum is considerably reduced as photic exposure and favoured prey changes (Novales Flamarique, 2013).

Regeneration of sws1:

Several studies have demonstrated that a few *sws1* positive cells retain their presence in the dorsal retina of certain salmonids (especially rainbow trout) into adulthood (Cheng et al., 2006; Cheng & Novales Flamarique, 2007a). This could indicate that the potential for perceiving UV light persists as the salmon grows older, maintaining a buffer of expressed cells for a possible regeneration when this would be required, likely associated with the upward migration into the rivers performed by sexually mature salmonids (Allison et al., 2006; Deutschlander et al., 2001; Hawryshyn et al., 2003). For the salmon studied in this thesis, *sws1* expression was still slightly observable in the retina adjacent to the CMZ after having spent 1 month in sea water. The constant downward trend of regulation seen through the period studied could indicate that expression would ultimately disappear completely, but further studies on later stages would be required to confirm this. A study by Novales Flamarique in 2002 showed a partial re-incorporation of UV sensitive corner cones in the dorsal retina of Atlantic salmon at sexual maturation, suggesting that a total loss of UV sensitivity is not the case for this species. The same study also suggested that the incorporation might start during the smolt stage (Novales Flamarique, 2002). In our study, one of the sections investigated from the scanned eye displayed a clear upregulation of *sws1* after 1 month in sea water. This contradicts the findings of all other sections and eyes studied, where expression is only slightly visible, and is unlikely to be representative for the species – but is an interesting find that could further support the theory presented by Novales Flamarique.

Does opsin changeover occur in all salmonids?

In the introduction, the background regarding the underlying cellular mechanisms responsible for the loss of UV sensitive opsins in corner cones was thoroughly discussed. In salmonids, the likely causations of this downregulatory development is two coherently working processes called apoptosis and opsin changeover (Cheng et al., 2006). The theory of opsin changeover, demonstrated that in order to fully understand the loss of *sws1* it would have to be studied in relation to the increased presence of *sws2* (Cheng et al., 2006; Cheng & Novales Flamarique,

2004, 2007a, 2007b). There are findings in Atlantic salmon, however, that question whether the opsin changeover process occurs at all in this species.

A study by Cheng et al. (2006) demonstrated that at a very early age, when the fish weighed approximately 1g, nearly all corner cones expressing *sws1* had been lost, with single cones in the centre of the mosaic square already expressing *sws2* (Cheng et al., 2006). Additionally, unpublished results by Eilertsen display how *sws2* expression is clearly present already at hatching. Hence, what this could indicate, and what was theorized by Cheng et al. (2006), is that if opsin changeover could be related to Atlantic salmon, the process would've had to commence during the embryonic stage (Cheng et al., 2006). This is in great contrast to most other species possessing this mechanism, where the opsin switch is initiated close to full yolk-sac absorption (Cheng & Novales Flamarique, 2007a). What this also indicates, is that if the opsin changeover actually occurs in Atlantic salmon, it is less related to smoltification than what is shown in other salmonid species – established in the literature as a mechanism working coherently with the smoltification process with the purpose of facilitating the adaptation of the fish's visual acuity as the environmental conditions change during the migratory transition (Carleton et al., 2020). Another finding that could further demonstrate how the downregulation of UV sensitivity occurs differently in Atlantic salmon, is that the expression of *sws1* seems to be equally apparent adjacent to the CMZ both in the dorsal and ventral retina. Cheng et al. (2006) displayed how these expression patterns were present in Atlantic salmon parr (Cheng et al., 2006), and by this demonstrating how the downregulation of UV sensitivity in Atlantic salmon differs to that of other salmonids, where the process proceeds from the ventral and towards the dorsal retina. In these species, and what is not the case for Atlantic salmon, is that the opsin changeover process ultimately depletes the ventral retina of *sws1* positive cells (Cheng et al., 2006; Cheng & Novales Flamarique, 2007a, 2007b). However, as is shown in Fig. 11, the few individual cells expressing *sws1* apart from the marginal areas were located in the dorsal retina during the parr and mid-smolt stage, potentially illustrating a resemblance to the dorsal domination of UV sensitivity observed in other salmonids (Cheng & Novales Flamarique, 2007a).

Expression of sws2 fluctuates as the smoltification process proceeds:

Having established through the presented literature how retinal transformations potentially differs in Atlantic salmon compared to other salmonids, it is natural to make a transition towards looking at the expression of *sws2* in our results. Fig. 12 and 15 makes for interesting viewing as the regulation of this opsin seems to follow a more fluctuating pattern. During the

earliest period, as a parr, *sws2* positive cells are distributed clearly throughout the retina, with expression readily observable adjacent to the CMZ both in the dorsal and ventral retina, diminishing slightly towards the central areas. Although being the earliest stage studied in this thesis, correlating these findings to the restricted presence of *sws1* during the same stage, indicates that if the opsin changeover process has occurred in the sampled fish, it has advanced considerably, having a clear effect on the single cone opsin distribution in the retina. Based on the opsin changeover theory, the likely scenario would be that the sensitivity to blue light would gradually increase from this stage forward. However, as the salmon grew and became a mid-smolt, the expression of *sws2* in cone photoreceptors decreased considerably, both adjacent to the CMZ and in the central retina, where expression is absent in the latter. From this stage onwards, however, and what is in accordance with the opsin changeover theory, expression proceeded to increase as the salmon developed, displaying a gradual upregulation through the smolt period and until having spent a month in sea water. The clear expression displayed during the parr stage differing considerably from the following stages was observed to be represented in the surrounding sections of the investigated eye, in addition to all three fish that ISH were performed on. This indicates that the displayed distribution of *sws2* positive cells in Fig. 12 reflects the real expression present in the retina during this stage, and not being a consequence of a faulty ISH-process. The considerable downregulation from parr to mid-smolt, followed by an upregulation during the smolt stage and after 1 month in sea water, was also determined to be represented across all sections and eyes studied, reflecting the actual expression in the retina. The observance of the *sws2* opsin expression fluctuating as noticeably in the Atlantic salmon studied could support the theory questioning whether opsin changeover is a process presented in this species at all (Cheng et al., 2006). However, this doesn't change the fact that the hypothesis of visual opsins undergoing alterations as the retina develops were confirmed for both *sws1* and *sws2*.

Sws2 in the central retina:

Another interesting finding that was established after a thorough examination of all sections treated with the *sws2* probe, determined the increased presence of expression in an area surrounding the optic nerve during the smolt-stage (Fig. 15, C3). As the optic nerve is located in the centro-ventral retina (Novales Flamarique & Hawryshyn, 1996), these findings could further support the observance of a ventral domination of blue sensitivity in the studied salmon. Knowing that the opsins expressed in photoreceptors are generally positioned in the retina according to where their spectral sensitivities are required (Temple, 2011), there is

likely no coincidence that the areas of utmost importance in the generation of new cone photoreceptors, like the ciliary marginal zone (CMZ) in teleosts (discussed in the following section), is located in the retina at positions where the requirement for visual acuity is most prominent. This information demonstrates the development of the teleost retina and the distribution of photoreceptors expressing opsins as a double-edged sword, two mechanisms working together towards the same purpose. These co-working adaptations likely presented the most effective method in the development of a complex visual system facilitated for the visual perception of the medium, having evolved universally in both aquatic- and land-based animals. The latter is reflected in the photoreceptor distribution in the fovea of primates, an eye structure unique to higher primates located in the central retina just dorsally of the optic nerve (Bringmann et al., 2018), almost solely consisting of photoreceptors expressing cone opsins (Bumsted et al., 1997; Packer et al., 1989). Additionally, the fovea is the "CMZ of primates", the proliferating area of the eye where photoreceptors are generated (Bumsted et al., 1997). This central distribution of cones, which is observed in a wide range of land-living animals, is a likely consequence of the food they forage for being located in their central field of vision (Carleton et al., 2020; Wikler et al., 1990). The same appears to be the case for salmonids, where the ventro-temporal domination of cones seems to be related to where their natural prey are located in the water column, typically in front and above the fish (Ahlbert, 1976). Hence, the centro-ventral expression of *sws2* adjacent to the optic nerve observed in this study during the smolt stage could further demonstrate the importance of the ventral retinal areas, while at the same time highlighting another proliferating zone in salmon, the embryonic fissure. Studies have shown how the embryonic fissure functions as the leading area of neurogenesis during the earliest embryonic stages in salmonids (Novales Flamarique & Hawryshyn, 1996), and continues to provide this function in the generation of *sws1* during later stages (Kunz, 1987; Novales Flamarique, 2000). Our findings, however, have in addition to providing further support to the importance of the embryonic fissure and its continued requirement in cone generation, displayed how this proliferating zone continues to generate *sws2* opsins during the smoltification process. What these findings demonstrate is that both single cones, *sws1* and *sws2*, are incorporated into the expanding retina in the areas surrounding the embryonic fissure, and could potentially indicate an evolutionary developed function in salmonids working to prevent that the ratio between double- and single cones becomes too large.

The distribution of rh2 and lws is more constant during smoltifcation:
By studying Fig. 13, 14 and 15, it becomes apparent that the topographic distribution of the double cones *rh2* and *lws* are more constant in their appearance through the smoltification process, with no clear signs of any alterations having occurred in these opsins. This could be supported by findings in the literature, demonstrating how the opsin changeover process doesn't occur in double cones (Cheng et al., 2006; Cheng & Novales Flamarique, 2007b). These findings indicate that the requirement for the photopic sensitivities these opsins provide are consistent throughout the studied period.

4.2.5. Visual opsins in ciliary marginal zone:

The appearance of visual opsins in ciliary marginal zone is reflected in the retinal transformation:
Neurogenesis is the physiological mechanism of neuron-synthesis, creating new nerve cells throughout the central nervous system (CNS) (Otteson & Hitchcock, 2003). Following the initial embryonic surge of photoreceptors in a fan-shaped manner common to salmonids (Cheng et al., 2007) and cyprinids (Raymond & Barthel, 2004; Deborah L. Stenkamp et al., 1996), at later stages there are two retinal areas of utmost importance in the creation of new photoreceptor cells. These areas are the outer nuclear layer (ONL) (rods) (Fadool, 2003) and the ciliary marginal zone (CMZ) where cones are created (Otteson & Hitchcock, 2003), and which will be the focus of this section. The importance of the CMZ in the generation of new cones can be readily observed in the figures, where expression is universally at its strongest in the areas adjacent to the CMZ. Hence, it was hypothesized that the appearance of visual opsins in the CMZ would be reflected in the retinal transformation. First, it is of importance to understand the developmental processes followed by the proliferating cells located in these areas. Multipotent stem cells have the potential of creating progenitor cells in the retina. These progenitor cells can either divide symmetrically, amplifying the population of progenitor cells - or asymmetrically, creating two dissimilar daughter cells with different fates. One is to become the former progenitor cell, while the other is differentiated into a newly formed neuron, potentially becoming rod- or cone photoreceptors (Otteson & Hitchcock, 2003). This differentiation into photoreceptor cells is assumed to occur in a step-wise process, which was shown by Stenkamp et al. in 1997 to be the case in the generation of cone photoreceptors (Deborah L. Stenkamp et al., 1997). First, the proliferating progenitor cell decides whether to create a photoreceptor (cone) cell or not. If the differentiation results

in a cone photoreceptor, the process proceeds by synthesizing a specialized specific phenotype (opsin) adapted for the purpose of receiving electromagnetic waves of different wavelengths (Deborah L. Stenkamp et al., 1997). In the CMZ, new neuronal cells are added to the retinal layers in a concentric annulus resembling the growth rings on a tree. This means that the most recently produced and least determined cells reside within the CMZ, newly differentiated cells are positioned just adjacent to the CMZ, and the more mature cells are pushed towards the central retina (Otteson & Hitchcock, 2003; Deborah L. Stenkamp, 2007). Relating the mechanisms occurring in the proliferation of cells in the CMZ to the results presented in Fig. 10-15, there is, as already mentioned, a clear trend between the various opsins in the importance of this zone, reflected in the prominent expression observed in the area. Additionally, the expression in this section of the retina seems to be maintained throughout the smoltification period studied, especially for *sws2, rh2* and *lws*. For these opsins, this ultimately verifies the presented hypothesis of a consistent incorporation of newly differentiated cone photoreceptors in the CMZ as the Atlantic salmon develops through smoltification. *Sws1,* however, which displays a different developmental pattern and is gradually downregulated, seems to contradict the presented hypothesis.

4.3. Visual transformation in a life history context and aquaculture impact:

4.3.1. Life history transition, life in fresh water and adaptation to sea water:

In order to fully understand the results presented in this study, it is of importance to make a relation to the life history context of the Atlantic salmon, and by this focusing towards the ecological aspect of the smoltification process. As an anadromous species migrating through a range of habitats as they transform from being a newly hatched alevin to a fully grown adult, the most profound change of environmental conditions exposed to the salmon occur during the period investigated in this study. Migrating from the natal river into the vast ocean provide tremendous challenges for the fish to handle. This is a transfer the salmon has prepared for through the profound smoltification process (Boeuf, 1993; Hoar, 1988; McCormick et al., 1998; Stefansson et al., 2008), a transformation proved to have occurred in the Atlantic salmon studied in this thesis. The changes occurring to penetration of electromagnetic waves in the aquatic medium as the salmon migrates has resulted in the retinal alterations to topographic patterns of photoreceptors observed in this study (Carleton et al., 2020; Temple, 2011). A fact that is especially related to the aquatic medium, is that the penetrating ability of light and how photons are distributed in the water column largely depends on in which part of

the visible spectrum it comes from. Hence, following the initial migration of photoreceptors through the retina during the earliest embryonic stages (Cheng et al., 2007), the more developed salmonid shows an expression of opsins in photoreceptors that are distributed according to from which part of the visual spectrum their received photons arrive (Temple, 2011). In most waters, wavelengths from the middle part of the spectrum (blue- and green light) penetrates the furthest, while the shorter and longer wavelengths (UV- and red light, respectively) are restricted to the upper few meters of the water column (Lin et al., 2017). However, it is important to state that the penetration varies greatly depending on the characteristics of the water, which is shown in Fig. 4 (Levine & Macnichol Jr, 1982). This figure demonstrates the profound transformation of photic environment experienced by the salmonid - with their life starting in shallow rivers (Fig. 4, C), where the fish is readily exposed to light from all parts of their visual field, before they later migrate into the oceans (Fig. 4, A), where light with wavelengths from the middle part of the spectrum penetrates the farthest (blue light travels further than green light, being the only electromagnetic waves present at greater depths), while UV- and red light with shorter- and longer wavelengths, respectively, are restricted to the upper few meters of the water column (Lin et al., 2017) (red light is completely absorbed by ocean water) (Levine & Macnichol Jr, 1982). Salmonids experiencing a range of depths during their life-history, have had to develop a visual system adapted to these changing conditions, a fact that is reflected in the general topographic distribution of photoreceptors and how transformations in expression patterns occur in certain opsins, especially relatable to *sws1* (Cheng et al., 2006; Cheng & Novales Flamarique, 2007a, 2007b; Kunz et al., 1994). The evolutionary development of a visual system adapted to its surrounding environment is readily apparent in the density of photoreceptors, and how these concentrations are fluctuating positively or negatively as the animal grows (Temple, 2011).

4.3.2. Square and row mosaic of cone photoreceptors in teleosts:

In order to make further relations between ecology and a specialized visual system, it becomes feasible to present another interesting topic related to the topographic placement of photoreceptors – how cones are arranged and positioned into the organized system seen in the vertebrate retina. In teleosts, these systems are arranged into two different mosaic patterns – the square- and the row mosaic. The morphology of the square mosaic previously discussed is an orderly fashioned and well organized system with the various cones located within the square at positions where they are best suited for visual detection, and is acknowledged as an advanced retinal organization known to certain teleost species (Cheng & Novales Flamarique,

2007a, 2007b). The second mosaic pattern, the row mosaics common to zebrafish, are arranged through the retina with alternating rows of single UV- and blue opsins, and double green- and red opsins (Raymond et al., 1995; Raymond & Barthel, 2004; Viets et al., 2016). In mammals like rodents and primates, on the other hand, photoreceptors expressing cone opsins are generally known to be arranged randomly in the retina. The blue cone is the only photoreceptor type organized into systematically arranged lattice-like mosaics (Hofer et al., 2005), while the green and red cones, which in primates are difficult to differentiate because of their similar spectral sensitivities, are distributed in a stochastic manner (Roorda et al., 2001; Viets et al., 2016). The more organized and less randomized arrangement of mosaics observed in teleosts compared to mammals is a likely consequence of the different environments they inhabit, where living in an aquatic environment requires a visual system more optimized, with the mentioned ability to perceive a wider range of spectral cues (Carleton et al., 2020; Viets et al., 2016). By further comparing the mosaic patterns seen in zebrafish and salmonids, a more advanced and specialized visual system is seen in the latter. The stationary life of a zebrafish is in great contrast to the migratory and highly dynamic life-style of salmonids, and is the likely causation of the differing retinal arrangements observed in these species (van der Meer, 1992; Viets et al., 2016).

4.3.3. Design of light environment related to visual photoreception in aquaculture:
Having related the findings in this study to the ecological aspect of development in the Atlantic salmon retina, a transition will be made towards discussing how the aquaculture industry can utilize this knowledge in order to enhance the artificial lighting systems used in farming. As the utilization of light regarding smoltification (Duncan et al., 1998; Duncan & Bromage, 1998; Thrush et al., 1994), growth (Maiolo et al., 2015; Oppedal et al., 2003) and sexual maturation (Oppedal et al., 2003; Taranger et al., 1999) in aquaculture has already been discussed, this section will be focused on the potential of using light with different wavelengths in salmon farming during the parr stage, through smoltification and in sea water. By looking at our results, the constant presence of both double cone members, *rh2* and *lws*, throughout the whole period investigated would indicate that farming could benefit from the continued utilization of these wavelengths. However, from Fig. 4 it is apparent that red light is restricted to the upper few meters in sea water. This theory is supported by findings in the aquaculture industry, which demonstrated how 80 % of the red light was absorbed by the sea water at 5 meters from the lighting sources (Stien et al., 2014). The same study showed how only 20 % of green light was absorbed by the water (Stien et al., 2014), and demonstrates that

in relation to the sensitivities of double cones in the Atlantic salmon retina, the utilization of green wavelengths in a sea water environment would be most beneficial, a knowledge that is renowned in the aquaculture industry through their usage of light emitting diodes (LEDs) (Migaud et al., 2007). Moving onto the single cone opsins, the development observed in *sws1* and *sws2* expression could be utilized in the aquaculture industry, likely associated with the foraging ability of the salmon as it migrates. The clear presence of *sws1* sensitivity during the parr stage suggests that the ability to perceive UV light is retained at this point, indicating that the utilization of these wavelengths could benefit the fish in its search for feed. The interesting find of a prominent presence of *sws2* during the same stage could potentially indicate that exposing the fish to blue light would be beneficial regarding foraging. As the fish develops further, the decreased presence of *sws1* would suggest that exposing the fish to these wavelengths would prove to be ineffective. In the case of *sws2*, however downregulated from the parr stage to the mid-smolt stage, maintains its presence in the retina throughout the whole period, especially adjacent to the CMZ and most prominently expressed in the ventral retina. In nature, the change in preferred prey from small, transparent zooplankton in fresh water to larger, opaque prey in sea water has likely facilitated this change in topography (Novales Flamarique, 2013). The utilization of this knowledge is present in current aquaculture, and especially in sea water, where the mentioned LEDs, in addition to green light, emits blue light (Migaud et al., 2007). Additionally, the ventral domination of *sws2* positive cells could indicate that exposing the reared fish to blue light emitted from sources located above would be beneficial during feeding. This indicates that the knowledge obtained from the findings in our study can provide the aquaculture industry with helpful information on how light of different wavelengths can be utilized to maintain a streamlined and economically favourable production.

5. Conclusion:

Through this study, the topographic distribution and the retinal development of all the acknowledged opsin classes present in Atlantic salmon were examined thoroughly and followed through the smoltification period, a process that was confirmed to have occurred in the sampled salmon through analysis of condition factor and gill NKA activity. This study not only builds on the knowledge from previous studies heavily focused towards the single cone opsins and their regulatory behaviour, but has also highlighted the more constant distribution

of *rh2* and *lws* - the double cone opsin classes and their expression patterns that have been slightly neglected in the past. The most profound topographic alterations were observed in the single cone photoreceptors, *sws1* and *sws2*, a finding in accordance with what has been detected in a range of other salmonids. However, if this regulation of opsin-expression is a consequence of the renowned opsin changeover mechanism, and whether this process can be related to smoltification, are factors that can be debated on the background of what was observed in this study. The fluctuating dynamic of *sws2* expression could indicate that Atlantic salmon differ in their way of regulating single cone opsins. Another interesting finding regarding *sws2*, that has not been discovered in the past, is the continued presence of this opsin in the central areas surrounding the optic nerve, providing further support to the importance of the embryonic fissure in the proliferation of single cones during the smoltification process. Future research should involve thorough analysis of the *sws2* opsin and its expression patterns in order to further establish this centro-ventral presence of blue sensitivity.

In addition, the topographic distribution of cone opsins generally varied in the retina, with the biggest differences observed between the single and double cones – while *rhodopsin* displayed an expression pattern different to that of the cone opsins. The appearance of photoreceptors expressing cone opsins in the CMZ through retinal transformations was confirmed for both the double cone opsins, *rh2* and *lws*, as well as the single cone opsin *sws2*. The downregulatory nature of *sws1* expression levels, however, demonstrated how this occurrence wasn't reflected and present in this opsin.

To ensure a strong expression in the tissue, which was of importance to this study, the probes utilized was generated to reveal the expression of all the various paralogues within an opsin. In order to fully understand the extent of expression in these opsins, especially in relation to *rh2* and *lws*, specific probes targeting each underlying gene is required. These specialized specific probes would determine the topographic patterning of the individual paralogues present. Hence, further research on this topic should include analysis based on these specialized probes, which has been done successfully in studies on Atlantic cod (Valen et al., 2016, 2018).

6. References:

Acloque, H., Wilkinson, D. G., & Nieto, M. A. (2008). In Situ Hybridization Analysis of Chick Embryos in Whole-Mount and Tissue Sections. In *Methods in Cell Biology* (Vol. 87, pp. 169–185). Academic Press. https://doi.org/10.1016/S0091-679X(08)00209-4

Ahlbert, I.-B. (1976). Organization of the Cone Cells in the Retinae of Salmon (Salmo salar) and Trout (Salmo trutta trutta) in Relation to Their Feeding Habits. *Acta Zoologica*, *57*(1), 13–35. https://doi.org/10.1111/j.1463-6395.1976.tb00208.x

Ali, M. A. (2008). Histophysiological studies on the juvenile Atlantic salmon (Salmo salar) retina: II: Responses to light intensities, wavelengths, temperatures, and continuous light or dark. *Canadian Journal of Zoology*. https://doi.org/10.1139/z61-055

Allison, W. T., Dann, S. G., Veldhoen, K. M., & Hawryshyn, C. W. (2006). Degeneration and regeneration of ultraviolet cone photoreceptors during development in rainbow trout. *The Journal of Comparative Neurology*, *499*(5), 702–715. https://doi.org/10.1002/cne.21164

Archer, S. N. (1999). Light and photoreception: Visual pigments and photoreception. In *Adaptive Mechanisms in the Ecology of Vision* (pp. 25–42). Springer Netherlands. https://doi.org/10.1007/978-94-017-0619-3_2

Baker, S. A., & Kerov, V. (2013). Photoreceptor inner and outer segments. In *Current Topics in Membranes* (Vol. 72, pp. 231–265). Academic Press Inc. https://doi.org/10.1016/B978-0-12-417027-8.00007-6

Balon, E. K. (1985). Early life histories of fishes: new developmental, ecological and evolutionary perspectives. *Biological Conservation*. https://doi.org/10.1007/978-94-010-9258-6

Balon, E. K. (1990). Epigenesis of an epigeneticist: the development of some alternative concepts on the early ontogeny and evolution of fishes. *Journal.Lib.Uoguelph.Ca*.

Beaudet, L., Novales Flamarique, I., & Hawryshyn, C. W. (1997). Cone photoreceptor topography in the retina of sexually mature Pacific salmonid fishes. *Journal of Comparative Neurology*, *383*(1), 49–59. https://doi.org/10.1002/(SICI)1096-9861(19970623)383:1<49::AID-CNE4>3.0.CO;2-L

Björnsson, B. T., Einarsdottir, I. E., & Power, D. (2012). Is salmon smoltification an example of vertebrate metamorphosis? Lessons learnt from work on flatfish larval development. *Aquaculture*, *362–363*, 264–272. https://doi.org/10.1016/j.aquaculture.2011.03.002

Björnsson, B. T., Stefansson, S. O., & McCormick, S. D. (2011). Environmental

endocrinology of salmon smoltification. *General and Comparative Endocrinology*. https://doi.org/10.1016/j.ygcen.2010.07.003

Blake, R. L., Roberts, F. L., & Saunders, R. L. (1984). Parr-smolt transformation of Atlantic salmon (Salmo salar): activities of two respiratory enzymes and concentrations of mitochondria in the liver. *Canadian Journal of Fisheries and Aquatic Sciences, 41(1)*, 199–203. https://doi.org/10.1139/f84-021

Blanton, M. L., & Specker, J. L. (2007). The Hypothalamic-Pituitary-Thyroid (HPT) Axis in Fish and Its Role in Fish Development and Reproduction. *Critical Reviews in Toxicology*, *37*(1–2), 97–115. https://doi.org/10.1080/10408440601123529

Boeuf, G. (1993). Salmonid smolting: a pre-adaptation to the oceanic environment. In *Fish Ecophysiology* (pp. 105–135). Springer Netherlands. https://doi.org/10.1007/978-94-011-2304-4_4

Bowmaker, J. K. (1998). Evolution of colour vision in vertebrates. *Eye (Basingstoke)*, *12*(3), 541–547. https://doi.org/10.1038/eye.1998.143

Bowmaker, J. K. (2008). Evolution of vertebrate visual pigments. *Vision Research*. https://doi.org/10.1016/j.visres.2008.03.025

Bowmaker, J. K., & Hunt, D. M. (2006). Evolution of vertebrate visual pigments. In *Current biology : CB*. https://doi.org/10.1016/j.cub.2006.06.016

Bringmann, A., Syrbe, S., Görner, K., Kacza, J., Francke, M., Wiedemann, P., & Reichenbach, A. (2018). The primate fovea: Structure, function and development. In *Progress in Retinal and Eye Research* (Vol. 66, pp. 49–84). Elsevier Ltd. https://doi.org/10.1016/j.preteyeres.2018.03.006

Bumsted, K., Jasoni, C., Szél, A., & Hendrickson, A. (1997). Spatial and temporal expression of cone opsins during monkey retinal development. *Journal of Comparative Neurology*, *378*(1), 117–134. https://doi.org/10.1002/(SICI)1096-9861(19970203)378:1<117::AID-CNE7>3.0.CO;2-7

Carleton, K. L., Escobar-Camacho, D., Stieb, S. M., Cortesi, F., & Marshall, N. J. (2020). Seeing the rainbow: mechanisms underlying spectral sensitivity in teleost fishes. *The Journal of Experimental Biology*, *223*(8), jeb193334. https://doi.org/10.1242/jeb.193334

Cheng, C. L., Gan, K. J., & Novales Flamarique, I. (2009). Thyroid hormone induces a time-dependent opsin switch in the retina of salmonid fishes. *Investigative Ophthalmology and Visual Science*, *50*(6), 3024–3032. https://doi.org/10.1167/iovs.08-2713

Cheng, C. L., Gan, L. J., & Novales Flamarique, I. (2007). The ultraviolet opsin is the first opsin expressed during retinal development of salmonid fishes. *Investigative*

Ophthalmology and Visual Science, *48*(2), 866–873. https://doi.org/10.1167/iovs.06-0442

Cheng, C. L., & Novales Flamarique, I. (2004). New mechanism for modulating colour vision. *Nature*, *428*(6980), 279. https://doi.org/10.1038/428279a

Cheng, C. L., & Novales Flamarique, I. (2007a). Photoreceptor distribution in the retina of adult Pacific salmon: Corner cones express blue opsin. *Visual Neuroscience*. https://doi.org/10.1017/S0952523807070137

Cheng, C. L., & Novales Flamarique, I. (2007b). Chromatic organization of cone photoreceptors in the retina of rainbow trout: Single cones irreversibly switch from UV (SWS1) to blue (SWS2) light sensitive opsin during natural development. *Journal of Experimental Biology*, *210*(23), 4123–4135. https://doi.org/10.1242/jeb.009217

Cheng, C. L., Novales Flamarique, I., Hárosi, F. I., Rickers-Haunerland, J., & Haunerland, N. H. (2006). Photoreceptor layer of salmonid fishes: Transformation and loss of single cones in juvenile fish. *Journal of Comparative Neurology*. https://doi.org/10.1002/cne.20879

Crescitelli, F. (1958). The natural history of visual pigments. *Annals of the New York Academy of Sciences*, *74*(2), 230–255. https://doi.org/10.1111/j.1749-6632.1958.tb39548.x

Cronin, T. W., & Marshall, J. (2011). Patterns and properties of polarized light in air and water. *Royalsocietypublishing.Org*, *366*(1565), 619–626. https://doi.org/10.1098/rstb.2010.0201

Dann, S. G. (1997). Opsin and Retinal Genomics in Salmonid Fishes: Implications for Phylogeny and Retinal Development. *Department of Biology*.

Dann, S. G., Allison, W. T., Levin, D. B., Taylor, J. S., & Hawryshyn, C. W. (2004). Salmonid opsin sequences undergo positive selection and indicate an alternate evolutionary relationship in Oncorhynchus. *Journal of Molecular Evolution*. https://doi.org/10.1007/s00239-003-2562-y

Davidsen, J. G., Plantalech Manel-la, N., Økland, F., Diserud, O. H., Thorstad, E. B., Finstad, B., Sivertsgård, R., McKinley, R. S., & Rikardsen, A. H. (2008). Changes in swimming depths of Atlantic salmon (Salmo salar) post-smolts relative to light intensity. *Journal of Fish Biology*, *73*(4), 1065–1074. https://doi.org/10.1111/j.1095-8649.2008.02004.x

De Busserolles, F., Cortesi, F., Helvik, J. V., Davies, W. I. L., Templin, R. M., Sullivan, R. K. P., Michell, C. T., Mountford, J. K., Collin, S. P., Irigoien, X., Kaartvedt, S., & Marshall, J. (2017). Pushing the limits of photoreception in twilight conditions: The rod-like cone

retina of the deep-sea pearlsides. *Science Advances*, *3*(11). https://doi.org/10.1126/sciadv.aao4709

Deutschlander, M. E., Greaves, D. K., Haimberger, T. J., & Hawryshyn, C. W. (2001). Functional mapping of ultraviolet photosensitivity during metamorphic transitions in a salmonid fish, Oncorhynchus mykiss. *Journal of Experimental Biology*, *204*(14).

Dickhoff, W. W., Beckman, B. R., Larsen, D. A., Duan, C., & Moriyama, S. (1997). The role of growth in endocrine regulation of salmon smoltification. In *Fish Physiology and Biochemistry* (Vol. 17). https://doi.org/10.1023/A:1007710308765

Duncan, N. J., Auchinachie, N., Robertson, D., Murray, R., & Bromage, N. (1998). Growth, maturation and survival of out-of-season 0 + and 1 + Atlantic salmon (Salmo salar) smolts. *Aquaculture*. https://doi.org/10.1016/S0044-8486(98)00359-7

Duncan, N. J., & Bromage, N. (1998). The effect of different periods of constant short days on smoltification in juvenile Atlantic salmon (Salmo salar). *Aquaculture*, *168*(1–4), 369–386. https://doi.org/10.1016/S0044-8486(98)00363-9

Ebbesson, L. O. E., Björnsson, B. T., Ekström, P., & Stefansson, S. O. (2008). Daily endocrine profiles in parr and smolt Atlantic salmon. *Comparative Biochemistry and Physiology - A Molecular and Integrative Physiology*, *151*(4), 698–704. https://doi.org/10.1016/j.cbpa.2008.08.017

Eilertsen, M., Drivenes, Ø., Edvardsen, R. B., Bradley, C. A., Ebbesson, L. O. E., & Helvik, J. V. (2014). Exorhodopsin and melanopsin systems in the pineal complex and brain at early developmental stages of Atlantic halibut (Hippoglossus hippoglossus). *Journal of Comparative Neurology*, *522*(18), 4003–4022. https://doi.org/10.1002/cne.23652

Ekström P., & Meissl H. (1997). The pineal organ of teleost fishes. *Reviews in Fish Biology and Fisheries*, *7*, 199–284. https://doi.org/10.1023/A:1018483627058

Evans, B. I., & Fernald, R. D. (1990). Metamorphosis and fish vision. *Journal of Neurobiology*, *21*(7), 1037–1052. https://doi.org/10.1002/neu.480210709

Fadool, J. M. (2003). Development of a rod photoreceptor mosaic revealed in transgenic zebrafish. *Developmental Biology*, *258*(2), 277–290. https://doi.org/10.1016/S0012-1606(03)00125-8

Flegler-Balon, C. (1989). Direct and indirect development in fishes — examples of alternative life-history styles. In *Alternative Life-History Styles of Animals* (pp. 71–100). Springer Netherlands. https://doi.org/10.1007/978-94-009-2605-9_5

Folkedal, O., Torgersen, T., Nilsson, J., & Oppedal, F. (2010). Habituation rate and capacity of Atlantic salmon (Salmo salar) parr to sudden transitions from darkness to light.

Aquaculture. https://doi.org/10.1016/j.aquaculture.2010.06.001

Gramage, E., Li, J., & Hitchcock, P. (2014). The expression and function of midkine in the vertebrate retina. *British Journal of Pharmacology*, *171*(4), 913–923. https://doi.org/10.1111/bph.12495

Handeland, S. O., Imsland, A. K., & Stefansson, S. O. (2008). The effect of temperature and fish size on growth, feed intake, food conversion efficiency and stomach evacuation rate of Atlantic salmon post-smolts. *Aquaculture*, *283*(1–4), 36–42. https://doi.org/10.1016/j.aquaculture.2008.06.042

Hansen, T., Stefansson, S., & Taranger, G. L. (1992). Growth and sexual maturation in Atlantic salmon, Salmon, salar L., reared in sea cages at two different light regimes. *Aquaculture Research*, *23*(3), 275–280. https://doi.org/10.1111/j.1365-2109.1992.tb00770.x

Hawryshyn, C. W., Arnold, M. G., Bowering, E., & Cole, R. L. (1990). Spatial orientation of rainbow trout to plane-polarized light: The ontogeny of E-vector discrimination and spectral sensitivity characteristics. *Journal of Comparative Physiology A: Sensory, Neural and Behavioral Physiology*. https://doi.org/10.1007/BF00192027

Hawryshyn, C. W., Martens, G., Allison, W. T., & Anholt, B. R. (2003). Regeneration of ultraviolet-sensitive cones in the retinal cone mosaic of thyroxin-challenged post-juvenile rainbow trout (Oncorhynchus mykiss). *Journal of Experimental Biology*, *206*(15), 2665–2673. https://doi.org/10.1242/jeb.00470

Helvik, J. V, Drivenes, Ø., Naess, T. H., Fjose, A., & Seo, H.-C. (2001). Molecular cloning and characterization of five opsin genes from the marine flatfish Atlantic halibut (Hippoglossus hippoglossus). *Visual Neuroscience*, *18*(5), 767–780. https://doi.org/10.1017/s095252380118510x

Hitchcock, P., Ochocinska, M., Sieh, A., & Otteson, D. (2004). Persistent and injury-induced neurogenesis in the vertebrate retina. In *Progress in Retinal and Eye Research* (Vol. 23, Issue 2, pp. 183–194). Pergamon. https://doi.org/10.1016/j.preteyeres.2004.01.001

Hoar, W. S. (1988). The physiology of smolting salmonids. *Fish Physiology*, *11*(PB), 275–343. https://doi.org/10.1016/S1546-5098(08)60216-2

Hofer, H., Carroll, J., Neitz, J., Neitz, M., & Williams, D. R. (2005). Organization of the Human Trichromatic Cone Mosaic. *The Journal of Neuroscience, 25(42)*, 9669–9679. https://doi.org/10.1523/JNEUROSCI.2414-05.2005

Hunt, D. M., Carvalho, L. S., Cowing, J. A., & Davies, W. L. (2009). Evolution and spectral tuning of visual pigments in birds and mammals. In *Philosophical Transactions of the*

Royal Society B: Biological Sciences (Vol. 364, Issue 1531, pp. 2941–2955). Royal Society. https://doi.org/10.1098/rstb.2009.0044

Iigo, M., Ikuta, K., Kitamura, S., Tabata, M., & Aida, K. (2005). Effects of Melatonin Feeding on Smoltification in Masu Salmon (Oncorhynchus masou). *Zoological Science*. https://doi.org/10.2108/zsj.22.1191

Ilyas, M. (1967). Effect of cloudiness on solar ultraviolet radiation reaching the surface. *Atmospheric Environment (1967)*, *21*(6), 1483–1484. https://doi.org/10.1016/0004-6981(67)90098-4

Jacobsen, J. A., & Hanse, L. P. (2001). Feeding habits of wild and escaped farmed Atlantic salmon, Salmo salar L., in the Northeast Atlantic. *ICES Journal of Marine Science*, *58*(4), 916–933. https://doi.org/10.1006/jmsc.2001.1084

Jerlov, N. (1976). Marine Optics. In *Elsevier Oceanography Series*. https://doi.org/10.1016/S0422-9894(08)70804-3

Johns, P. R. (1982). Formation of photoreceptors in larval and adult Goldfish. In *The Journal of Neuroscience Copyright 0 Society for Neuroscience* (Vol. 2, Issue 2). https://doi.org/10.1523/jneurosci.02-02-00178.1982

Johns, Pamela Raymond, & Easter, S. S. (1977). Growth of the adult goldfish eye. II. Increase in retinal cell number. *The Journal of Comparative Neurology*, *176*(3), 331–341. https://doi.org/10.1002/cne.901760303

Johns, Pamela Raymond, & Fernald, R. D. (1981). Genesis of rods in teleost fish retina. *Nature*, *293*(5828), 141–142. https://doi.org/10.1038/293141a0

Johnston, C. E., & Eales, J. G. (2011). Purines in the Integument of the Atlantic Salmon (Salmo salar) During Parr–Smolt Transformation . *Journal of the Fisheries Research Board of Canada*. https://doi.org/10.1139/f67-085

Julian, D., Ennis, K., & Korenbrot, J. I. (1998). Birth and fate of proliferative cells in the inner nuclear layer of the mature fish retina. *Journal of Comparative Neurology*, *394*(3), 271–282. https://doi.org/10.1002/(SICI)1096-9861(19980511)394:3<271::AID-CNE1>3.0.CO;2-Z

Kipanyula, M. J., & Maina, K. W. (2016). Morphological and adaptational changes associated with fish migration from fresh to marine water bodies. *International Journal of Fisheries and Aquatic Studies*, *4*(4), 125–129. https://doi.org/10.1007/BF01945524

Kirk, J. T. O. (1994). Light and photosynthesis in aquatic ecosystems. In *Choice Reviews Online* (Vol. 32, Issue 05). https://doi.org/10.5860/CHOICE.32-2716

Kunz, Y. W. (1987). Tracts of putative ultraviolet receptors in the retina of the two-year-old

brown trout (Salmo trutta) and the Atlantic salmon (Salmo salar). *Experientia*, *43(11-12)*, 1202–1204. https://doi.org/10.1007/BF01945524

Kunz, Y. W., Wildenburg, G., Goodrich, L., & Callaghan, E. (1994). The fate of ultraviolet receptors in the retina of the atlantic salmon (Salmo salar). *Vision Research*. https://doi.org/10.1016/0042-6989(94)90136-8

Lamb, T. D., Collin, S. P., & Pugh, E. N. (2007). Evolution of the vertebrate eye: Opsins, photoreceptors, retina and eye cup. In *Nature Reviews Neuroscience*. https://doi.org/10.1038/nrn2283

Landgren, E., Fritsches, K., Brill, R., & Warrant, E. (2014). The visual ecology of a deep-sea fish, the escolar Lepidocybium flavobrunneum (Smith, 1843). *Philosophical Transactions of the Royal Society B: Biological Sciences*. https://doi.org/10.1098/rstb.2013.0039

Levine, J. S., & Macnichol Jr, E. F. (1982). Color Vision in Fishes. *Source: Scientific American*, *246*(2), 140–149. https://doi.org/10.2307/24966528

Li, L., & Maaswinkel, H. (2006). Visual Sensitivity And Signal Processing In Teleosts. In *Fish Physiology* (Vol. 25, pp. 179–241). Academic Press. https://doi.org/10.1016/S1546-5098(06)25005-2

Lin, J.-J., Wang, F.-Y., Li, W.-H., & Wang, T.-Y. (2017). The rises and falls of opsin genes in 59 ray-finned fish genomes and their implications for environmental adaptation. *Scientific Reports*, *7(1)*. https://doi.org/10.1038/s41598-017-15868-7

Lythgoe, J. N. (1988). Light and Vision in the Aquatic Environment. In *Sensory Biology of Aquatic Animals* (pp. 57–82). Springer New York. https://doi.org/10.1007/978-1-4612-3714-3_3

Maiolo, S., Hansen, T., Parisi, G., & Olsen, R. E. (2015). Effects of Photoperiod and Melatonin Implants on Feed Intake in Atlantic Salmon *(Salmo Salar* L.) Postsmolts. *Italian Journal of Animal Science*, *14*(4), 4098. https://doi.org/10.4081/ijas.2015.4098

Martin, P., Rancon, J., Segura, G., Laffont, J., Boeuf, G., & Dufour, S. (2012). Experimental study of the influence of photoperiod and temperature on the swimming behaviour of hatchery-reared Atlantic salmon (Salmo salar L.) smolts. *Aquaculture*, *362–363*, 200–208. https://doi.org/10.1016/j.aquaculture.2011.11.047

McCormick, S. D. (1993). Methods for Non Biopsy and Measurement of Na+, K+-ATPase Activity. *Canadian Journal of Fisheries and Aquatic Sciences*, *50(3)*, 656–658. https://doi.org/10.1139/f93-075

McCormick, S. D., Hansen, L. P., Quinn, T. P., & Saunders, R. L. (1998). Movement,

migration, and smolting of Atlantic salmon (Salmo salar). *Canadian Journal of Fisheries and Aquatic Sciences, 55(S1)*, 77–92. https://doi.org/10.1139/d98-011

McCormick, S. D., & Saunders, R. L. (1987). Preparatory Physiological Adaptations for Marine Life of Salmonids: Osmoregulation, Growth, and Metabolism. In *American Fisheries Society Symposium* (Vol. 1).

McCormick, S. D., Shrimpton, J. M., Moriyama, S., & Björnsson, B. T. (2002). Effects of an advanced temperature cycle on smolt development and endocrinology indicate that temperature is not a zeitgeber for smolting in Atlantic salmon. *The Journal of Experimental Biology*, *205(Pt 22)*, 3553–3560.

McCormick, S. D., Shrimpton, J. M., Moriyama, S., & Björnsson, B. T. (2007). Differential hormonal responses of Atlantic salmon parr and smolt to increased daylength: A possible developmental basis for smolting. *Aquaculture*. https://doi.org/10.1016/j.aquaculture.2007.10.015

McDowall, R. M. (2006). Diadromy: Origins and Definitions of Terminology. *Copeia*. https://doi.org/10.2307/1446563

Migaud, H., Cowan, M., Taylor, J., & Ferguson, H. W. (2007). The effect of spectral composition and light intensity on melatonin, stress and retinal damage in post-smolt Atlantic salmon, Salmo salar. *Elsevier*, *270*(1–4), 390–404. https://doi.org/10.1016/j.aquaculture.2007.04.064

Nash, C. (2010). *The history of aquaculture*. Blackwell Publishing Ltd.

Nathans, J., Thomas, D., & Hogness, D. (1986). Molecular genetics of human color vision: the genes encoding blue, green, and red pigments. *Science*, *232*(4747), 193–202. https://doi.org/10.1126/science.2937147

Nilsen, T. O., Ebbesson, L. O. E., Madsen, S. S., McCormick, S. D., Andersson, E., Bjornsson, B. T., Prunet, P., & Stefansson, S. O. (2007). Differential expression of gill Na+,K+-ATPase - and -subunits, Na+,K+,2Cl- cotransporter and CFTR anion channel in juvenile anadromous and landlocked Atlantic salmon Salmo salar. *Journal of Experimental Biology*. https://doi.org/10.1242/jeb.002873

Nordgarden, U., Oppedal, F., Taranger, G. L., Hemre, G.-I., & Hansen, T. (2003). Seasonally changing metabolism in Atlantic salmon (Salmo salar L.) I - Growth and feed conversion ratio. *Aquaculture Nutrition*, *9*(5), 287–293. https://doi.org/10.1046/j.1365-2095.2003.00256.x

Novales Flamarique, I. (2000). The ontogeny of ultraviolet sensitivity, cone disappearance and regeneration in the sockeye salmon Oncorhynchus nerka. *Journal of Experimental*

Biology, *203*(7), 1161–1172.

Novales Flamarique, I. (2002). Partial re-incorporation of corner cones in the retina of the Atlantic salmon (Salmo salar). *Vision Research*, *42*(25), 2737–2745. https://doi.org/10.1016/S0042-6989(02)00360-7

Novales Flamarique, I. (2005). Temporal shifts in visual pigment absorbance in the retina of Pacific salmon. *Journal of Comparative Physiology A: Neuroethology, Sensory, Neural, and Behavioral Physiology*, *191*(1), 37–49. https://doi.org/10.1007/s00359-004-0573-9

Novales Flamarique, I. (2013). Opsin switch reveals function of the ultraviolet cone in fish foraging. *Proceedings of the Royal Society B: Biological Sciences*, *280*(1752), 20122490. https://doi.org/10.1098/rspb.2012.2490

Novales Flamarique, I. (2018). Light exposure during embryonic and yolk-sac alevin development of Chinook salmon (Oncorhynchus tshawytscha) does not alter the spectral phenotype of photoreceptors. *Journal of Fish Biology*, *95*(1). https://doi.org/10.1111/jfb.13850

Novales Flamarique, I., & Hawryshyn, C. W. (1994). Ultraviolet photoreception contributes to prey search behaviour in two species of zooplanktivorous fishes. *The Journal of Experimental Biology*, *186*, 187–198.

Novales Flamarique, I., & Hawryshyn, C. W. (1996). Retinal development and visual sensitivity of young pacific sockeye salmon (Oncorhynchus Nerka). *Journal of Experimental Biology*, *199*(4), 869–882.

Nuovo, G. J. (1994). PCR in situ hybridization. *Methods in Molecular Biology (Clifton, N.J.)*, *33*, 223–241. https://doi.org/10.1385/0-89603-280-9:223

Oppedal, F., Dempster, T., & Stien, L. H. (2011). Environmental drivers of Atlantic salmon behaviour in sea-cages: A review. In *Aquaculture*. https://doi.org/10.1016/j.aquaculture.2010.11.020

Oppedal, F., Taranger, G. L., & Hansen, T. (2003). Growth performance and sexual maturation in diploid and triploid Atlantic salmon (Salmo salar L.) in seawater tanks exposed to continuous light or simulated natural photoperiod. *Aquaculture*, *215*(1–4), 145–162. https://doi.org/10.1016/S0044-8486(02)00223-5

Otteson, D. C., & Hitchcock, P. F. (2003). Stem cells in the teleost retina: Persistent neurogenesis and injury-induced regeneration. *Vision Research*, *43*(8), 927–936. https://doi.org/10.1016/S0042-6989(02)00400-5

Packer, O., Hendrickson, A. E., & Curcio, C. A. (1989). Photoreceptor topography of the retina in the adult pigtail macaque (Macaca nemestrina). *The Journal of Comparative*

Neurology, *288*(1), 165–183. https://doi.org/10.1002/cne.902880113

Peirson, S. N., Haiford, S., & Foster, R. G. (2009). The evolution of irradiance detection: Melanopsin and the non-visual opsins. In *Philosophical Transactions of the Royal Society B: Biological Sciences* (Vol. 364, Issue 1531, pp. 2849–2865). Royal Society. https://doi.org/10.1098/rstb.2009.0050

Pichaud, F., & Desplan, C. (2016). Evolution of color vision. In *Results and problems in cell differentiation* (Vol. 37, pp. 135–149). Springer, Cham. https://doi.org/10.1007/978-3-319-44978-4_11

Porter, M. J. R., Duncan, N., Handeland, S. O., Stafansson, S. O., & Bromage, N. R. (2001). Temperature, light intensity and plasma melatonin levels in juvenile Atlantic salmon. *Journal of Fish Biology*, *58*(2), 431–438. https://doi.org/10.1111/j.1095-8649.2001.tb02262.x

Raymond, P. A., & Barthel, L. K. (2004). A moving wave patterns the cone photoreceptor mosaic array in the zebrafish retina. *The International Journal of Developmental Biology*, *48*(8–9), 935–945. https://doi.org/10.1387/ijdb.041873pr

Raymond, P. A., Barthel, L. K., & Curran, G. A. (1995). Developmental patterning of rod and cone photoreceptors in embryonic zebrafish. *The Journal of Comparative Neurology*, *359*(4), 537–550. https://doi.org/10.1002/cne.903590403

Reddin, D. G., Downton, P., Fleming, I. A., Hansen, L. P., & Mahon, A. (2011). Behavioural ecology at sea of Atlantic salmon (Salmo salar L.) kelts from a Newfoundland (Canada) river. *Fisheries Oceanography*, *20*(3), 174–191. https://doi.org/10.1111/j.1365-2419.2011.00576.x

Reece, J., Urry, L. A., Meyers, N., Cain, M. L., Wasserman, S. A., Minorsky, P. V., Jackson, R. B., & Cooke, B. N. (2015). Biology: A Global Approach, 10th edition. In *Pearson Education Ltd.*

Roorda, A., Metha, A. B., Lennie, P., & Williams, D. R. (2001). Packing arrangement of the three cone classes in primate retina. *Vision Research*, *41*(10–11), 1291–1306. https://doi.org/10.1016/S0042-6989(01)00043-8

Sabouhanian, A.-A. (2015). Correlated Evolution of Teleost Fish Rhodopsin with Habitat: Linking Molecular Changes to Ecology. In *Biology*.

Sandbakken, M., Ebbesson, L., Stefansson, S., & Helvik, J. V. (2012). Isolation and characterization of melanopsin photoreceptors of atlantic salmon (Salmo salar). *Journal of Comparative Neurology*. https://doi.org/10.1002/cne.23125

Schachtel, E. G. (2013). *Metamorphosis: On the conflict of human development and the*

development of creativity (1st ed.). Routledge.

Schmitt, E. A., & Dowling, J. E. (1996). Comparison of topographical patterns of ganglion and photoreceptor cell differentiation in the retina of the zebrafish, Danio rerio. *Journal of Comparative Neurology*, *371*(2), 222–234. https://doi.org/10.1002/(SICI)1096-9861(19960722)371:2<222::AID-CNE3>3.0.CO;2-4

Sheridan, M. A. (1989). Alterations in lipid metabolism accompanying smoltification and seawater adaptation of salmonid fish. *Aquaculture*, *82*(1–4), 191–203. https://doi.org/10.1016/0044-8486(89)90408-0

Sigholt, T., Staurnes, M., Jakobsen, H. J., & Åsgård, T. (1995). Effects of continuous light and short-day photoperiod on smolting, seawater survival and growth in Atlantic salmon (Salmo salar). *Aquaculture*, *130*(4), 373–388. https://doi.org/10.1016/0044-8486(94)00349-S

Solbakken, V. A., Hansen, T., & Stefansson, S. O. (1994). Effects of photoperiod and temperature on growth and parr-smolt transformation in Atlantic salmon (Salmo salar L.) and subsequent performance in seawater. *Aquaculture*, *121*(1–3), 13–27. https://doi.org/10.1016/0044-8486(94)90004-3

Staurnes, M., Sigholt, T., Åsgård, T., & Baeverfjord, G. (2001). Effects of a temperature shift on seawater challenge test performance in Atlantic salmon (Salmo salar) smolt. *Aquaculture*, *201*(1–2), 153–159. https://doi.org/10.1016/S0044-8486(01)00654-8

Stefansson, S. O., Björnsson, B. T., Ebbesson, L. O., & McCormick, S. D. (2008). Smoltification. In *Fish Larval Physiology* (pp. 639–681).

Stefansson, S. O., Björnsson, B. T., Hansen, T., Haux, C., Taranger, G. L., & Saunders, R. L. (1991). Growth, Parr-Smolt Transformation, and Changes in Growth Hormone of At Salmo salar) Reared under Different Photoperiods. *Canadian Journal of Fisheries and Aquatic Sciences*, *48*, 63–68.

Stenkamp, D. L., & Raymond, P. A. (1994). Photoreceptor patterning in embryonic and adult goldfish retina. *Molecular Biology Cell*.

Stenkamp, Deborah L. (2007). Neurogenesis in the Fish Retina. In *International Review of Cytology* (Vol. 259, pp. 173–224). https://doi.org/10.1016/S0074-7696(06)59005-9

Stenkamp, Deborah L., Barthel, L. K., & Raymond, P. A. (1997). Spatiotemporal coordination of rod and cone photoreceptor differentiation in goldfish retina. *Journal of Comparative Neurology*, *382*(2), 272–284. https://doi.org/10.1002/(SICI)1096-9861(19970602)382:2<272::AID-CNE10>3.0.CO;2-U

Stenkamp, Deborah L., Hisatomi, O., Barthel, L. K., Tokunaga, F., & Raymond, P. A. (1996).

Temporal expression of rod and cone opsins in embryonic goldfish retina predicts the spatial organization of the cone mosaic. *Investigative Ophthalmology and Visual Science*, *37*(2), 363–376.

Stien, L. H., Fosseidengen, J. E., Malm, M. E., Sveier, H., Torgersen, T., Wright, D. W., & Oppedal, F. (2014). Low intensity light of different colours modifies Atlantic salmon depth use. *Aquacultural Engineering*, *62*, 42–48. https://doi.org/10.1016/j.aquaeng.2014.05.001

Strand, J. E. T., Hazlerigg, D., & Jørgensen, E. H. (2018). Photoperiod revisited: is there a critical day length for triggering a complete parr–smolt transformation in Atlantic salmon Salmo salar? *Journal of Fish Biology*, *93*(3), 440–448. https://doi.org/10.1111/jfb.13760

Taranger, G. L., Haux, C., Hansen, T., Stefansson, S. O., Björnsson, B. T., Walther, B. T., & Kryvi, H. (1999). Mechanisms underlying photoperiodic effects on age at sexual maturity in Atlantic salmon, Salmo salar. *Aquaculture*, *177*(1–4), 47–60. https://doi.org/10.1016/S0044-8486(99)00068-X

Temple, S. E. (2011). Why different regions of the retina have different spectral sensitivities: A review of mechanisms and functional significance of intraretinal variability in spectral sensitivity in vertebrates. *Visu*, *28(4)*, 281–293. https://doi.org/10.1017/S0952523811000113

Temple, S. E., Plate, E. M., Ramsden, S., Haimberger, T. J., Roth, W. M., & Hawryshyn, C. W. (2006). Seasonal cycle in vitamin A1/A2-based visual pigment composition during the life history of coho salmon (Oncorhynchus kisutch). *Journal of Comparative Physiology A: Neuroethology, Sensory, Neural, and Behavioral Physiology*, *192*(3), 301–313. https://doi.org/10.1007/s00359-005-0068-3

Temple, S. E., Veldhoen, K. M., Phelan, J. T., Veldhoen, N. J., & Hawryshyn, C. W. (2008). Ontogenetic changes in photoreceptor opsin gene expression in coho salmon (Oncorhynchus kisutch, Walbaum). *Journal of Experimental Biology*, *211*(24), 3879–3888. https://doi.org/10.1242/jeb.020289

Terakita, A. (2005). The opsins. *Genome Biology*, *6(3)*. https://doi.org/10.1186/gb-2005-6-3-213

Thrush, M. A., Duncan, N. J., & Bromage, N. R. (1994). The use of photoperiod in the production of out-of-season Atlantic salmon (Salmo salar) smolts. *Aquaculture*, *121*(1–3), 29–44. https://doi.org/10.1016/0044-8486(94)90005-1

Tipsmark, C. K., Sorensen, K. J., & Madsen, S. S. (2010). Aquaporin expression dynamics in osmoregulatory tissues of Atlantic salmon during smoltification and seawater

acclimation. *Journal of Experimental Biology*. https://doi.org/10.1242/jeb.034785

Valen, R., Eilertsen, M., Edvardsen, R. B., Furmanek, T., Rønnestad, I., van der Meeren, T., Karlsen, Ø., Nilsen, T. O., & Helvik, J. V. (2016). The two-step development of a duplex retina involves distinct events of cone and rod neurogenesis and differentiation. *Developmental Biology*. https://doi.org/10.1016/j.ydbio.2016.06.041

Valen, R., Karlsen, R., & Helvik, J. V. (2018). Environmental, population and life-stage plasticity in the visual system of Atlantic cod. *Journal of Experimental Biology, 221(Pt 1)*. https://doi.org/10.1242/jeb.165191

van der Meer, H. J. (1992). Constructional morphology of photoreceptor patterns in percomorph fish. *Acta Biotheoretica*, *40*(1), 51–85. https://doi.org/10.1007/BF00046551

Veldhoen, K., Allison, W. T., Veldhoen, N., Anholt, B. R., Helbing, C. C., & Hawryshyn, C. W. (2006). Spatio-temporal characterization of retinal opsin gene expression during thyroid hormone-induced and natural development of rainbow trout. *Visual Neuroscience*, *23(2)*, 169–179. https://doi.org/10.1017/S0952523806232139

Verspoor, E., Stradmeyer, L., & Nielsen, J. (2007). The Atlantic salmon: Genetics, Conservation and Management. In *Blackwell Publishing Ltd*.

Viets, K., Eldred, K. C., & Johnston, R. J. (2016). Mechanisms of Photoreceptor Patterning in Vertebrates and Invertebrates. In *Trends in Genetics* (Vol. 32, Issue 10, pp. 638–659). Elsevier Ltd. https://doi.org/10.1016/j.tig.2016.07.004

Wikler, K. C., Williams, R. W., & Rakic, P. (1990). Photoreceptor mosaic: Number and distribution of rods and cones in the rhesus monkey retina. *The Journal of Comparative Neurology*, *297*(4), 499–508. https://doi.org/10.1002/cne.902970404

Woo, N. Y. S., Bern, H. A., & Nishioka, R. S. (1978). Changes in body composition associated with smoltification and premature transfer to seawater in Coho salmon (Oncorhynchus kisutch) and King salmon (O. tschawytscha). *Journal of Fish Biology*. https://doi.org/10.1111/j.1095-8649.1978.tb03450.x

Wozniak, B., & Dera, J. (2007). Light absorption in sea water. In *Light Absorption in Sea Water* (Vol. 33). Springer New York. https://doi.org/10.1007/978-0-387-49560-6

Wu, A. R., Neff, N. F., Kalisky, T., Dalerba, P., Treutlein, B., Rothenberg, M. E., Mburu, F. M., Mantalas, G. L., Sim, S., Clarke, M. F., & Quake, S. R. (2014). Quantitative assessment of single-cell rnA-sequencing methods. *Nature Methods*, *11*(1), 41. https://doi.org/10.1038/nmeth.2694

Xiaowei, Z., & Junning, C. (2018). *World Fisheries and Aquaculture*. Food and Agriculture Organization of the United Nations.

Yokoyama, S. (2000). Molecular evolution of vertebrate visual pigments. In *Progress in Retinal and Eye Research* (Vol. 19, Issue 4, pp. 385–419). https://doi.org/10.1016/S1350-9462(00)00002-1

Young, G., Björnsson, B. T., Prunet, P., Lin, R. J., & Bern, H. A. (1989). Smoltification and seawater adaptation in coho salmon (Oncorhynchus kisutch): Plasma prolactin, growth hormone, thyroid hormones, and cortisol. *General and Comparative Endocrinology, 74*(3), 335–345. https://doi.org/10.1016/s0016-6480(89)80029-2

Zar, J. H. (1996). Biostatistical Analysis. 3rd Edition. *Prentice Hall, Upper Saddle River, 662 P.*

7. Appendix:

Buffers and solutions:

4% paraformaldehyde (4% PF):

- 40 g PF (Cat. No P6148, Sigma-Aldrich) was dissolved in 500 ml dH_2O.
- The solution was heated to 65 °C while stirring and stirred for 15 min at 65 °C.
- Some drops of NaOH was added to make the solution blank.
- The solution was cooled down on ice.
- 200 ml 5xPBS in DEPC H_2O was added.
- The pH was then adjusted to 7,4 by using NaOH.
- The volume was then adjusted to 1 litre.
- The 4% PF solutions were stored at -20°C.

0.1 M Triethanolamine (TEA) (pH 8,0):

- 665 µl of TEA (Triethanolamine) (Cat. No 90279, Sigma) was pipetted into 50 ml DEPC water.
- The pH was adjusted to 8,0 using HCl.

0.25% acetic anhydride in 0.1 M TEA (pH 8.0):

- 665 µl of TEA (Triethanolamine) (Cat. No 90279, Sigma) and 125 µl acetic anhydride (Cat. No A-6404, Sigma) was pipetted into 50 ml DEPC water.
- The pH was adjusted to 8,0.

10% Blocking solution:

- 15 g of Blocking Reagent (Cat. No 11096176001, Roche Diagnostic) was added to 30 ml of 5x Maleate (pH 7.5), and then added DEPC water to a total volume of 150 ml.
- The solution was dissolved by heating it carefully in a microwave.
- The solution was then autoclaved and stored at -20°C.

50% deionised formamide in 2xSSC (50 ml):

- 25 ml Formamide (low quality) (Cat. No 47671, Sigma) and 25 ml 2xSSC in dH_2O were mixed together in a falcon tube.

70% glycerol:

- 35 ml glycerol (98%) (Cat. No G5516, Sigma) was mixed with 15 ml of 1xPBS.
- The solution was prepared in advance to prevent bubbles.

5xPBS in DEPC water:

- 40 g NaCl (Cat. No 31434, Sigma-Aldrich), 1g KCl (Cat. No 60130, Sigma-Aldrich), 7,2 g Na2HPO4 (Cat.No 71640, Sigma-Aldrich) and 1,2 g KH_2PO4 (Cat.No P5655, Sigma) was dissolved in 800mL dH_2O.
- The pH was adjusted to 7,4.
- The volume was adjusted to 1 litre.
- 0,5 ml DEPC was added and the solution placed in room temperature overnight.
- The following morning, the solutions were autoclaved.

RNase buffer (10 mM Tris-HCl pH 7.5, 1 mM EDTA, 0.5 M NaCl):

- 10 ml 1 M Tris-HCl (pH 7.5), 2 ml 0.5 M EDTA and 100 ml 5 M NaCl was added dH_2O to a volume of 1 litre.

5x Maleate buffer:

- 58 g maleic acid (Cat. No M0375, Sigma) was dissolved in 850ml dH_2O (100 mM).
- The pH was adjusted to 7.5 with sodium hydroxide pellets (Cat. No 30620, Sigma-Aldrich) .
- 43.8 g NaCl (Cat. No 31434N, Sigma-Aldrich) was added (150 mM).
- The volume was adjusted to 1 litre.

Visualization buffer (100 mM Tris pH 9.5, 100 mM NaCl, 50 mM $MgCl_2$):

- 20 ml 5 M NaCl, 100 ml 1 M Tris (pH 9.5) and 100 ml 0.5 M $MgCl_2x6H_2O$ was added dH_2O to a volume of 1 litre.
- The pH was adjusted to 9.5 using HCl.

Stop buffer (10 mM Tris-HCl pH 7.5, 1 mM EDTA, 150 mM NaCl):

- 10 ml 1 M Tris-HCl (pH 7.5), 2 ml 0.5 M EDTA and 30 ml 5 M NaCl was added dH_2O to a volume of 1 litre.
- The pH was adjusted to 7.5.

PAP pen:

- (Cat. No S2002, Dako).

Proteinase K:

- 10 mg of Proteinase K (Cat. No P2308, Sigma-Aldrich) (2 mg/ml) was dissolved in 5 ml of 0.1 M Tris pH 8.0 and 0.05 M EDTA pH 8.0 (Proteinase K buffer).
- The solution was made into aliquots of 250 µl and stored at -20 °C.
- The aliquot of 250 µl was then diluted in 50 ml 0.1 M Tris pH 8.0 and 0.05 M EDTA pH 8.0 to a concentration of 10 µg/ml before use.

Proteinase K buffer (0.1 M Tris pH 8.0 and 0.05 M EDTA pH 8.0):

- 100 ml 1 M Tris (pH 8.0) and 100 ml 0,5 M EDTA (pH 8.0) was added 800 ml DEPC water.

20xSSC in DEPC water:

- 175.3 g NaCl (Cat. No 31434N, Sigma-Aldrich) and 88.2 g tri-Sodium citrate-dihydrate (Cat. No 71402, Sigma) was dissolved in 800 ml dH_2O.
- The pH was adjusted to 7.
- The volume was adjusted to 1 litre and then added 0,5 ml DEPC.
- The solution was incubated at room temperature overnight.
- The following morning the solution was autoclaved.

2x SSC, 0.05% Triton X-100, 2% Blocking reagent:

- 40 ml 2x SSC, 25 µl Triton X-100 (Cat. No T8787, Sigma) and 10 ml 10% Blocking reagent were mixed together.

Antibody solution (1 ml for 10 glasses):

- 0.5 µl antibody (Anti-DIG-AF (1:2000) (Cat. No 11093274910, Roche Diagnostics), 200 µl 5x Maleate buffer, 100 µl 10x Blocking solution, 3 µl Triton X-100 (Cat. No T8787, Sigma) was added dH_2O to a total volume of 1 litre.

0.02 mg/ml RNase A:

- 0,05 g (50 mg) of RNase A (Cat. No R4875, Sigma) was dissolved in 0,01 M NaOAc (pH 5,2) (166,7 µl of 3 M NaOAc in 45 ml dH_2O) by heating to approximately 100 °C. The solution was left at this temperature for approximately 15 min.
- The solution was then slowly cooled down to room temperature .
- Following this, the pH was adjusted by adding 0,1x volume of 1M Tris pH 7,4 (5 ml).
- Now being a concentration of 1 mg/ml, aliquots of 1 ml were made in 50 separate tubes and stored at -20 °C.
- Prior to use, one aliquot of 1 ml was added to 49 ml of RNase buffer, resulting in a final concentration of 0.02 mg/ml.

Staining solution (NBT/BCIP):

- 10 ml Visualization buffer was added 45 µl NBT (Cat. No 11383213001, Roche Diagnostics) and 35 µl BCIP (Cat. No 11383221001, Roche Diagnostics).
- The falcon tube was enclosed in aluminium to protect the solution from light.

50% deionised formamide in 2xSSC (50 ml):

- 25 ml Formamide (low quality) (Cat. No 47671, Sigma) was added preheated 25 ml 2xSSC in dH_2O.

Hybridization solution (500 µl) (Hyb^+ (with probe)):

- 387 µl of Hyb^- and 50 µl 10% Blocking solution was added to a falcon tube and heated to 65 °C.
- x µl probe and x µl dH_2O with a total volume of 63 µl was added to a eppendorf tube. (RHOD: 0.5 µl probe + 62.5 µl dH_2O; LWS, SWS1, SWS2 and RH2: 1.0 µl probe + 62.0 µl dH_2O).
- The "probe+dH_2O"-solution was heated at 100 °C for 5 minutes, directly put on ice for 2 minutes, before it was added to the "Hyb- + 10% blocking"-solution.

Anaesthetics:

- MS222 (Cat. No 140729, Finquel vet. 100%. Tricainmesiat 100%, Metacain, Anaesthetics used on Atlantic salmon, Cod and Rainbow trout).
- 5 g MS222 was dissolved in 1 litre of dH_2O.
- The solution was buffered with 1 g $NaHCO_3$ (Merck, K31721929311).
- The pH was adjusted to 7.0 using NaOH.
- The solution was kept in a bottle protecting it from light.
- The concentration of the solution was 5 mg/ml.
- The fish was killed by adding 40 ml of this stock solution to 1 litre of system water (fresh water). (200 mg/litre).

Info (fish used in ISH):

***Table 1*:** Relevant information about the individuals of Atlantic salmon of which the eyes were performed ISH on. Samplings were performed at four stages after a certain daydegrees (dd), at which weight (g), length (cm), sex (male (M) or female (F)) and maturity were determined. For eyes 7, 9 and 10 during the 1st sampling, sex was not established (N/E).

Sampling number	Eye number	Weight	Length	Sex
SS01/19 (4280 dd)	Ey7	66.9 g	17.2 cm	N/E
	Ey9	72.3 g	17.8 cm	N/E
	Ey10	59.8 g	16,2 cm	N/E
SS02/19 (4515 dd)	Ey15	72.9 g	18.1 cm	M
	Ey16	66.2 g	17.6 cm	F
	Ey17	64.8 g	17.6 cm	M
SS03/19 (4835 dd)	Ey7	79.4 g	19.5 cm	M
	Ey10	77.9 g	19.3 cm	F
	Ey11	90.4 g	20.3 cm	F
SS04/19 (5370 dd)	Ey13	129.9 g	24 cm	M
	Ey14	142.3 g	24.1 cm	F
	Ey17	135.6 g	23.5 cm	F

Table 2: Adjustments made in photoshop in creation of the figures.

		Zoom (%) and brightness				Scalebar (µm)			
Gene	**Eye (size)**	**Whole**	**Central**	**Dorsal**	**Ventral**	**Whole**	**Central**	**Dorsal**	**Ventral**
Rhod	7 (24%)	24	300 0,55/250	280 0,65/250	280 0,65/250	1000	100	100	100
	16 (101%)	24	300 0,70/250	260 0,65/250	260 0,65/250	1000	100	100	100
	11 (97%)	24	300 1,00/255	220 0,75/250	220 0,75/250	1000	100	100	100
	17 (152%)	24	300 0,75/250	220 0,75/250	220 0,75/250	1000	100	100	100
Sws1	7 (27%)	27	300 0,60/250	280 0,60/250	280 0,60/250	1000	100	100	100
	16 (84%)	27	300 0,60/250	280 0,60/250	280 0,60/250	1000	100	100	100
	11 (87%)	27	300 0,90/250	280 0,70/250	280 0,70/250	1000	100	100	100
	17 (112%)	27	300 0,65/250	250 0,60/250	250 0,60/250	1000	100	100	100
Sws2	7 (31%)	31	300 0,60/250	260 0,60/250	260 0,60/250	1000	100	100	100
	16 (85%)	31	300 0,65/250	260 0,60/250	260 0,60/250	1000	100	100	100
	11 (79,5%)	31	300 0,60/250	260 0,60/250	260 0,60/250	1000	100	100	100
	17 (116%)	31	300 0,60/250	220 0,60/250	220 0,60/250	1000	100	100	100
	7 (31%)	31	300 0,60/250	260 0,60/250	260 0,60/250	1000	100	100	100

Rh2	16 (78%)	31	300 0,60/250	280 0,60/250	280 0,60/250	1000	100	100	100
	11 (73%)	31	300 0,60/250	260 0,60/250	260 0,60/250	1000	100	100	100
	17 (100%)	31	300 0,70/250	240 0,75/250	240 0,75/250	1000	100	100	100
Lws	7 (27%)	27	300 0,70/250	280 0,65/250	280 0,65/250	1000	100	100	100
	16 (91,5%)	27	300 0,60/250	250 0,60/250	250 0,60/250	1000	100	100	100
	11 (88%)	27	300 0,65/250	280 0,65/250	280 0,65/250	1000	100	100	100
	17 (135%)	27	300 0,60/250	250 0,65/250	250 0,65/250	1000	100	100	100

Statistical analysis:

Descriptive statistics:

Table 3*:* Mean weight (g), standard error of mean (SEM), minimum and maximum values for each sampling during smoltification in Atlantic salmon. Number of individuals (N) in each group and time points are included.

Time point	Mean Weight	N	SEM	Maximum	Minimum
Ss10/18	17,9	18	0,959	26,3	9,1
Ss01/19	70,6	18	3,61	98,9	50,7
Ss02/19	90,1	18	4,86	143	64,8
Ss03/19	101	18	4,58	140	66,2

Table 4*:* Mean length (cm), standard error of mean (SEM), minimum and maximum values for each sampling during smoltification in Atlantic salmon. Number of individuals (N) in each group and time points are included.

Time point	Mean Length	N	SEM	Maximum	Minimum
Ss10/18	11,5	18	0,218	13,2	9,2
Ss01/19	17,6	18	0,309	19,7	15,7
Ss02/19	19,2	18	0,308	22	17,6
Ss03/19	21,1	18	0,327	23,6	18,7

Table 5*:* Mean condition factor (CF), standard error of mean (SEM), minimum (min) and maximum (max) values for each sampling during smoltification in Atlantic salmon. Number of individuals (N) in each group and time points are included.

Time point	Mean CF	N	SEM	Maximum	Minimum
Ss10/18	1,17	18	0,00896	1,24	1,08
Ss01/19	1,29	18	0,017	1,41	1,07
Ss02/19	1,24	18	0,012	1,34	1,18
Ss03/19	1,06	18	0,012	1,14	0,974

Table 6*:* Gill NKA activity (µmol ADP mg prot h^{-1}) standard error of mean (SEM), minimum (min) and maximum (max) values for each sampling during smoltification in Atlantic salmon. Number of individuals (N) in each group and time points are included.

Time point	Mean NKA activity	N	SEM	Maximum	Minimum
Ss10/18	2,09	16	0,446	5,85	0,184
Ss01/19	1,78	18	0,276	4,61	0,598
Ss02/19	2,24	17	0,638	11,1	0,366
Ss03/19	4,41	18	0,663	9,08	1,08

Normality test:

Table 7: Test results from Shapiro-Wilks test of goodness of fit. W = 1 if data are perfectly normal in distribution. Bold W values are significantly smaller than 1 (p<0,05), indicating that the hypothesis of normal distribution should be rejected.

Time point	Condition factor	Length	Weight	Gill NKA acitivity
Ss10/18	W = 0,9856	W = 0,9204	W = 0,9716	W = 0,8887
Ss01/19	**W = 0,8598**	W = 0,9334	W = 0,9293	**W = 0,8587**
Ss02/19	W = 0,9145	W = 0,9319	W = 0,9216	**W = 0,6424**
Ss03/19	W = 0,9459	W = 0,9671	W = 0, 9779	**W = 0,8835**

One-way Analysis of Variance (ANOVA) test:

Table 8: One-way Analysis of Variance (ANOVA) test on the weight (g) of the Atlantic salmon. P<0,05 indicates that there was a general significant difference in weight between the sampling points.

Weight	SS	Degrees of freedom	MS	F (DFn, DFd)	P value
Treatment (between timepoints)	0,5301	3	0,1767	F (3, 68) = 59,47	P<0,0001
Residual (within timepoint)	0,202	68	0,002971		
Total	0,7321	71			

Table 9: One-way Analysis of Variance (ANOVA) test on the length (cm) of the Atlantic salmon. P<0,05 indicates that there was a general significant difference in length between the sampling points.

Length	SS	Degrees of freedom	MS	F (DFn, DFd)	P value
Treatment (between timepoints)	941,9	3	314	F (3, 68) = 202,2	P<0,0001
Residual (within timepoint)	105,6	68	1,552		
Total	1047	71			

Table 10: One-way Analysis of Variance (ANOVA) test on the condition factor (CF) of the Atlantic salmon. P<0,05 indicates that there was a general significant difference in condition factor between the sampling points.

Condition factor	SS	Degrees of freedom	MS	F (DFn, DFd)	P value
Treatment (between timepoints)	0,5301	3	0,1767	F (3, 68) = 59,47	P<0,0001
Residual (within timepoint)	0,202	68	0,002971		
Total	0,7321	71			

Table 11: One-way Analysis of Variance (ANOVA) test on gill NKA activity (µmol ADP mg prot h^{-1}) of the Atlantic salmon. P<0,05 indicates that there was a general significant difference in gill NKA activity between the sampling points.

Gill NKA activity	SS	Degrees of freedom	MS	F (DFn, DFd)	P value
Treatment (between timepoints)	77,15	3	25,72	F (3, 65) = 5,283	P=0,0025
Residual (within timepoint)	316,4	65	4,868		
Total	393,6	68			

Tukey's post-hoc test:

Table 12: Tukey's post-hoc test for wet weight (g) in Atlantic salmon. The timepoints are represented by samplings at 09.10.18 (SS10/18), 22.01.19 (SS01/19), 12.02.19 (SS02/19) and 12.03.19 (SS03/19).

Timepoints, weight	Adjusted P Value
Ss10/18 vs. Ss01/19	<0,0001
Ss10/18 vs. Ss02/19	<0,0001
Ss10/18 vs. Ss03/19	<0,0001
Ss01/19 vs. Ss02/19	<0,005
Ss01/19 vs. Ss03/19	<0,0001
Ss02/19 vs. Ss03/19	0,1886

Table 13: Tukey's post-hoc test for length (cm) in Atlantic salmon. The timepoints are represented by samplings at 09.10.18 (SS10/18), 22.01.19 (SS01/19), 12.02.19 (SS02/19) and 12.03.19 (SS03/19).

Timepoints, length	Adjusted P Value
Ss10/18 vs. Ss01/19	<0,0001
Ss10/18 vs. Ss02/19	<0,0001
Ss10/18 vs. Ss03/19	<0,0001
Ss01/19 vs. Ss02/19	<0,0003
Ss01/19 vs. Ss03/19	<0,0001
Ss02/19 vs. Ss03/19	<0,0001

Table 14: Tukey's post-hoc test for condition factor (CF) in Atlantic salmon. The timepoints are represented by samplings at 09.10.18 (SS10/18), 22.01.19 (SS01/19), 12.02.19 (SS02/19) and 12.03.19 (SS03/19).

Timepoints, condition factor	Adjusted P Value
Ss10/18 vs. Ss01/19	<0,0001
Ss10/18 vs. Ss02/19	<0,0003
Ss10/18 vs. Ss03/19	<0,0001
Ss01/19 vs. Ss02/19	0,0831
Ss01/19 vs. Ss03/19	<0,0001
Ss02/19 vs. Ss03/19	<0,0001

Table 15: Tukey's post-hoc test for gill NKA activity (µmol ADP mg prot h^{-1}) in Atlantic salmon. The timepoints are represented by samplings at 09.10.18 (SS10/18), 22.01.19 (SS01/19), 12.02.19 (SS02/19) and 12.03.19 (SS03/19).

Timepoints, NKA activity	Adjusted P Value
NKA Ss10/18 vs. NKA Ss01/19	0,9767
NKA Ss10/18 vs. NKA Ss02/19	0,9973
NKA Ss10/18 vs. NKA Ss03/19	<0,05
NKA Ss01/19 vs. NKA Ss02/19	0,9258
NKA Ss01/19 vs. NKA Ss03/19	<0,05
NKA Ss02/19 vs. NKA Ss03/19	<0,05